NUMERICAL STUDIES IN NON-LINEAR BOUNDARY LAYER STABILITY THEORY

Thesis

Submitted by

DAVID FRANCIS CORNER, B.Sc.,

for the degree of

DOCTOR OF PHILOSOPHY

University of Edinburgh

SEPTEMBER, 1973.

C O N T E N T S

C O N T E N T S (Contd.)

C O N T E N T S (Contd.)

ABSTRACT

The main part of this thesis is devoted to the study of a finite periodic perturbation imposed on a Blasius boundary layer.

Some non-linear terms are included, causing distortion of the mean flow by the perturbation, generation of second and third harmonics, and modification of the fundamental of the perturbation by the second harmonic. The problem requires the solution of a set of three non-linear coupled equations.

The linearised problem of an infinitesimal perturbation is also stated, and the equation for the perturbation, the Orr-Sommerfeld equation is given.

The numerical methods used to solve the individual equations are derived. The undistorted mean flow is found by a step-by-step method, but in the application of this step-by-step method to the distorted mean flow, an initial value has first to be found.

An iterative method is used for the solution of the Orr-Sommerfeld equation. It has been used previously, but a more concise derivation is given. A development of the iteration is derived in order to solve for the fundamental of the non-linear problem. The method of solution for the higher harmonics is also given.

The solution of the set of coupled equations is accomplished by iteration of the individual equations until convergence is attained.

The results of some solutions of the coupled equations at

ABSTRACT (Contd.)

different amplitudes, Reynolds numbers, and frequencies are presented, and a few cases considered in more detail.

In addition, the results of some investigations into the existence of other modes of solution of the Orr-Sommerfeld equation are presented. The possibility of non-linear interaction between these modes is suggested.

LIST OF SYMBOLS

The following symbols are used to describe the quantities indicated in this list, unless otherwise stated in the text.

c	Amplitude of fundamental perturbation.
c	Non-dimensional complex wave velocity $= c_r + ic_i = \beta/\alpha$.
C_g	Group velocity $= \partial\beta/\partial\alpha$.
D	$= d/dz$.
$f(\eta)$	Dependent variable in the Blasius equation.
F	Non-dimensional frequency parameter.
g	New dependent variable in the finite difference approximation.
h	Steplength.
h_n	Vorticity of the n-th harmonic.
k	Constant = 1.720788.
k_r	Parameter expressing the effect of the non-linear terms.
M	Matrix in the iteration process.
n	Number of points in the finite difference approximation.
p	Pressure.
R	Reynolds number.
u	Velocity component in the x-direction.
U	Mean flow velocity in the x-direction.
U_o	Velocity of the mainstream outside the boundary layer.
w	Velocity component in the z-direction.
W	Mean flow velocity in the z-direction.
W_∞	Limiting value of W outside the boundary layer.
x	Downstream co-ordinate.
z	Normal co-ordinate.

LIST OF SYMBOLS (Contd.)

z_c	Critical layer.
z_n	Position of minimum of $\lvert\phi_1'\rvert$.
α	Non-dimensional complex wave number = $\alpha_r + i\alpha_i$.
β	Non-dimensional frequency.
γ	Parameter in asymptotic form of ϕ_1.
δ	Boundary layer thickness.
δ_1	Boundary layer displacement thickness (Blasius).
δ_1^*	Boundary layer displacement thickness (Distorted Mean Flow). Non-dimensional.
δ_2	Boundary layer momentum thickness.
η	Independent variable in Blasius equation.
ν	Kinematic viscosity.
ρ	Density.
ϕ_1	Fundamental z-distribution.
ϕ_n	n-th Harmonic. z-distribution.
ψ_o	Stream function of mean flow.
ψ_n	Stream function of n-th harmonic.

CHAPTER 1

INTRODUCTION

Brief Historical Review

The theoretical study of laminar flows has been well established for many years, although in a large number of cases exact numerical solutions have only been made possible with the development of the digital computer. In most cases, agreement with experiment is good, but under certain conditions, the flow does not behave in a well-behaved laminar manner. Instead, the flow has a random structure, called turbulence.

The first observations of turbulence were made by Reynolds (1883). Flow in a pipe, Hagen-Poiseuille flow, was examined by means of a coloured filament. In a laminar flow, the filament remained a narrow line for the entire length of the pipe, but if the flow were turbulent the filament was dispersed to fill the entire cross-section of the pipe with colour. It was observed that the transition from laminar to turbulent flow occurred when a non-dimensional parameter, later called the Reynolds number, was exceeded. Further investigations revealed that the value of this critical Reynolds number was reduced when an initial disturbance was imposed on the flow, but that below the critical Reynolds number, initial disturbances were damped out.

Similar effects were observed in a variety of other flows, including boundary layer flows. Boundary layers are

very interesting to the experimenter for, since the Reynolds number increases in the downstream direction, laminar and turbulent behaviour may be observed in the same experiment.

Stability theory was developed in order to predict the critical Reynolds number. A perturbation is imposed on the mean flow, and the perturbation becomes damped or amplified, depending on whether the flow is stable or unstable. Orr (1907), proposed a perturbation in the form of a wave, and, making the assumption of linearity, derived the equation for the perturbation now known as the Orr-Sommerfeld equation. The equation is an eigenvalue equation, employing complex arithmetic, and the sign of the imaginary part of the eigenvalue determines the stability. Even for a mean flow of simple form, such as plane Poiseuille flow, numerical methods must be used for an exact solution, but analytical methods were used to approximate the solution asymptotically. The object of the solution was to predict a neutral curve, a curve of frequency against Reynolds number for waves which are neither amplified nor damped. Notable papers dealing with the solution include Heisenberg (1924), and Tollmein (1929), who approximated the Blasius boundary layer by curves. Further work by Schlichting (1935) predicted the distribution of the wave in the boundary layer, and the perturbations became known as Tollmein-Schlichting waves.

For a long time, these waves were only hypothetical, and experimental confirmation had to await the work of Schubauer and Skramstad (1947). Previous boundary layer experiments had proved inconclusive because of the level of natural turbulence. Using a wind tunnel designed to have

particularly low turbulence, it was possible to observe naturally occurring waves in the region of transition. In further experiments, waves were created by a vibrating ribbon in the boundary layer, and the properties of the waves were found and compared with existing theoretical predictions.

The analytical methods used for the solution of the Orr-Sommerfeld equation involved a series expansion in inverse powers of the Reynolds number, and had the disadvantage that the omission of viscosity in the first approximation caused a singularity at a position called the critical layer. There is no singularity in the complete equation, but it was not until the development of the digital computer that it became feasible to attempt to solve the complete equation exactly. The first "exact" solution was made by Thomas (1953).

The theory of linear perturbations is in itself insufficient to explain the breakdown to turbulence. The assumption of linearity limits the theory to very small disturbances, and ignores the non-linear effects of mean flow distortion and the generation of harmonics. There are large discrepancies between experiment and linear theory, particularly in the prediction of a critical Reynolds number. In many cases turbulence occurs at a much lower Reynolds number than linear theory predicts, and in the extreme cases of plane Couette and Hagen-Poiseuille flow, no critical Reynolds number can be calculated since all linear disturbances are stable. Boundary layer flow appears to differ, since transition does not occur until after the critical Reynolds number of linear theory. For this reason, Tollmein-Schlichting waves can be generated, and transition does not occur until a sufficient

amplitude of perturbation is attained through downstream growth.

It appears necessary to postulate that under certain circumstances a sufficiently large perturbation can become unstable, even if linear theory predicts stability. The first non-linear calculations by Meksyn and Stuart (1951) found this to be the case. In a study of plane Poiseuille flow, they calculated the critical Reynolds number corresponding to various amplitudes of perturbation. With increasing amplitude the critical Reynolds number first fell, then rose. A minimum value was found, as an improvement on linear theory.

A large number of papers on non-linear stability have appeared since 1951. Most of these have dealt with time-amplified perturbations, since these are easier to handle mathematically, and, because of its simple form, plane Poiseuille flow has been a popular choice. In an experiment in boundary layer stability, it is not the time amplification but the space amplification which is measured. It is therefore of more assistance in making comparisons with experiment to calculate space amplification. Little of this has been done, but results for the space amplified case in plane Poiseuille flow have been given by Watson (1962) and Stewartson and Stuart (1971).

It is of interest to know which non-linear effect is of most importance, and in a paper, Lin (1958) concluded that in the vicinity of the critical layer, the harmonics became important before there was significant distortion of the mean flow.

Further experimental studies of the transition process have examined the detailed nature of the processes involved in transition. Emmons (1951), using a water table, observed that natural turbulence began as a random breakdown into turbulent spots, travelling downstream and growing in size and number until they coalesced into complete turbulence.

Klebanoff and Tidstrom (1959) observed the transition of a perturbed boundary layer, and found similar behaviour. A spot appeared at a precise point in each cycle, to be joined a little downstream by others, until there was little trace of periodicity, and only turbulence observed. The experiment was intended to be two-dimensional, but it was found that there were three-dimensional irregularities. The initial spot occurred at a position linked to these irregularities, and was itself three-dimensional in nature. The experiment was repeated with a controlled three-dimensionality by Klebanoff, Tidstrom and Sargent (1962), and their conclusion was that there was a secondary instability in the flow.

The equation for three-dimensional linear perturbations was first given by Squire (1933), who proved that the first unstable linear perturbation is two-dimensional. An attempt to extend non-linear theory to three dimensions was made by Benney (1961).

While three-dimensional effects may make a contribution towards breakdown, they will not be included here.

The Edinburgh Work

The Fluid Dynamics Unit at Edinburgh has been under the directorship of Dr. M.A.S. Ross. A wind tunnel of low natural turbulence was completed in Edinburgh in 1964, and its main use has been for boundary layer stability experiments.

First, the experiments of Schubauer and Skramstad were repeated. Using amplitudes small enough to satisfy linear theory, measurements of wavelength and amplification rate, and determination of the neutral curve and perturbation distribution were made by Barnes (1966) and Ross (1970).

Very little calculated data was available for space-amplified perturbations in boundary layers. In order to provide data for comparison with experiment, a solution method for the Orr-Sommerfeld equation was developed by Osborne (1967). Given an approximation to the eigenvalue the method iterated to the eigenvalue, and simultaneously calculated the eigenvector, to give the distribution of the perturbation. In its original form, Osborne's method was applied to the time-amplified problem, but a modification by Jordinson (1968) enabled solution of the space-amplified problem. A further modification by Barry (1970) took into account the effects on the perturbation of the growth of the boundary layer by including terms involving the normal component of mean velocity.

A few observations of the effects of large perturbations were made by Ross, but a more detailed study was made by Robertson (1971), who observed the distribution of the

second harmonic, and the distortion of the mean flow, and also measured the amplitudes of the fundamental perturbation and its second harmonic throughout the transition region.

Some effects of non-linearity were included in calculations made by Barry. Non-linear terms in the perturbation were added to the mean flow equation, and a solution for the distorted mean flow was found. This distorted mean flow modifies the perturbation and it was necessary to iterate the solutions for the mean flow and the perturbation until a simultaneous solution was attained.

The present aim is to extend this a stage further, and to take into account another non-linear interaction, that between the fundamental and its second harmonic. This requires the simultaneous solution for three things: the distorted mean flow, the perturbation, and its second harmonic.

Other modes of solution

To a large extent, non-linear theory has concentrated on the eigenstate solution of the Orr-Sommerfeld equation which is known to be unstable over a range of frequency and Reynolds number. For many flow profiles, it is known that there are a number of further modes of solution, all stable. For Poiseuille flow, Pekeris and Shkoller (1969) and (1971a) took into consideration non-linear interactions between these modes, and found that, if the initial amplitude of perturbation was sufficiently large, after a period of time, there was an

abrupt increase in amplitude of a number of modes, apparently without limit. This appears to correspond with breakdown, and it would be interesting to repeat the calculations with Blasius flow. This is not possible at present because there is very little known about the spectrum of modes of solution of the Orr-Sommerfeld equation for Blasius flow. A chapter of this work has been devoted to an investigation of the spectrum of eigenvalues. Some results were found by Jordinson (1968) and these were used as guidelines for the present investigation.

CHAPTER 2

DERIVATION OF EQUATIONS

The Mean Flow

A semi-infinite flat plate positioned in the plane $z = 0$, with the y-axis as its leading edge, is surrounded by fluid moving parallel to the x-axis. The situation is entirely two dimensional, with no variation in the y-direction.

Due to the no-slip requirement on the surface of the plate, there will be a region near the plate where the fluid velocity is affected by the presence of the plate. This region is called the boundary layer and is thin in comparison with the downstream distance from the leading edge.

The motion must satisfy the Navier-Stokes equations:

$$\frac{\partial u}{\partial t} + u\frac{\partial u}{\partial x} + w\frac{\partial u}{\partial z} = -\frac{1}{\rho}\frac{\partial p}{\partial x} + \nu\left(\frac{\partial^2 u}{\partial x^2} + \frac{\partial^2 u}{\partial z^2}\right) \qquad (2.1a)$$

$$\frac{\partial w}{\partial t} + u\frac{\partial w}{\partial x} + w\frac{\partial w}{\partial z} = -\frac{1}{\rho}\frac{\partial p}{\partial z} + \nu\left(\frac{\partial^2 w}{\partial x^2} + \frac{\partial^2 w}{\partial z^2}\right) \qquad (2.1b)$$

and the equation of continuity

$$\frac{\partial u}{\partial x} + \frac{\partial w}{\partial z} = 0 \quad . \qquad (2.2)$$

The latter may be satisfied by the choice of a stream function ψ such that

$$\frac{\partial \psi}{\partial z} = u, \qquad \frac{\partial \psi}{\partial x} = -w \quad . \qquad (2.3)$$

Because of the small extent of the boundary layer, certain terms in (2.1) are of small order and may be ignored.

The components u, $\frac{\partial u}{\partial t}$, $\frac{\partial u}{\partial x}$, $\frac{\partial^2 u}{\partial x^2}$ are of order unity. Since u changes in a small distance δ from zero on the plate to its mainstream velocity U_o, $\frac{\partial u}{\partial z}$ is $O(\delta^{-1})$. From (2.2), $\frac{\partial w}{\partial z}$ is $O(1)$, therefore w, $\frac{\partial w}{\partial t}$, $\frac{\partial w}{\partial x}$, $\frac{\partial^2 w}{\partial x^2}$ are $O(\delta)$. Taking the viscous and inertial terms in (2.1a) to be of equal order gives that δ is $O(\nu^{1/2})$.

Equations (2.1) now become

$$\frac{\partial u}{\partial t} + u\frac{\partial u}{\partial x} + w\frac{\partial u}{\partial z} = -\frac{1}{\rho}\frac{\partial p}{\partial x} + \nu\frac{\partial^2 u}{\partial z^2}$$

$$-\frac{1}{\rho}\frac{\partial p}{\partial z} = O(\delta) \qquad (2.4)$$

These equations were first derived by Prandtl (1904).

Since the flow is in a steady state, there is no time variation. In addition the assumption of zero pressure gradient is made, leaving the following equation to be solved:

$$u\frac{\partial u}{\partial x} + w\frac{\partial u}{\partial z} = \nu\frac{\partial^2 u}{\partial z^2} \qquad (2.5)$$

with the requirements $u = w = 0$ on $z = 0$, $u \longrightarrow U_o$ as $z \longrightarrow \infty$.

This equation was first solved by Blasius (1908), but the method of solution here follows Jones & Watson (1963). The stream function ψ is expressed in terms of a function $f(\eta)$, by

$$\psi = (2\nu U_o x)^{1/2} f(\eta), \quad \text{with} \quad \eta = \left(\frac{U_o}{2\nu x}\right)^{1/2} z \qquad (2.6)$$

This gives

$$u = U_o f' \qquad w = \left(\frac{\nu U_o}{2x}\right)^{1/2} (\eta f' - f)$$

$$\frac{\partial u}{\partial x} = -\frac{U_o}{2x}\eta f'' \qquad \frac{\partial u}{\partial z} = U_o\left(\frac{U_o}{2\nu x}\right)^{1/2} f''$$

$$\frac{\partial^2 u}{\partial z^2} = U_o\left(\frac{U_o}{2\nu x}\right) f''' ,$$

and substitution into (2.5) leads to the Blasius equation

$$f''' + ff'' = 0 \qquad (2.7)$$

with boundary conditions $f(0) = f'(0) = 0$,
$f'(\eta) \longrightarrow 1$ as $\eta \longrightarrow \infty$.

(2.7) must be solved numerically, and a starting value, $f''(0)$ is required. The Jones & Watson value, .469600, was adopted.

The displacement thickness, δ_1, of a boundary layer is defined by

$$\delta_1 = \int_0^\infty \left(1 - \frac{u}{U_o}\right) dz .$$

In the Blasius boundary layer, $\delta_1 = k\left(\frac{\nu x}{U_o}\right)^{1/2}$, where the constant, k, has the value 1.720788 (Jones & Watson).

This thickness is used to form the boundary layer Reynolds number $R = \frac{U_o \delta_1}{\nu}$.

Non-dimensional Form

The boundary layer equations may be non-dimensionalised, using the boundary layer displacement thickness δ_1, and the mean stream velocity U_o as units of length and velocity. The non-dimensional components x', u', etc. are then given by

$$x' = x/\delta_1 \qquad u' = u/U_o$$

$$z' = z/\delta_1 \qquad w' = w/U_o$$

$$t' = U_o t/\delta_1 \qquad p' = p/\rho U_o^2 .$$

In the rest of the work, the non-dimensional form will be used, and for convenience, the primes will be omitted.

In the non-dimensional form, the Navier-Stokes equations (2.1) are

$$\begin{aligned} \frac{\partial u}{\partial t} + u\frac{\partial u}{\partial x} + w\frac{\partial u}{\partial z} &= -\frac{\partial p}{\partial x} + \frac{1}{R}\nabla^2 u \\ \frac{\partial w}{\partial t} + u\frac{\partial w}{\partial x} + w\frac{\partial w}{\partial z} &= -\frac{\partial p}{\partial z} + \frac{1}{R}\nabla^2 w \end{aligned} \qquad (2.8)$$

where $\nabla^2 = \frac{\partial^2}{\partial x^2} + \frac{\partial^2}{\partial z^2}$.

The pressure can be eliminated by taking the curl of the vector form of (2.8), and, writing $\frac{\partial u}{\partial z} - \frac{\partial w}{\partial x} = \eta$, (2.8) becomes

$$\frac{\partial \eta}{\partial t} + u\frac{\partial \eta}{\partial x} + w\frac{\partial \eta}{\partial z} = \frac{1}{R}\nabla^2 \eta$$

or in terms of the stream function ψ, $\eta = \nabla^2\psi$, and (2.8) becomes

$$\frac{\partial \eta}{\partial t} + J(\psi,\eta) - \frac{1}{R}\nabla^2\eta = 0 \qquad (2.9)$$

where $J(\psi,\eta) = \frac{\partial \psi}{\partial z}\frac{\partial \eta}{\partial x} - \frac{\partial \psi}{\partial x}\frac{\partial \eta}{\partial z}$.

Equations of the Perturbed Flow

The stability of the mean flow is examined by superimposing on it a periodic disturbance of small amplitude. It is therefore necessary to assume a stream function of the form

$$\psi = \psi_o(x,z) + \psi_p(x,z,t) \qquad (2.10)$$

where ψ_o represents the mean flow, and ψ_p a disturbance of period $\frac{2\pi}{\beta}$. ψ_p may be expanded as a Fourier Series,

$$\psi_p = \sum_{n=1}^{\infty} c_n(\psi_n(x,z)e^{-in\beta t} + \tilde{\psi}_n(x,z)e^{+in\beta t}) \qquad (2.11)$$

where $\sim$ denotes a complex conjugate, and c_n is the amplitude factor of ψ_n, the nth harmonic, a suitably normalised function.

(2.10) and (2.11) may be substituted in (2.9). Equating coefficients of like powers of $e^{-i\beta t}$, a series of equations is obtained:

$$J(\psi_o,\nabla^2\psi_o) - \tfrac{1}{R}\nabla^4\psi_o = -\sum_{m=1}^{\infty} c_m^2(J(\psi_m,\nabla^2\tilde{\psi}_m) + J(\tilde{\psi}_m,\nabla^2\psi_m)) \qquad (2.12)$$

$$c_1G_1(\psi_1) = -\sum_{m=1}^{\infty} c_m c_{m+1}(J(\psi_{m+1},\nabla^2\tilde{\psi}_m) + J(\tilde{\psi}_m,\nabla^2\psi_{m+1})) \qquad (2.13)$$

$$c_nG_n(\psi_n) = -\sum_{m=1}^{n-1} c_m c_{n-m}\, J(\psi_m,\nabla^2\psi_{n-m}) - \sum_{m=1}^{\infty} c_m c_{m+n}(J(\psi_{m+n},\nabla^2\tilde{\psi}_m) + J(\tilde{\psi}_m,\nabla^2\psi_{m+n})) \qquad (2.14)$$

where

$$G_n(\psi_n) = -in\beta\nabla^2\psi_n + J(\psi_o,\nabla^2\psi_n) + J(\psi_n,\nabla^2\psi_o) - \tfrac{1}{R}\nabla^4\psi_n \ .$$

Since i occurs explicitly in $G_n(\psi_n)$, it is expected that the solution of ψ_n will be complex.

The case of interest is one where c_1 is initially very small, and the other c_n's negligible. It is known that boundary layer amplification may occur, and with sufficient amplification, the higher harnonics can be generated.

In the set of equations (2.14), the nth harmonic is

excited by the non-linear terms on the right hand side of the equation. It can be seen that the non-linear presence of the second harmonic is necessary in order to excite the third and fourth harmonics, and in general excitation of the (2n-1)th and (2n)th harmonics requires the presence of at least the nth harmonic.

Now suppose that only the fundamental is large enough to enter the equations non-linearly. If the fundamental, ψ_1, is normalised, then in order to normalise ψ_2, it is necessary to relate c_2 to c_1. If, further, the product of the fundamental and the second harmonic is not negligible, then, to normalise ψ_3, it is necessary to relate c_3 to c_1c_2. Inclusion of further non-linear terms makes necessary further relationships. The most convenient general relationship is $c_n = c_1^n$.

Assuming now that terms of order higher than c_1^3 are negligible, the equations may be truncated to this order. This leaves a set of four equations.

For the mean flow:

$$J(\psi_o,\nabla^2\psi_o) - \frac{1}{R}\nabla^4\psi_o = -c_1^2(J(\psi_1,\nabla^2\tilde{\psi}_1) + J(\tilde{\psi}_1,\nabla^2\psi_1)) \quad (2.15)$$

For the fundamental perturbation:

$$G_1(\psi_1) = -c^2(J(\psi_2,\nabla^2\tilde{\psi}_1) + J(\tilde{\psi}_1,\nabla^2\psi_2)) \quad (2.16)$$

For the second harmonic:

$$G_2(\psi_2) = -J(\psi_1,\nabla^2\psi_1) \quad (2.17)$$

For the third harmonic:

$$G_3(\psi_3) = -J(\psi_1,\nabla^2\psi_2) - J(\psi_2,\nabla^2\psi_1) \qquad (2.18)$$

As yet, no consideration has been given to the boundary layer nature of the mean flow. In order to neglect mean flow terms of small order, the Prandtl boundary layer assumption is made in the form

$$\nabla^2\psi_o = \frac{\partial^2\psi_o}{\partial z^2} \quad ; \qquad \nabla^4\psi_o = \frac{\partial^4\psi_o}{\partial z^4} \; .$$

This form retains terms containing w in (2.16), (2.17) and (2.18) to the same order as the viscous term $\frac{1}{R}\nabla^4\psi_n$. The mean flow terms retained in these three equations are

$$U = \frac{\partial\psi_o}{\partial z} \qquad W = -\frac{\partial\psi_o}{\partial x}$$

$$\frac{\partial^2 U}{\partial z^2} = \frac{\partial^3\psi_o}{\partial z^3} \qquad \frac{\partial^2 W}{\partial z^2} = -\frac{\partial^3\psi_o}{\partial x\partial z^2} \; .$$

Separability

It is expected that the solution for the perturbation will in addition be periodic in space. It is therefore customary in stability theory to assume a solution of the form

$$\psi_n(x,z) = \phi_n(z)e^{in\alpha x} \qquad (2.19)$$

where $n\alpha$ is the wave number of the perturbation, and α, which may take complex values, must be determined. A negative imaginary part indicates a disturbance which is amplified as it moves downstream, and a positive imaginary part indicates a decaying disturbance.

This form of solution assumes that the equations are separable in x and z. It is known, however, that the assumption of separability does not introduce serious error. For the purpose of x differentiation, a is assumed to be a local constant. This is the fundamental simplification introduced into the theory, and as a result, equations (2.16), (2.17) and (2.18) are reduced from partial to ordinary differential equations.

With the substitution of (2.19), and the rewriting of ψ_o in terms of U and W, (2.15), (2.16), (2.17) and (2.18) respectively become:

$$\frac{\partial}{\partial z}\left(U\frac{\partial U}{\partial x} + W\frac{\partial U}{\partial z} - \frac{1}{R}\frac{\partial^2 U}{\partial z^2}\right) =$$

$$-c_1^2 e^{-2a_i x}\left\{\begin{array}{l} i\tilde{a}\tilde{\phi}_1(\phi_1''' - a^2\phi_1') + ia\tilde{\phi}_1'(\phi_1'' - a^2\phi_1) \\ \qquad\qquad + \text{complex conjugate} \end{array}\right\} \tag{2.20}$$

$$L_1(\phi_1) = -c_1^2 e^{-2a_i x}\left\{\begin{array}{l} \tilde{\phi}_1'(2a\phi_2'' - 8a^3\phi_2) + \tilde{a}\,\tilde{\phi}_1(\phi_2''' - 4a^2\phi_2') \\ \quad - \phi_2'(\tilde{a}\,\tilde{\phi}_i'' - \tilde{a}^3\tilde{\phi}_1) - 2a\phi_2(\tilde{\phi}_1''' - \tilde{a}^2\tilde{\phi}_1') \end{array}\right\} \tag{2.21}$$

$$L_2(\phi_2) = a(\phi_1\phi_1''' - \phi_1'\phi_1'') \tag{2.22}$$

$$L_3(\phi_3) = a(2\phi_2\phi_1''' - \phi_2'\phi_1'' + \phi_1\phi_2''' - 2\phi_1'\phi_2'') + a^3(6\phi_1'\phi_2 - 3\phi_2'\phi_1) \tag{2.23}$$

where

$$L_n(\phi_n) = \left[n(aU - \beta)(D^2 - (na)^2) - naD^2U - iW(D^3 - (na)^2 D) + iD^2WD + \frac{i}{R}(D^2 - (na)^2)^2\right]\phi_n$$

and $D = \frac{d}{dz}$.

The factor $e^{-2\alpha_i x}$ in (2.20) and (2.21) occurs in conjunction with the amplitude factor c_i^2. It indicates that at a different x position, the amplitude c_i increases or decreases. When the calculation is to be carried out at one particular point, this factor is ignored.

Linear Problem

In the linear case, only perturbation terms of $O(c)$ are included. The equation for the perturbation is then

$$L_1(\phi_1) = 0 \quad . \tag{2.24}$$

Because of the presence of terms in W, (2.24) is an extended form of the Orr-Sommerfeld equation.

To the same order of approximation, the equation for the mean flow is obtained by setting the right hand side of (2.20) to zero:

$$\frac{\partial}{\partial z}\left(U \frac{\partial U}{\partial x} + W \frac{\partial U}{\partial z} - \frac{1}{R} \frac{\partial^2 U}{\partial z^2}\right) = 0 \tag{2.25}$$

(2.25) may be integrated with respect to z, with zero constant of integration, since the assumption of zero pressure gradient has been made for the mean flow.

CHAPTER 3

NUMERICAL METHODS FOR SOLVING THE MEAN FLOW EQUATION

Undistorted Mean Flow

In the undistorted situation, the equation for the mean flow reduces to the Blasius equation (2.7), when the substitution

$$\psi = \left(\frac{2x}{R}\right)^{1/2} f(\eta) \qquad \eta = \left(\frac{R}{2x}\right)^{1/2} z \qquad (3.1)$$

is made. From the form of the non-dimensionalising process, it is found that $R = k^2 x$, and hence $\eta = \frac{k}{\sqrt{2}} z$. Now the Blasius equation has the property that it is also satisfied by a function $F(\alpha\eta)$ such that $f(\eta) = \alpha F(\alpha\eta)$. A choice of $\alpha = \frac{\sqrt{2}}{k}$ makes the dependent variable z, and gives

$$U = \frac{2}{k^2} F'(z) \qquad \frac{\partial^2 u}{\partial z^2} = \frac{2}{k^2} F'''(z)$$

$$W = \frac{1}{R}(zF'(z) - F(z)) \qquad \frac{\partial^2 w}{\partial z^2} = \frac{1}{R}(F''(z) + zF'''(z)).$$

The boundary conditions are

$$F(0) = F'(0) = 0$$

$$F'(z) \longrightarrow \frac{k^2}{2} \quad \text{as} \quad z \longrightarrow \infty .$$

The initial value $F''(0) = .469600 \times \frac{k^3}{2\sqrt{2}}$ is required to satisfy the outer boundary condition.

Using the initial values at $z = 0$, a fourth order Runge-Kutta integration method was used. Applied to a first order equation $y' = f(x,y)$ the calculation of the function at $x = x_o + h$ from the known value y_o at $x = x_o$ requires the calculation of four intermediate values.

$$k_1 = hf(x_o, y_o)$$

$$k_2 = hf(x_o + \frac{h}{2}, y_o + \frac{k_1}{2})$$

$$k_3 = hf(x_o + \frac{h}{2}, y_o + \frac{k_2}{2})$$

$$k_4 = hf(x_o + h, y_o + k_3)$$

The calculated value of $y(x_o+h)$ is $\frac{1}{6}(k_1 + 2k_2 + 2k_3 + k_4)$ with an error proportional to h^5.

In the application of this method to a higher order equation, it may be considered as a set of simultaneous first order equations.

Distorted Mean Flow

In order to solve the distorted mean flow equation (2.20), it is necessary to know the z-dependent function on the right hand side of the equation. To represent these non-linear terms we write

$$h(z) = i\alpha \tilde{\phi}_1'(\phi_1'' - \alpha^2\phi_1) + i\tilde{\alpha}\tilde{\phi}_1(\phi_1''' - \alpha^2\phi_1') + \text{complex conjugate} .$$

It is then required to solve

$$\frac{\partial\psi_o}{\partial z}\frac{\partial^3\psi_o}{\partial x\partial z^2} - \frac{\partial\psi_o}{\partial x}\frac{\partial^3\psi_o}{\partial z^3} - \frac{1}{R}\frac{\partial^4\psi_o}{\partial z^4} = -\alpha^2 h(z) . \quad (3.2)$$

The Blasius similarity substitution (3.1) is not strictly applicable to this equation, since the equation is to be solved at constant x^*, but as an approximation it

---

* The x-dependence in the mean flow is very small, and in boundary layer stability theory is usually neglected. It is included in (2.24), since terms in W relating to the growth of boundary layer thickness have been added to the standard Orr-Sommerfeld equation. Pretsch (1941) used a similar approach when dealing with boundary layers with a pressure gradient.

was applied, to give

$$f^{iv}(\eta) + f f''' + f'f'' = \frac{2\sqrt{2}}{k^3} R c^2 h(z) \quad . \qquad (3.3)$$

Changing from $f(\eta)$ to $F(z)$ gives

$$F^{iv}(z) + F F''' + F' F'' = \frac{k^2}{2} R c^2 h(z) \quad . \qquad (3.4)$$

(3.4) may be integrated, to produce an equation of similar form to the Blasius equation

$$F''' + F F'' = \frac{k^2}{2} Rc^2 \int_0^z h(z)dz + C \qquad (3.5)$$

where C is a constant of integration to be determined.

Writing the right hand side of (3.5) as $H(z)$, and $K = \frac{k^2}{2}$, the equation is

$$F''' + F F'' = H(z) \qquad (3.6)$$

with asymptotic boundary condition $F'(z) \longrightarrow K$ as $z \longrightarrow \infty$. At moderately large z, where $H(z)$ may be assumed constant, an error function ε, of small value, may be defined by

$$F'(z) = K - \varepsilon'(z) \quad . \qquad (3.7)$$

Integration and differentiation of (3.7) gives

$$F(z) = Kz - \beta - \varepsilon(z) \quad \text{where} \quad \beta = \lim_{z \to \infty} (Kz - F(z))$$

$$F''(z) = - \varepsilon''(z)$$

$$F'''(z) = - \varepsilon'''(z) \quad .$$

Substitution into (3.6) gives

$$- \varepsilon''' + (Kz - \beta - \varepsilon)(-\varepsilon'') = H(\infty) \quad .$$

Neglecting products of ε

$$\varepsilon''' + (Kz - \beta)\varepsilon'' = - H(\infty) \quad . \tag{3.8}$$

(3.8) has the approximate solution

$$\varepsilon'' = A \exp\left(- \frac{(Kz-\beta)^2}{2K}\right) - \frac{H(\infty)}{Kz-\beta}$$

$$\varepsilon' = - \frac{A\exp\left(- \frac{(Kz-\beta)^2}{2K}\right)}{Kz - \beta} - \frac{H(\infty)}{K} \log (Kz-\beta) \quad .$$

Now $\varepsilon' \longrightarrow 0$ as $z \longrightarrow \infty$. This can only hold if $H(\infty) = 0$. Thus the constant of integration in (3.5), $C = - \frac{k^2}{2} Rc^2 \int_0^\infty h(z)dz$, and $H(z) = - \frac{k^2}{2} Rc^2 \int_z^\infty h(z)dz$.

The Initial Values of (3.6)

$F(0) = F'(0) = 0$ are known, but the value of $F''(0) = s$ is not known, and before the equation can be integrated by the Runge-Kutta method, the value of s must be found. An iteration based on one described by Fox (1960) was used.

The function $F(z)$ is also a function of s, and its partial derivative $G = \frac{\partial F}{\partial s}$ can be defined. G satisfies the equation found by differentiation of (3.6), and also its initial conditions, with respect to s.

$$G''' + FG'' + F''G = 0 \tag{3.9}$$

$$G(0) = G'(0) = 0$$

$$G''(0) = 1 \quad .$$

Using an estimate for s (initially the Blasius value),

(3.6) and (3.9) were integrated by the Runge-Kutta method, An application of Newton's Rule gives a correction $\triangle s$ from

$$F'(\infty) - K + \triangle s\, G'(\infty) = 0 .$$

The iteration has second order convergence.

In practice, it is unnecessary to integrate much beyond $z = 6$. At $z = 6$, the error of the Blasius U from unity is of the order of 10^{-9}, and the magnitude of $h(z)$ is also of this order.

CHAPTER 4

NUMERICAL METHODS FOR SOLVING THE ORR-SOMMERFELD EQUATION

The modified Orr-Sommerfeld equation

$$\left[(\alpha U - \beta - iWD)(D^2 - \alpha^2) - \alpha U'' + iW''D + \frac{i}{R}(D^2 - \alpha^2)^2\right]\phi = 0 \qquad (4.1)$$

with boundary values $\phi(0) = \phi'(0) = 0$, $\phi(z) \longrightarrow 0$ as $z \longrightarrow \infty$, is an eigenvalue equation, with, in the present case, α as eigenvalue. In much previous research, the simpler quantity $c = \frac{\beta}{\alpha}$, the wave velocity, was chosen as eigenvalue, since it occurs only once in the equation. In a physical situation, a constant dimensional angular frequency is used, and α is unknown. It is more difficult to solve for α, since it occurs to fourth power in (4.1).

At $z = 0$, the large ratio $\frac{D^4\phi}{D^2\phi} = (2\alpha^2 - i\beta R)$ requires careful treatment. When explicit methods of solution are used, a highly accurate integration formula is necessary. Instead, an implicit method of solution which would give specially accurate values for $D^4\phi$ was chosen.

The function ϕ is to be calculated at a finite number of equally spaced net points, with interval h. Central difference formulae approximate the derivatives at each net point.

$$hD\,\phi_{(i)} = (\mu\delta - \tfrac{1}{6}\mu\,\delta^3 + \tfrac{1}{30}\mu\,\delta^5)\phi_{(i)} + O(\mu\delta^7)$$

$$h^2D^2\,\phi_{(i)} = (\delta^2 - \tfrac{1}{12}\delta^4 + \tfrac{1}{90}\,\delta^6)\phi_{(i)} + O(\delta^8)$$

$$h^3D^3\,\phi_{(i)} = (\mu\delta^3 - \tfrac{1}{4}\mu\,\delta^5 + \tfrac{7}{120}\mu\,\delta^7)\phi_{(i)} + O(\mu\delta^9)$$

$$h^4D^4\,\phi_{(i)} = (\delta^4 - \tfrac{1}{6}\,\delta^6 + \tfrac{7}{240}\,\delta^8)\phi_{(i)} + O(\delta^{10}) \ .$$

Retention of only the first term in the expansion for $D^4\phi$ gives an error $O(h^2)$. It is desirable to compensate for the higher differences, but it is convenient to use no difference higher than δ^4. A device to achieve both these aims is a Noumerov transformation (1924).

A function g is defined such that $\phi_{(i)} = (1 + k_1\delta^2 + k_2\delta^4)g_{(i)}$, where k_1, k_2 are arbitrary constants.

Then, in terms of g

$$h^4D^4\phi_{(i)} = (\delta^4 - \tfrac{1}{6}\delta^6 + \tfrac{7}{240}\delta^8)(1 + k_1\delta^2 + k_2\delta^4)g_{(i)}$$

$$= (\delta^4 + (k_1 - \tfrac{1}{6})\delta^6 + (k_2 - \tfrac{1}{6}k_1 + \tfrac{7}{240})\delta^8)g_{(i)} + O(\delta^{10}).$$

With the choice of $k_1 = \frac{1}{6}$, $k_2 = -\frac{1}{720}$, the coefficients of δ^6 and δ^8 are eliminated, so that

$$h^4D^4\phi_{(i)} = \delta^4 g_{(i)} + O(\delta^{10})$$

with truncation error $O(h^6)$. Taking $O(h^4)$ truncation error for the other derivatives, the formulae are

$$h\,D\,\phi_{(i)} = \mu\,\delta g_{(i)} + O(\mu\,\delta^5)$$

$$h^2D^2\phi_{(i)} = (\delta^2 + \tfrac{1}{12}\delta^4)g_{(i)} + O(\delta^6)$$

$$h^3D^3\phi_{(i)} = (\mu\,\delta^3 - \tfrac{1}{12}\mu\delta^5)g_{(i)} + O(\mu\delta^7).$$

The only difference higher than δ^4 is $\mu\delta^5$, but it will be shown that this can easily be accommodated.

Application of these difference equations to (4.1) produces a set of simultaneous equations

$$\sum_{j=-3}^{3} t_{(i,j)}\, g_{(i+j)} = 0, \quad i = 0, 1, \ldots, n$$

where the coefficients $t_{(i,j)}$ are functions of α, β, R, U and W.

Additional equations are obtained from the boundary conditions to eliminate $g_{(-1)}$, $g_{(-2)}$, $g_{(n+1)}$, $g_{(n+2)}$ and $g_{(n+3)}$. $g_{(-3)}$ is automatically eliminated, since $t_{(0,-3)} = 0$ because it contains W(0).

From the condition $D\phi(0) = 0$

$$h\, D\phi_{(0)} = \mu\, \delta g_{(0)} = \tfrac{1}{2}(g_{(1)} - g_{(-1)})$$

$$\therefore \quad g_{(-1)} = g_{(1)} \ .$$

From the condition $\phi(0) = 0$

$$\phi_{(0)} = (1 + \tfrac{1}{6}\delta^2 - \tfrac{1}{720}\delta^4)g_{(0)}$$

$$= \tfrac{1}{720}(-g_{(-2)} + 124g_{(-1)} + 474g_{(0)} + 124g_{(1)} - g_{(2)})$$

$$\therefore \quad g_{(-2)} = 474g_{(0)} + 248g_{(1)} - g_{(2)} \ .$$

The outer limit must be taken at some finite value. At sufficiently large z, U, U", W, W" are to a good approximation at their asymptotic values. It was found that there was no significant difference between solutions using $z = 6$, and $z = 9$ as the outer limit, and the former was taken as standard.

The asymptotic form of the equation is

$$(\alpha - \beta - iW_\infty D)(D^2 - \alpha^2) + \tfrac{i}{R}(D^2 - \alpha^2)^2 \ \phi = 0$$

with general solution

$$\phi = Ae^{-\alpha z} + Be^{+\alpha z} + Ce^{-\gamma_1 z} + De^{-\gamma_2 z} \ ,$$

where γ_1, γ_2 are the roots of $\gamma^2 + RW_\infty\gamma - \alpha^2 - iR(\alpha-\beta) = 0$. One of the roots, γ_1 say, has positive, the other negative real part, of magnitude $O(R^{1/2})$. The exponentially growing terms must have zero coefficient to satisfy the asymptotic boundary condition. Also the term $Ce^{-\gamma_1 z}$ decays very rapidly, and quickly becomes negligible. Thus ϕ has an asymptotic form $\phi = Ae^{-\alpha z}$.

Values of $g_{(i)}$ at net points outside the outer limit were found using

$$g_{(n+s)} = g_{(n)}\, e^{-sh\alpha}, \qquad s = 1,2,3.$$

The set of simultaneous equations may be combined to form a matrix equation

$$M\underline{g} = 0 \qquad (4.2)$$

where M is a heptadiagonal matrix, i.e. a matrix with the only non-zero elements in a band seven wide centred on the diagonal. The vector $\underline{g}$ must be normalised, and the method chosen was to impose the condition $\underline{s}^T.\underline{g} = 1$, where $\underline{s} = \underline{e}_i$, a vector whose only non-zero component, the i-th, is unity. In order to make the maximum component of $\underline{g}$ unity, i is chosen to be the suffix of the maximum component of $\underline{g}$.

An iteration was derived by Osborne (1967) to solve a problem of this form. A more concise derivation is given here.

The iteration is formulated for the non-linear eigenvalue problem

$$M(\lambda)\underline{v} = 0$$

with scaling condition

$$\underline{s}^T\underline{v} = k\ .$$

If, at the ith stage of the iteration, approximations $\underline{v}^{(i)}$, $\lambda^{(i)}$ are known, then corrections $\Delta\underline{v}^{(i)}$, $\Delta\lambda^{(i)}$ are sought such that

$$M(\lambda^{(i)} + \Delta\lambda^{(i)})(\underline{v}^{(i)} + \Delta\underline{v}^{(i)}) = 0 \qquad (4.3)$$

$$\underline{s}^{T} (\underline{v}^{(i)} + \Delta\underline{v}^{(i)}) = k \ . \qquad (4.4)$$

By means of a Taylor expansion, (4.3) becomes

$$M(\lambda^{(i)})(\underline{v}^{(i)} + \Delta\underline{v}^{(i)}) + \Delta\lambda^{(i)} \frac{\partial M}{\partial \lambda}(\lambda^{(i)})\underline{v}^{(i)} = O(\Delta^2). \qquad (4.5)$$

Ignoring second order terms, and left multiplying (4.5) by M^{-1}

$$\underline{v}^{(i)} + \Delta\underline{v}^{(i)} + \Delta\lambda^{(i)} M^{-1} \frac{\partial M}{\partial \lambda} \underline{v}^{(i)} = 0 \ . \qquad (4.6)$$

Eliminating $\underline{v}^{(i)} + \Delta\underline{v}^{(i)}$ from (4.4) and (4.6)

$$\Delta\lambda^{(i)} \underline{s}^{T} M^{-1} \frac{\partial M}{\partial \lambda} \underline{v}^{(i)} + k = 0$$

$$\Delta\lambda^{(i)} = - \frac{k}{\underline{s}^{T} M^{-1} \frac{\partial M}{\partial \lambda} \underline{v}^{(i)}} \ . \qquad (4.7)$$

Substitution of (4.7) into (4.6) gives

$$\underline{v}^{(i+1)} = \underline{v}^{(i)} + \Delta\underline{v}^{(i)} = \frac{k\, M^{-1} \frac{\partial M}{\partial \lambda} \underline{v}^{(i)}}{\underline{s}^{T} M^{-1} \frac{\partial M}{\partial \lambda} \underline{v}^{(i)}} \qquad (4.8)$$

Equations (4.7) and (4.8) comprise the iteration, which is second order. Initial values $\underline{v}^{(0)}$ and $\lambda^{(0)}$ are required. $\lambda^{(0)}$ is normally known to a good approximation, but a poor estimate, a vector with each component unity, was used for $\underline{v}^{(0)}$. It was observed that the first step of the iteration was generally poor, and an alternative iteration was used.

Expanding (4.3) to include second order terms

$$M(\lambda^{(i)})(\underline{v}^{(i)}+\Delta\underline{v}^{(i)}) + \Delta\lambda^{(i)}\left[\frac{\partial M}{\partial\lambda}(\underline{v}^{(i)}+\Delta\underline{v}^{(i)}) + \frac{1}{2}\Delta\lambda\frac{\partial^2 M}{\partial\lambda^2}\underline{v}\right] = O(\Delta^3) \qquad (4.9)$$

The terms in (4.9) enclosed in square brackets are only required to second order. Substituting (4.7) and (4.8) inside the square bracket

$$M(\underline{v}+\Delta\underline{v}) + \frac{k\Delta\lambda}{\underline{s}^T\underline{x}}\left[\frac{\partial M}{\partial\lambda}\underline{x} - \frac{1}{2}\frac{\partial^2 M}{\partial\lambda^2}\underline{v}\right] = 0 \qquad (4.10)$$

where $\underline{x} = M^{-1}\frac{\partial M}{\partial\lambda}\underline{v}$.

The elimination of $\underline{v}^{(i)} + \Delta\underline{v}^{(i)}$ from (4.4) and (4.10) leads to a third order iteration

$$\left.\begin{aligned}\Delta\lambda^{(i)} &= -\frac{\underline{s}^T\underline{x}}{\underline{s}^T M^{-1}\left(\frac{\partial M}{\partial\lambda}\underline{x} - \frac{1}{2}\frac{\partial^2 M}{\partial\lambda^2}\underline{v}\right)}\\ \underline{v}^{(i+1)} &= \frac{k M^{-1}\left(\frac{\partial M}{\partial\lambda}\underline{x} - \frac{1}{2}\frac{\partial^2 M}{\partial\lambda^2}\underline{v}\right)}{\underline{s}^T M^{-1}\left(\frac{\partial M}{\partial\lambda}\underline{x} - \frac{1}{2}\frac{\partial^2 M}{\partial\lambda^2}\underline{v}\right)}\end{aligned}\right\} \qquad (4.11)$$

If the terms involving $\frac{\partial^2 M}{\partial\lambda^2}$ are omitted, the matrices involved in the iteration are the same as for the second order iteration (4.7), (4.8), and the extra programming required for the longer iteration is minimal. The iteration is reduced to second order, but is better able to cope with a poor initial eigenvector estimate than (4.7), (4.8).

The Neutral Curve

Of particular interest in the solution of the Orr-Sommerfeld equation is the evaluation of the neutral stability curve, the curve linking those perturbations which are neither damped nor amplified, i.e. $\alpha_i = 0$. In order to solve for a point on the neutral stability curve, an iteration was derived which solved for two independent parameters α_r, and either R or β.

The iteration may be derived for a general real problem

$$\left.\begin{aligned} M(\lambda_1, \lambda_2)\underline{v} &= 0, \\ \text{with scaling condition } s\underline{v} &= \underline{k}, \end{aligned}\right\} \qquad (4.12)$$

where M is an $n \times n$ matrix, s is a constant $n \times 2$ matrix $\underline{v}$ is an n vector, $\underline{k}$ is a constant non-zero 2 vector.

The scaling condition must take the form used in order to determine the system of equations. There are n+2 quantities to be determined (λ_1, λ_2 and the n components of $\underline{v}$), therefore there must be n+2 equations.

To approximations $\lambda_1^{(i)}$, $\lambda_2^{(i)}$, $\underline{v}^{(i)}$ are sought corrections $\Delta\lambda_1^{(i)}$, $\Delta\lambda_2^{(i)}$, $\Delta\underline{v}^{(i)}$ such that

$$M(\lambda_1^{(i)}+\Delta\lambda_1^{(i)}, \lambda_2^{(i)}+\Delta\lambda_2^{(i)})(\underline{v}^{(i)}+\Delta\underline{v}^{(i)}) = 0 \qquad (4.13)$$

$$s(\underline{v}^{(i)} + \Delta\underline{v}^{(i)}) = \underline{k} \ . \qquad (4.14)$$

Expanding (4.13) as a Taylor Series

$$M(\lambda_1^{(i)},\lambda_2^{(i)})(\underline{v}+\Delta\underline{v}^{(i)}) + \Delta\lambda_1^{(i)} \frac{\partial M}{\partial\lambda_1}\underline{v}^{(i)} + \Delta\lambda_2^{(i)} \frac{\partial M}{\partial\lambda_2}\underline{v}^{(i)} = O(\Delta^2) \ . \qquad (4.15)$$

Neglecting second order terms, and left multiplying by M^{-1}

$$\underline{v}^{(i)} + \Delta\underline{v}^{(i)} + \Delta\lambda_1 \underline{x} + \Delta\lambda_2 \underline{y} = 0 \qquad (4.16)$$

where

$$\underline{x} = M^{-1} \frac{\partial M}{\partial \lambda_1} \underline{v}^{(i)} , \qquad \underline{y} = M^{-1} \frac{\partial M}{\partial \lambda_2} \underline{v}^{(i)} .$$

Eliminating $\underline{v}^{(i)} + \Delta\underline{v}^{(i)}$ from (4.14) and (4.16)

$$\underline{k} + \Delta\lambda_1 s\underline{x} + \Delta\lambda_2 s\underline{y} = 0 . \qquad (4.17)$$

If the 2×2 matrix T is defined by columns to be

$$T = \begin{bmatrix} s\underline{x} & s\underline{y} \end{bmatrix}$$

then

$$\begin{bmatrix} \Delta\lambda_1^{(i)} \\ \Delta\lambda_2^{(i)} \end{bmatrix} = - T^{-1} \underline{k} . \qquad (4.18)$$

Substitution of these values in (4.16) gives the next approximation to the eigenvector

$$\underline{v}^{(i+1)} = \underline{v}^{(i)} + \Delta\underline{v}^{(i)} = - \Delta\lambda_1^{(i)} \underline{x} - \Delta\lambda_2^{(i)} \underline{y} . \qquad (4.19)$$

The iteration (4.18), (4.19) is second order.

Before this iteration can be applied to the calculation of the neutral curve, the discretised form of the Orr-Sommerfeld (4.2) must be changed from complex to real.

The complex equation $(M_r + iM_i)(g_r + ig_i) = 0$ is equivalent to a pair of real equations

$$\begin{bmatrix} M_r & -M_i \\ M_i & M_r \end{bmatrix} \begin{bmatrix} g_r \\ g_i \end{bmatrix} = 0 .$$

Thus a real $2n$ vector and a $2n \times 2n$ matrix are produced. The real equivalent of the scaling condition is

$$\begin{bmatrix} \underline{e}_i^T & \underline{0}^T \\ \underline{0}^T & \underline{e}_i^T \end{bmatrix} \begin{bmatrix} \underline{g}_r \\ \underline{g}_i \end{bmatrix} = \begin{bmatrix} 1 \\ 0 \end{bmatrix}$$

i.e. the real part of a component is scaled to unity, and its imaginary part set to zero.

The transformation from complex to real is only necessary for the mathematical formulation of the iteration. Using complex arithmetic, the operations carried out in the evaluation of, for example, $M^{-1} \frac{\partial M}{\partial \alpha} \underline{g}$, are the same as those which would have been carried out in the evaluation of the real expression

$$\begin{bmatrix} M_r & -M_i \\ M_i & M_r \end{bmatrix}^{-1} \begin{bmatrix} \frac{\partial M_r}{\partial \lambda_r} & -\frac{\partial M_i}{\partial \lambda_r} \\ \frac{\partial M_i}{\partial \lambda_r} & \frac{\partial M_r}{\partial \lambda_r} \end{bmatrix} \begin{bmatrix} \underline{g}_r \\ \underline{g}_i \end{bmatrix} .$$

It is therefore not difficult to modify the procedure to solve for α, to a procedure to solve for α_r and either R or β.

Calculation of Partial Derivatives

Partial derivatives $\left[\frac{\partial \alpha}{\partial R}\right]_\beta$, $\left[\frac{\partial \alpha}{\partial \beta}\right]_R$, $\left[\frac{\partial \beta}{\partial R}\right]_{\alpha_i}$, calculated at a known eigenvalue, may be used in an extrapolation to approximate a neighbouring eigenvalue. The latter is the slope of the neutral curve, and may be used for extrapolation of the neutral curve.

At an eigenvalue α, it is known that

$$\begin{aligned} M(\alpha, \beta, R)\underline{g} &= 0 \\ \underline{s}^T \underline{g} &= k \quad . \end{aligned} \tag{4.19}$$

At an adjacent eigenvalue $\alpha + \Delta\alpha$

$$\begin{aligned} M(\alpha + \Delta\alpha, \beta + \Delta\beta, R + \Delta R)(\underline{g} + \Delta\underline{g}) &= 0 \\ \underline{s}^T(\underline{g} + \Delta\underline{g}) &= k \quad . \end{aligned} \tag{4.20}$$

(4.20) may be expanded as a Taylor Series

$$M(\alpha, \beta, R)(\underline{g} + \Delta\underline{g}) + \Delta\alpha \frac{\partial M}{\partial \alpha}\underline{g} + \Delta\beta \frac{\partial M}{\partial \beta}\underline{g} + \Delta R \frac{\partial M}{\partial R}\underline{g} = O(\Delta^2) \; . \tag{4.21}$$

Ignoring second order terms and subtracting (4.19)

$$\begin{aligned} M(\alpha, \beta, R)\Delta\underline{g} + \Delta\alpha \frac{\partial M}{\partial \alpha}\underline{g} + \Delta\beta \frac{\partial M}{\partial \beta}\underline{g} + \Delta R \frac{\partial M}{\partial R}\underline{g} &= 0 \\ \underline{s}^T \Delta\underline{g} &= 0. \end{aligned} \tag{4.22}$$

Now M is singular and therefore its inverse M^{-1} does not exist. A non-singular matrix M' can be obtained by interchanging a row of M with $\underline{s}^T$

$$M' = \begin{bmatrix} m_1 \\ \vdots \\ \underline{s}^T \\ \vdots \\ m_n \end{bmatrix}, \qquad \underline{s}'^T = m_r \quad .$$

Equations (4.22) now become

$$M'\Delta\underline{g} + \Delta\alpha \frac{\partial M'}{\partial \alpha}\underline{g} + \Delta\beta \frac{\partial M'}{\partial \beta}\underline{g} + \Delta R \frac{\partial M'}{\partial R}\underline{g} = 0 \tag{4.23}$$

$$\underline{s}'^T\Delta\underline{g} + \Delta\alpha \frac{\partial \underline{s}'^T}{\partial \alpha}\underline{g} + \Delta\beta \frac{\partial \underline{s}'^T}{\partial \beta}\underline{g} + \Delta R \frac{\partial \underline{s}'^T}{\partial R}\underline{g} = 0 \tag{4.24}$$

$\Delta\underline{g}$ can be eliminated from (4.23), (4.24), to give

$$\Delta\alpha\, k_\alpha + \Delta\beta\, k_\beta + \Delta R\, k_R = 0 \qquad (4.25)$$

where

$$k_\alpha = (\underline{s}'^{T} M'^{-1} \frac{\partial M'}{\partial \alpha} - \frac{\partial \underline{s}'^{T}}{\partial \alpha})\underline{g}$$

$$k_\beta = (\underline{s}'^{T} M'^{-1} \frac{\partial M'}{\partial \beta} - \frac{\partial \underline{s}'^{T}}{\partial \beta})\underline{g}$$

$$k_R = (\underline{s}'^{T} M'^{-1} \frac{\partial M'}{\partial R} - \frac{\partial \underline{s}'^{T}}{\partial R})\underline{g} \quad .$$

If $\Delta R = 0$, then from (4.25)

$$\left[\frac{\partial \alpha}{\partial \beta}\right]_R = \frac{\Delta\alpha}{\Delta\beta} = -\frac{k_\beta}{k_\alpha} \quad .$$

Similarly

$$\left[\frac{\partial \alpha}{\partial R}\right]_\beta = -\frac{k_R}{k_\alpha} \quad .$$

On a curve of constant α_i, $\Delta\alpha$ is real. Elimination of $\Delta\alpha$ from the real and imaginary parts of (4.25) gives

$$\left[\frac{\partial \beta}{\partial R}\right]_{\alpha_i} = \frac{(k_R)_r (k_\alpha)_i - (k_R)_i (k_\alpha)_r}{(k_\alpha)_r (k_\beta)_i - (k_\alpha)_i (k_\beta)_r} \quad .$$

CHAPTER 5

NUMERICAL METHODS FOR THE NON LINEAR PROBLEM

Solution of the equation for the distorted fundamental.

Equation (2.21) is the equation for the distorted fundamental to the order of perturbation adopted. It is non-analytic, but homogeneous and linear in ϕ_1. It remains an eigenvalue type of equation, but with the complication that complex conjugates $\tilde{\phi}_1$, $\tilde{\alpha}$ are explicit. The equation may be expressed in terms of two operators:

$$A(\alpha, \beta, R, U, W)\phi_1 + B(\tilde{\alpha}, \alpha, \phi_2)\tilde{\phi}_1 = 0 \qquad (5.1)$$

The occurrence of α in the operator B is solely in conjunction with ϕ_2, caused by x differentiation of ψ_2. For the solution of (5.1) ϕ_2 is assumed to be known, and constant, and its associated coefficients of α are held constant.

(5.1) may be expressed in real and imaginary parts as a pair of equations

$$\begin{bmatrix} A_r + B_r & B_i - A_i \\ A_i + B_i & A_r - B_r \end{bmatrix} \begin{bmatrix} \phi_{1r} \\ \phi_{1i} \end{bmatrix} = 0 \quad . \qquad (5.2)$$

α_r and α_i can be considered as independent parameters. The boundary conditions are as for the Orr-Sommerfeld equation, but expressed in real and imaginary parts.

Application of the Noumerov transformation produces a matrix equation

$$M(\alpha_r, \alpha_i)g = 0 \qquad (5.3)$$

where M is a $2n \times 2n$ matrix. If the components of $\underline{g}$ are arranged to correspond to alternatively real and imaginary parts of the complex vector $\underline{g}_r + i\underline{g}_i$, i.e.

$$\underline{g} = (\ldots\ldots (g_r)_i, (g_i)_i, (g_r)_{(i+1)}, (g_i)_{(i+1)} \ldots\ldots)$$

then M has a band structure, with non-zero elements lying in a band fifteen wide, centred on the diagonal.

The iteration (4.18), (4.19) is applicable to solve (5.3). Since a reasonable approximation to the eigenvector is known, there is no initial difficulty.

Solution of the Equations for Higher Harmonics

The equations for the second and third harmonics (2.22) and (2.23) are inhomogeneous, and can be solved directly. Boundary conditions are applied in a similar manner as for the Orr-Sommerfeld equation. In both equations $\phi_n(0) = D\phi_n(0) = 0$. At the outer limit the asymptotic form is e^{-2az} for the second harmonic, and e^{-3az} for the third harmonic. The right hand sides of the equations can be calculated, and the left hand side discretised with the aid of the Numerov transformation, to give an equation of the form

$$M\,\underline{g}_n = \underline{z}_n$$

where $\underline{z}_n$ is the vector found by evaluating the right hand side of the equation. A matrix inversion gives

$$\underline{g}_n = M_n^{-1}\,\underline{z}_n .$$

Complete Solution

For a complete solution, the simultaneous solution of equations (2.20), (2.21) and (2.22) is required. The methods

of solution of each of these equations requires knowledge of the solution of the other equations. It is necessary to solve iteratively until a consistent solution has been found. To commence the iteration the linear problem (2.7) and (2.24) was solved, to give initial values for the mean flow and the fundamental perturbation. Then the sequence of solutions (2.20), (2.22), and (2.21) was carried out repetitively, using for each solution the most recently calculated value for the others, as shown in the following diagram.

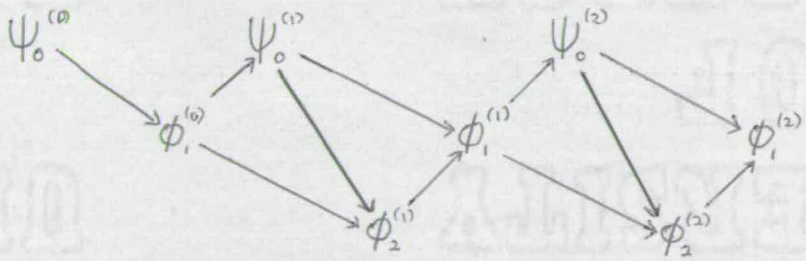

The magnitude of the change of eigenvalue over one cycle was used as a test of convergence. If the criterion $\Delta a < 10^{-7}$ was met, the iteration was terminated.

In order to improve convergence, an Aitken Δ^2 acceleration device was applied. The results of three consecutive solutions of (2.21) were used to produce an improved value, both to the eigenvalue and, point by point, to the eigenvector, using the formula

$$a^{(i)'} = a^{(i)} - \frac{(a^{(i)} - a^{(i-1)})^2}{(a^{(i)} - 2a^{(i-1)} + a^{(i-2)})} .$$

This device was found to assist the convergence moderately well.

CHAPTER 6

RESULTS

With a view to comparison with experiment, calculations were carried out using several values of amplitude c and Reynolds number R. The parameter β was found from $\beta = FR$, where F is the non-dimensional frequency parameter. F is related to the dimensional frequency f used in an experiment by

$$F = \frac{2\pi\nu}{U_o^2} f \ ,$$

and hence is independent of the downstream position or Reynolds number. For the most part, the value $F = 80\times10^{-6}$ was used.

The Eigenvalue α

Tables (6.1) and (6.2) present the calculated values of α_r and α_i respectively, tabulated against R and c, for $F = 80 \times 10^{-6}$.

An equation relating the eigenvalues of the linear and non-linear cases was given by Stewartson and Stuart (1971), and is similar to that used by other authors:

$$\tfrac{1}{2} \frac{\partial}{\partial x} (\log A^2) = -\alpha_i(c,R) = -\alpha_i(0,R) + \frac{K_r}{C_g} A^2 \ ,$$

where the amplitude factor $A = 2c$, C_g is the local group velocity $\frac{\partial\beta}{\partial\alpha}$, and K_r is a parameter expressing the effect

TABLE 6.1 Values of α_r

c	Reynolds No. 500	800	1000	1250	1500	1750
0	.1229764	.1869243	.2304583	.2864213	.3409959	.3844376
.0035	-	-	-	-	-	.3844326
.007	-	-	.2300424	.2856230	.3395638	.3835453
.014	.1229772	.1864369	.2288320	.2834682	.3358039	.3788549
.021	-	-	-	.2804744	.3309467	
.028	.1229853	.1850090	.2246105	.2770922		
.042	-	.1828237				
.056	.1230927					

TABLE 6.2 Values of $a_i \times 10^3$

$C \times 10^2$	Reynolds Number					
	500	800	1000	1250	1500	1750
0	16.7342	0.6923	-6.6047	-8.0589	2.2218	26.3145
0.35	-	-	-	-	-	23.2038
0.7	-	-	-6.4591	-8.1085	0.6624	17.1793
1.4	16.8204	1.0995	-6.0833	-8.1713	-1.8975	7.7350
2.1	-	-	-	-8.1229	-3.6302	-
2.8	17.0686	2.0568	-5.1620	-7.9306	-	-
4.2	-	3.0231	-	-		
5.6	17.9734	-	-	-		

of the non-linear terms. $\frac{K_r}{C_g}$, and C_g for the linear case, are tabulated in Table (6.3).

When K_r is negative, the effect of the perturbation is stabilising; an unstable perturbation tends towards stability, or a stable perturbation becomes even more damped. The opposite takes place when K_r is positive. A stable perturbation then tends towards instability, or an unstable perturbation becomes further amplified.

The former occurs when $R < 1250$, and the latter when $R > 1250$. $R = 1250$ appears to be a borderline case; its instability is enhanced for small amplitudes, but diminished at larger amplitudes. In addition, the magnitude of K_r/C_g when positive becomes much greater at larger Reynolds numbers, but it is reduced by increasing amplitude. It appears that although the trend is towards instability, further effects appear which hinder this aim.

Calculations were made at two further values of F, and the results are listed in Table (6.4). The same type of stabilisation/destabilisation behaviour is found. Again there is a Reynolds number at which the changeover occurs, and at higher Reynolds numbers, the value of K_r/C_g becomes very large The Reynolds number of the changeover is lower in these cases, as are the Reynolds numbers of the neutral curve.

Ease of Convergence of the Iteration

Corresponding to the large values of K_r/C_g, the iteration becomes slower to converge. For this reason, it

TABLE 6.3 K_r/C_g

C	500	800	1000	1250	1500	1750
.0035	-	-	-	-	-	63.48
.007	-	-	-.7429	+.2529	7.956	46.61
.014	-.1100	-.5195	-.6651	+.1433	5.254	23.70
.021	-	-	-	+.0363	3.317	-
.028	-.1067	-.4351	-.4601	-.0409	-	-
.042	-	-	-	-	-	-
.056	-.0988	-	-	-	-	-
C_g	.4022	.4155	.4112	.4063	.4027	.4371

TABLE 6.4

R	$Fx10^6$	$Cx10^2$	$\alpha_r(0)$	$\alpha_i(0)x10^3$	$\alpha_r(c)$	$\alpha_i(c)x10^3$	$\frac{Kr}{Cg}$
800	120	1.4	.2617178	-5.5084	.2598294	-5.2132	-0.3766
1000	"	1.4	.3256595	-4.1611	.3222560	-5.1528	1.265
1100	"	1.4	.3570683	1.8233	.3524822	-1.4075	4.121
1250	"	1.4	.4000451	18.9668	.3936296	6.9272	15.36
1400	"	0.7	.4287146	43.4883	.4300782	28.3177	77.40
500	160	1.4	.2133123	5.3299	.2128534	5.6643	-0.4265
800	"	1.4	.3348542	-2.9561	.3317416	-3.8777	1.176
1000	"	1.4	.4138349	17.3723	.4077709	7.4948	12.60
1250	"	0.35	.4671387	62.1740	.4714039	53.2602	181.9
"	"	0.7	"	"	.4746216	39.5314	115.5

was not possible to use higher values of C at the larger Reynolds numbers.

Table (6.5) represents a typical difficult iteration. The value of a at each stage is shown, together with the approximate error from the final value. The effectiveness of the Δ^2 correction is apparent at the early stages of the iteration, where it is difficult to estimate whether the sequence converges or diverges, but it appears to be of little effect in the later stages of the iteration.

The Functions Obtained on Iteration

Figures (6.1) to (6.6) show a number of features of the functions obtained on iteration for $F = 80 \times 10^{-6}$, and the largest amplitude for each of the Reynolds numbers used. Each figure consists of eight graphs.

a) The relative distortion of the mean flow $(U - U_B)/U_B$ where U_B is the Blasius mean flow. This is always small, of the order of 1 or 2°/o, and therefore a graph of the distorted mean flow will differ only slightly from the shape of the Blasius mean flow, and plotting the graphs in that form would show little information.

b) The Reynolds stress, $-\overline{uw}$. u and w are the x and z components of the perturbation, and the bar denotes a time average. The Reynolds stress is important in the study of turbulence, and indicates the interchange of energy between the mean flow and the disturbance. A positive sign means that energy is being supplied to the perturbation from the mean flow, and vice versa.

TABLE 6.5

Iteration R= 1750, C= .014, F= 80×10^{-6}

	αr	$\alpha i \times 10^2$	approx. error from final value
$\alpha(0)$	.38443765	2.631453	2.10^{-2}
	.38121867	-1.054752	2.10^{-2}
	.36842243	+3.316500	3.10^{-2}
	.37626916	-1.385302	2.10^{-2}
Δ^2 correction:	.37366081	+1.042731	5.10^{-3}
	.37625305	0.452671	4.10^{-3}
	.37954877	1.301363	5.10^{-3}
	.37885890	0.199946	6.10^{-3}
Δ^2correction:	.37839130	0.810027	6.10^{-4}
	.37916597	0.747114	4.10^{-4}
	.37880285	0.799766	3.10^{-4}
	.37887425	0.742201	3.10^{-4}
Δ^2correction	.37891071	0.770367	6.10^{-5}
	.37886037	0.774318	9.10^{-6}
	.37885384	0.772450	1.10^{-5}
	.37885458	0.774664	1.10^{-5}
Δ^2correction	.37885587	0.773488	9.10^{-7}
	.37885368	0.773468	1.10^{-6}
	.37885502	0.773516	2.10^{-7}
	.37885496	0.773468	3.10^{-7}
Δ^2correction	.37885487	0.773479	2.10^{-7}
final value ($\lvert\Delta\alpha\rvert<3.10^{-7}$)	.37885490	0.773500	

The components of the perturbation are

$$u = c(\phi_1' e^{i(\alpha x-\beta t)} + \tilde{\phi}_1' e^{-i(\tilde{\alpha} x-\beta t)})$$

and $$w = c(-i\alpha\phi_1 e^{i(\alpha x-\beta t)} + i\tilde{\alpha}\tilde{\phi}_1 e^{-i(\tilde{\alpha} x-\beta t)}),$$

from which $$-\overline{uw} = 2Re(i\alpha\phi_1\tilde{\phi}_1')c^2 e^{-2\alpha_i x}$$

where Re denotes the real part of a complex number.

The normalised function, $2Re(i\alpha\phi_1\tilde{\phi}_1')$ is shown.

c) The u velocity distribution of the fundamental $|\phi_1'|$. It is this function which is observed in experiment.

d) The distribution of vorticity of the fundamental,

$$h_1 = |\phi_1'' - \alpha^2\phi_1| .$$

e) and f) As for c) and d) but for the second harmonic.

g) and h) As for c) and d) but for the third harmonic.

In addition, e) to h) also show the corresponding function in the linear case, $c = 0$. This function is marked in order to distinguish between the graphs.

Three of this set will now be considered in more detail, one from the first damping region, the second at a higher Reynolds number and amplified, and the third, at the highest Reynolds number considered, in the second damping region.

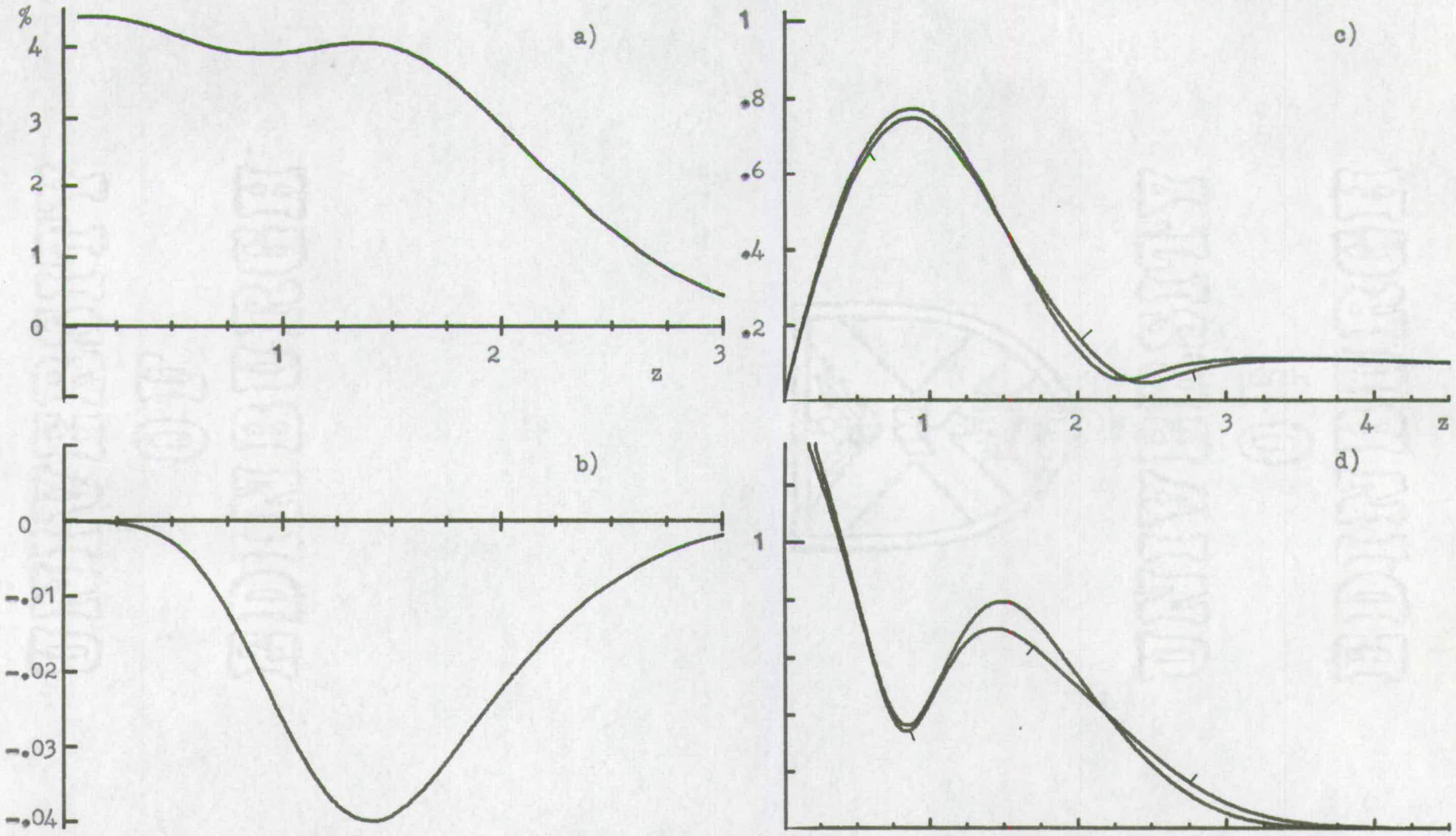

Figure 6.1 Functions at R= 500, c= .056, graphs a) to d).

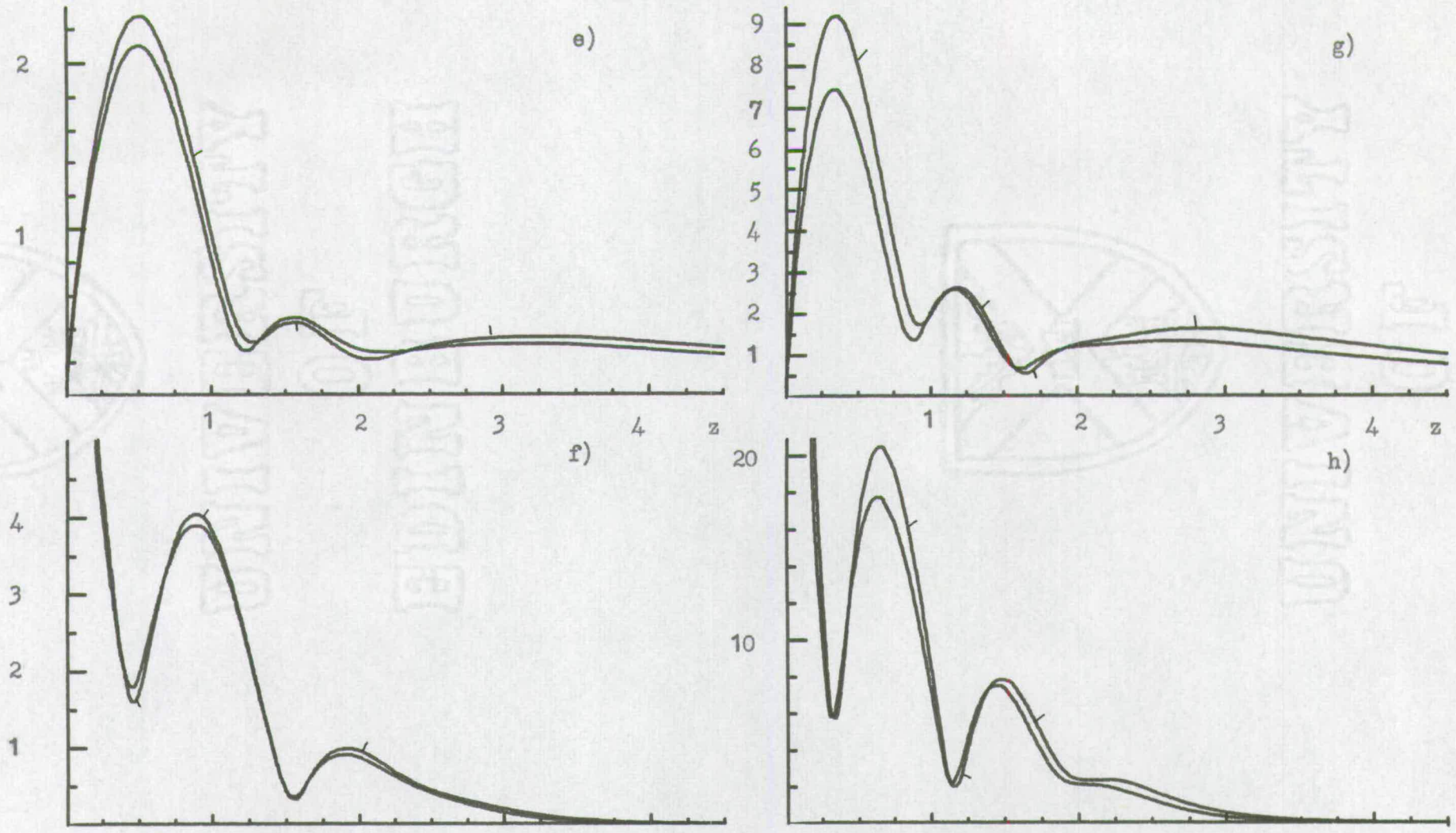

Figure 6.1 Functions at R= 500, c= .056, graphs e) to h).

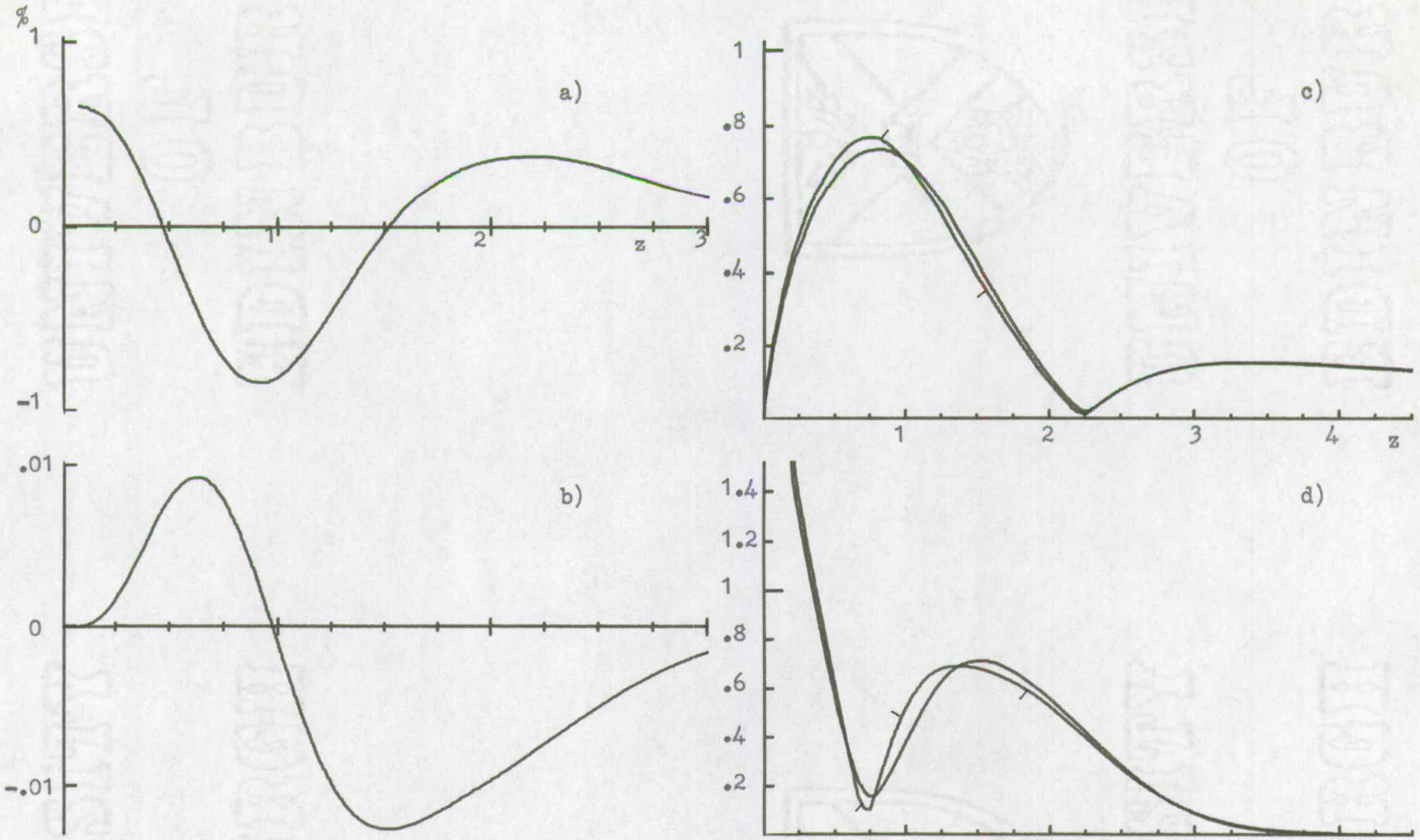

Figure 6.2 Functions at R= 800 , c = .042 , graphs a) to d).

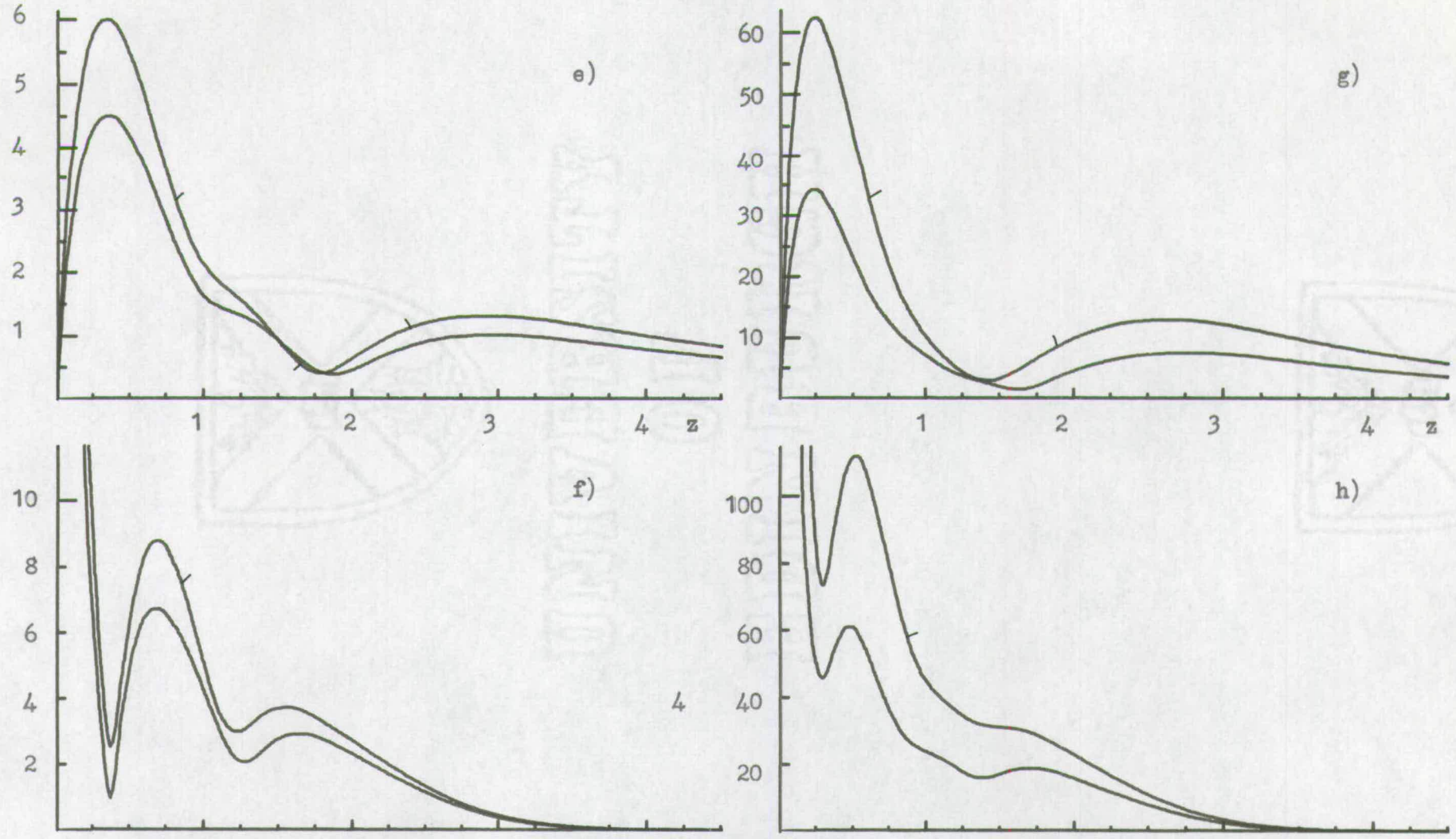

Figure 6.2 Functions at R= 800 , c = .042 , graphs e) to h).

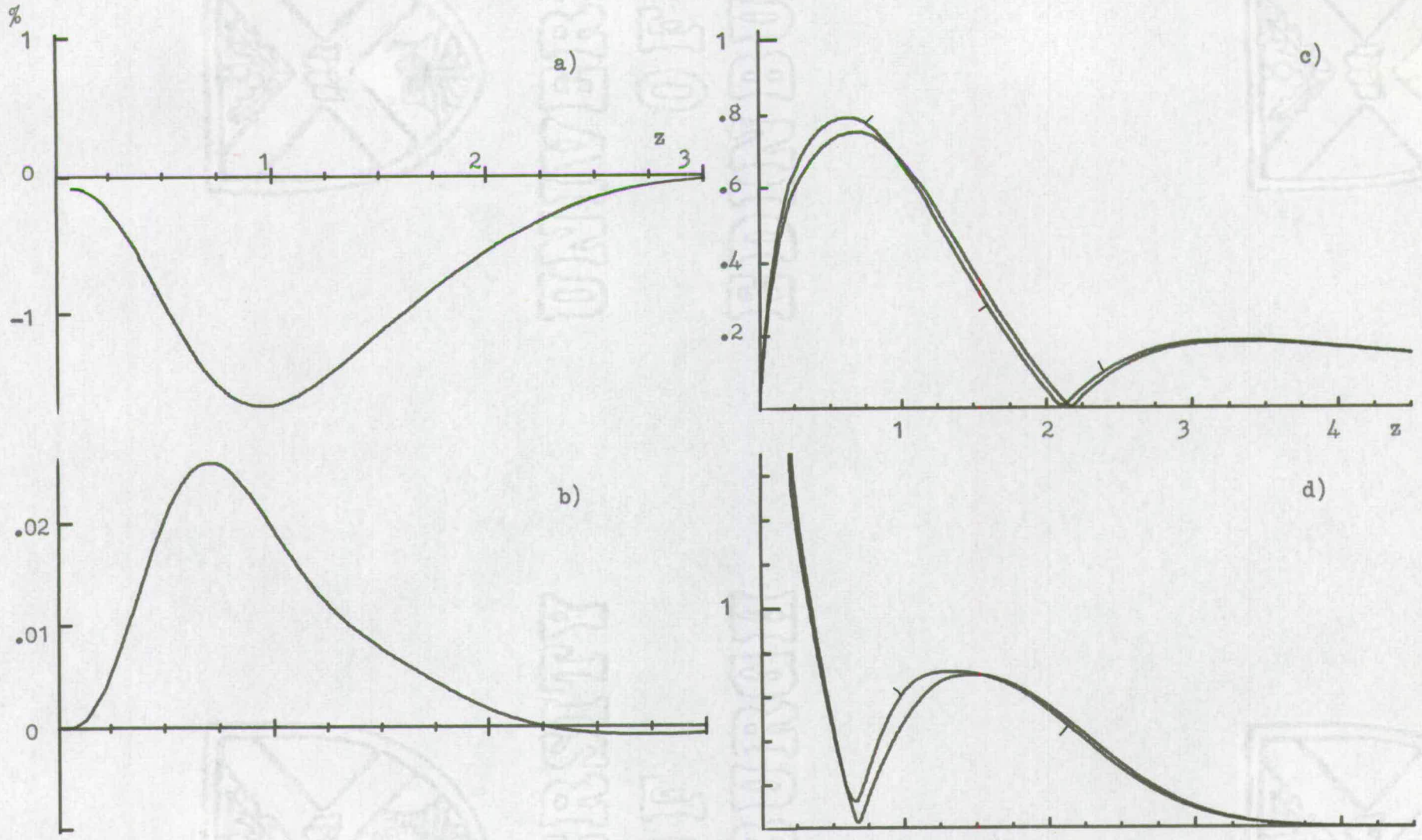

Figure 6.3 Functions at R= 1000, c= .028, graphs a) to d)

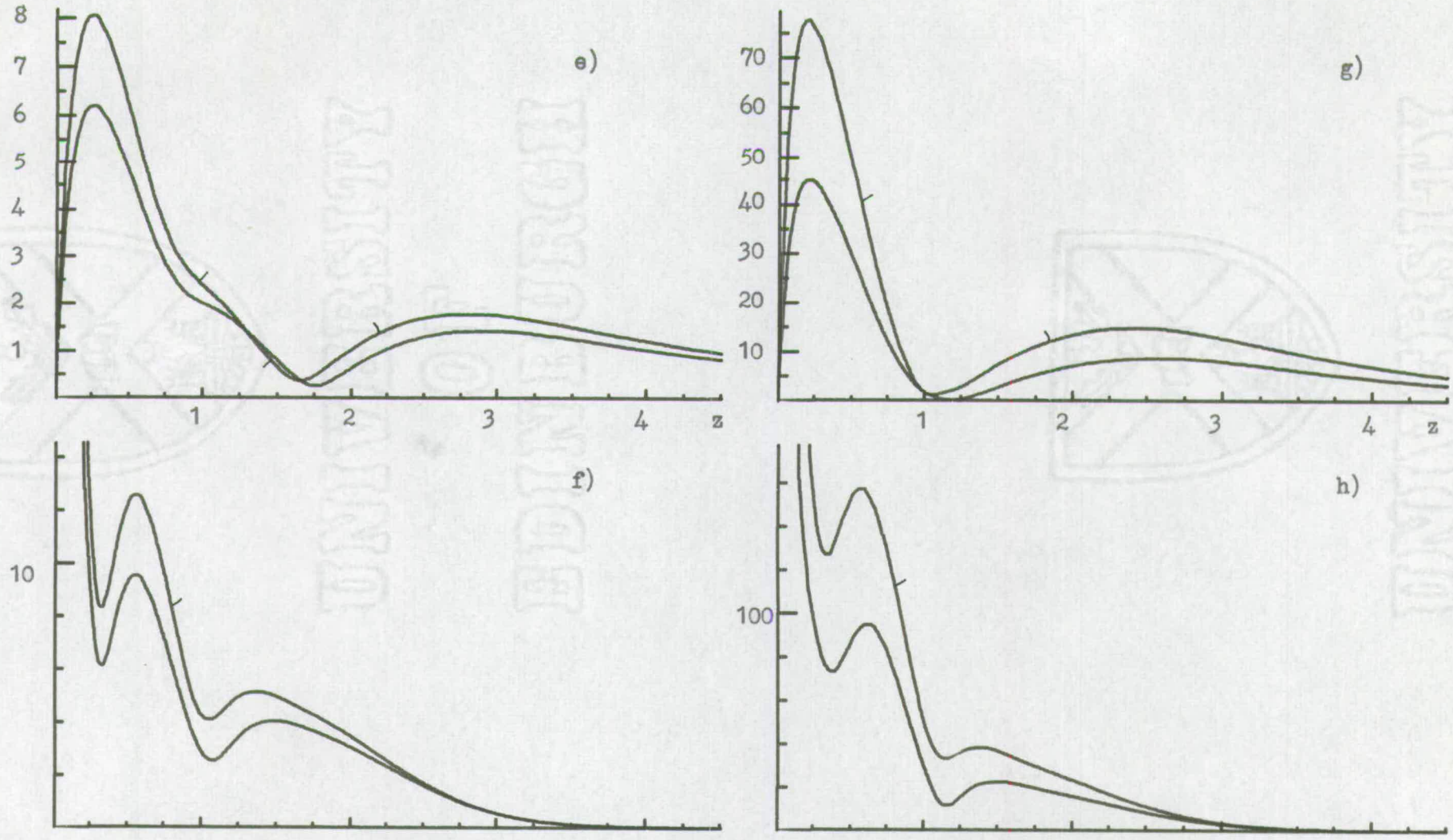

Figure 6.3 Functions at R= 1000, c= .028, graphs e) to h).

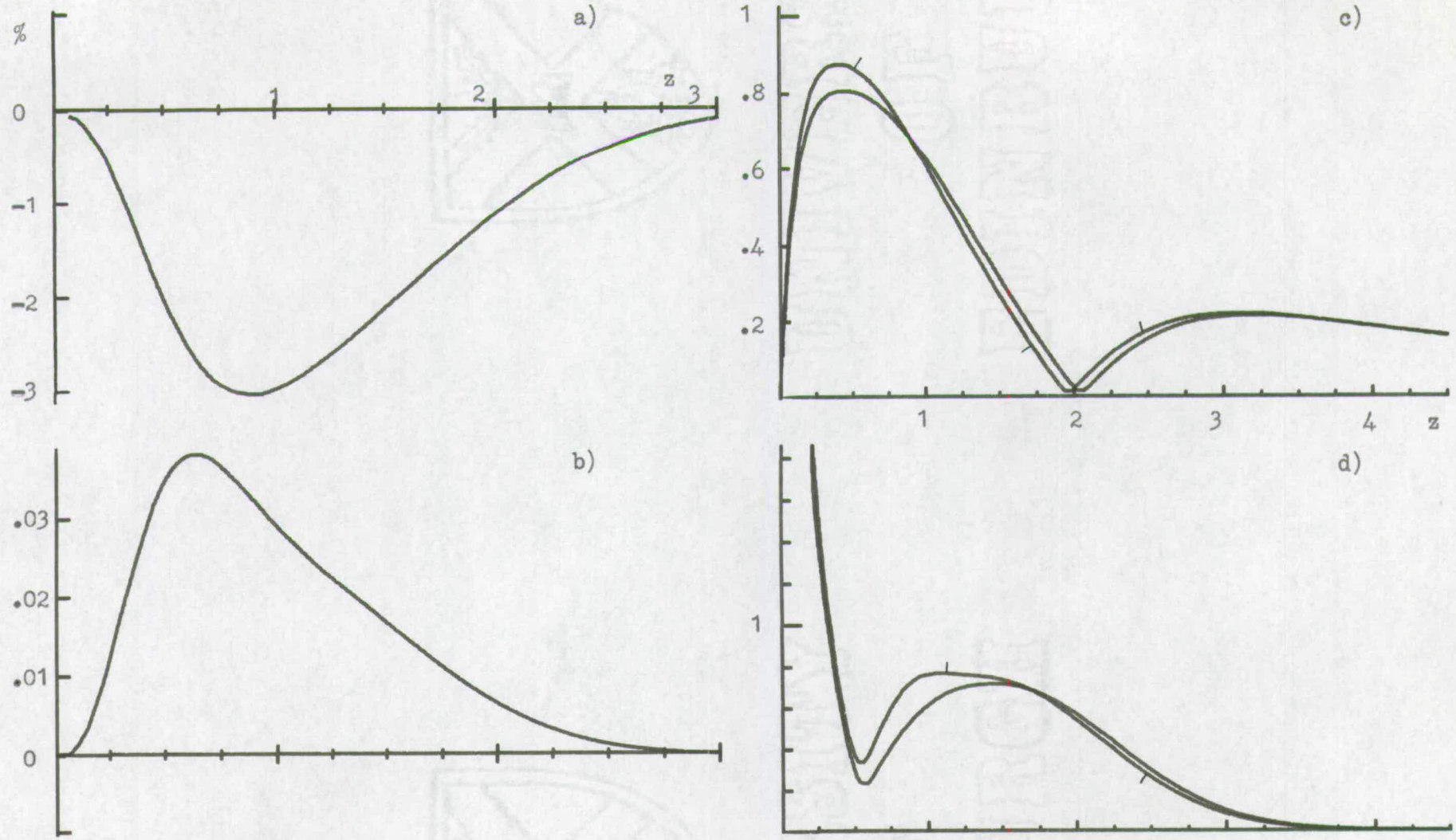

Figure 6.4 Functions at R= 1250, c= .028, graphs a) to d).

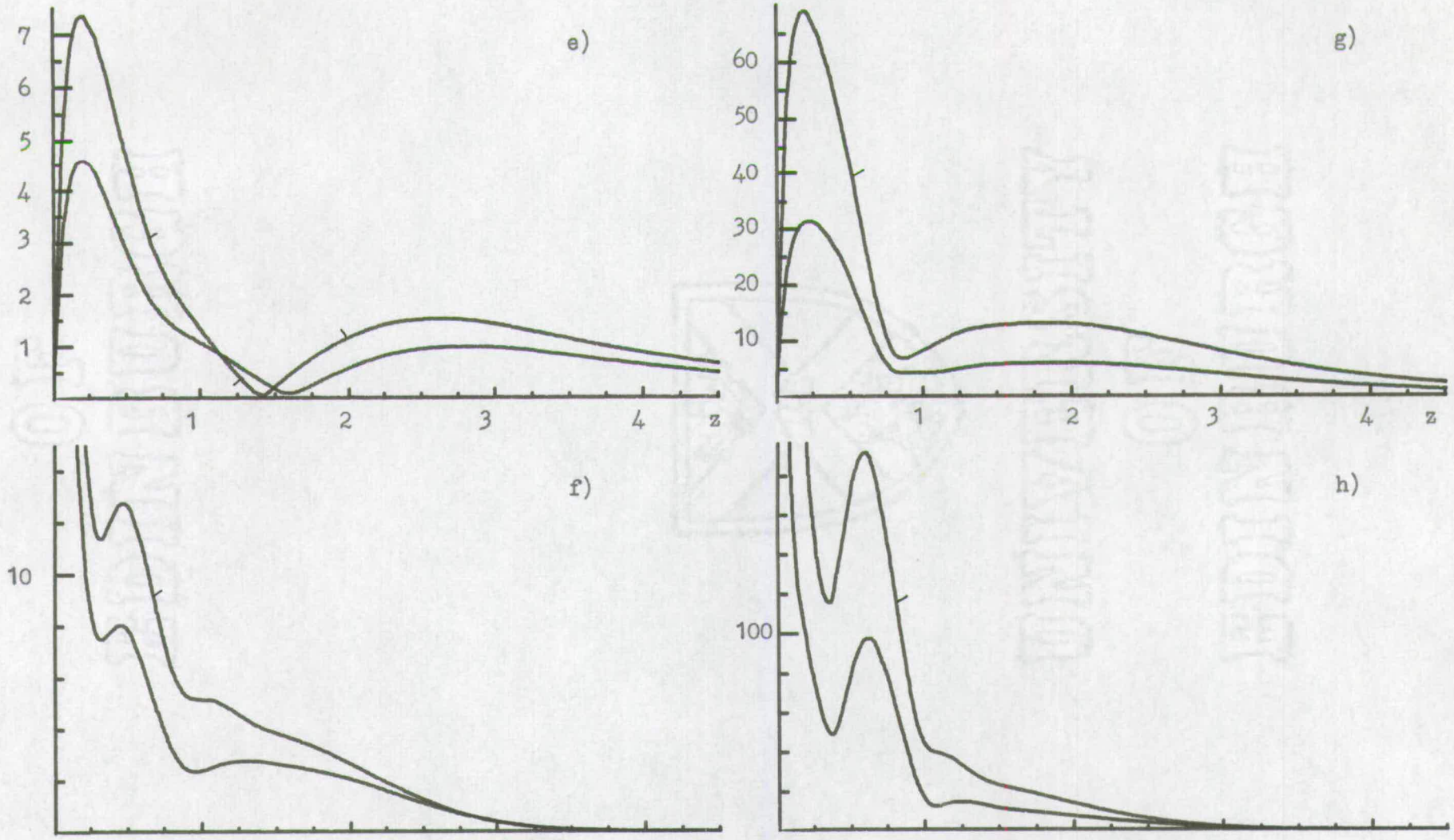

Figure 6.4 Functions at R= 1250, c= .028, graphs e) to h).

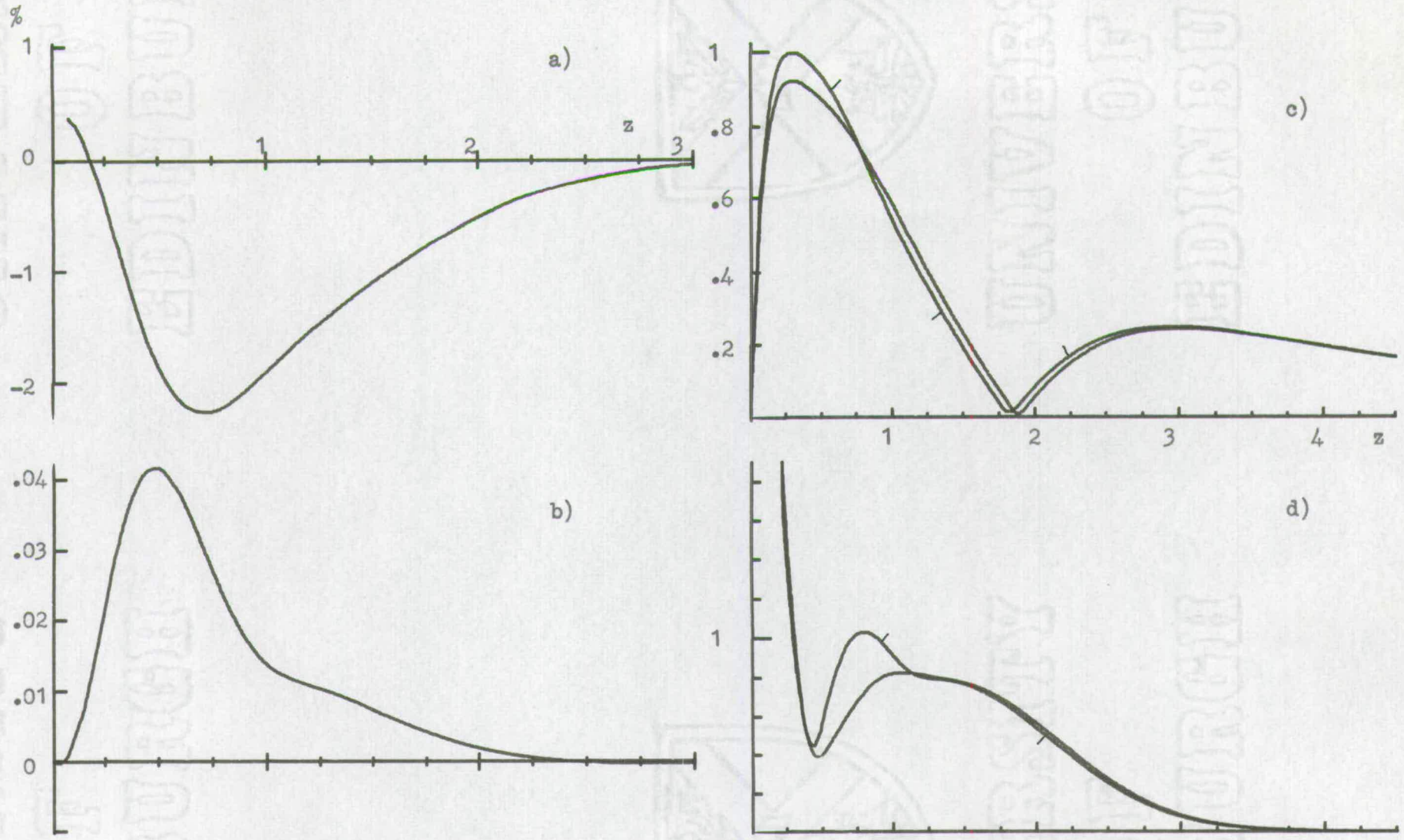

Figure 6.5 Functions at R= 1500, c= .021, graphs a) to d)

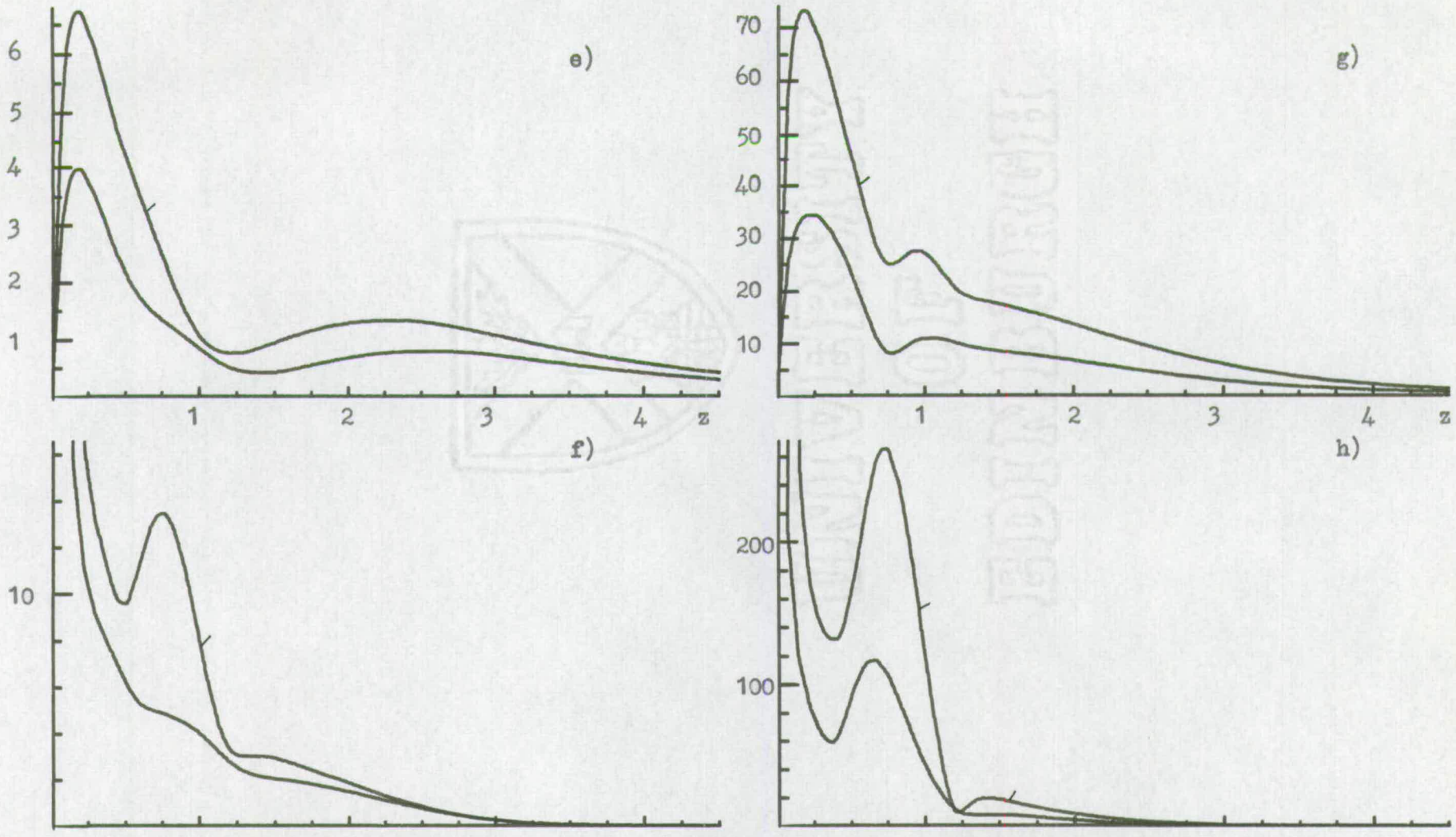

Figure 6.5 Functions at R= 1500, c= .021, graphs e) to h).

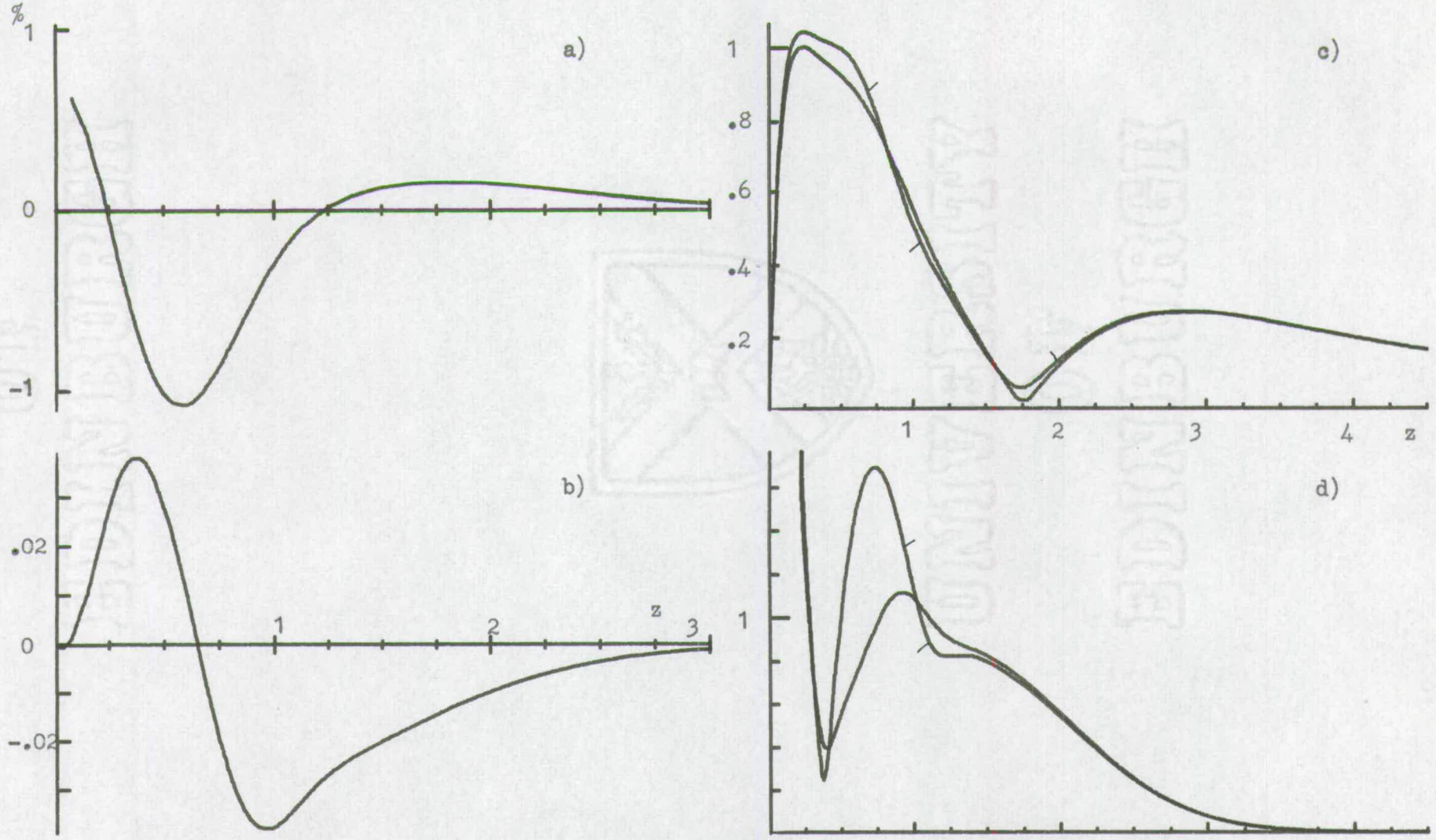

Figure 6.6 Functions at R= 1750, c= .014, graphs a) to d).

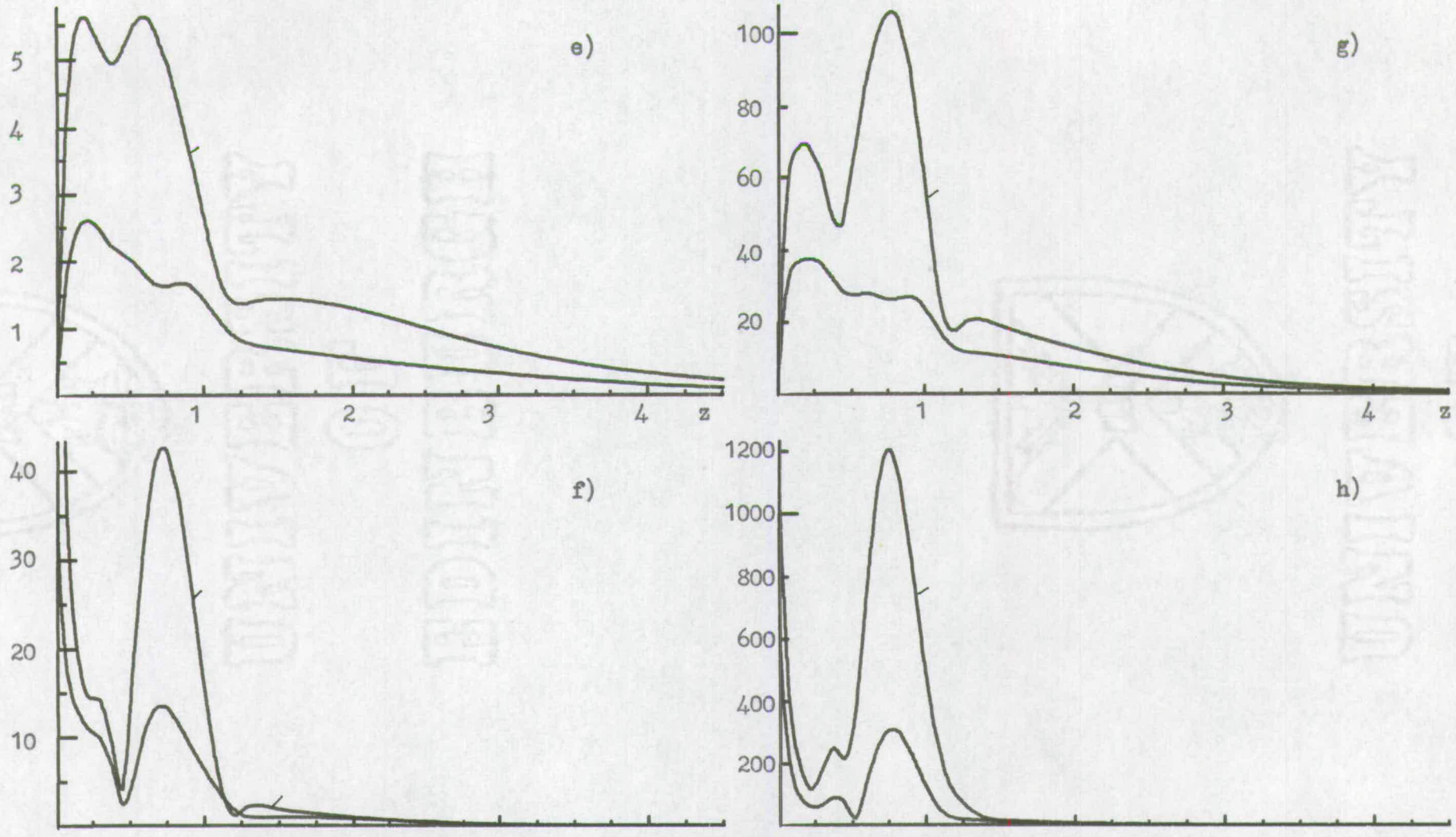

Figure 6.6 Functions at R= 1750, c= .014, graphs e) to h).

The Results at $R = 500$, $F = 80 \times 10^{-6}$

Numerical values derived from the functions in Figure (6.1) are compared with the corresponding values for the linear case and a smaller amplitude in Table (6.6).

$R = 500$ is in the first damping region, and the effect of the perturbation is to increase the amount of damping.

δ is the boundary layer thickness, which is defined to be the distance at which the flow attains 99°/o of its mainstream value.

δ_1^* is the displacement thickness of the perturbed mean flow. It has to be distinguished from δ_1, the displacement thickness of the undistorted Blasius flow used in the non-dimensionalisation.

δ_2 is the momentum thickness of a boundary layer, and is found from $\delta_2 = \int_0^\infty U(1 - U)dz$.

Each of these measures of boundary layer thickness indicates that the boundary layer is reduced in thickness by the perturbation.

The Reynolds stress is everywhere negative, thus energy is taken from the perturbation to increase the mean flow. This causes the boundary layer to appear thinner.

W_∞ is the limiting value of W as $z \longrightarrow \infty$. It is always non-zero, since the boundary layer grows in thickness downstream but it also is reduced by the perturbation.

Z_c is the position of the "critical layer", important in analytical theory. At this point the mean flow has the

TABLE 6.6

Computed values with R = 500, F = 80×10^{-6}

C	0	.028	.056
α_r	0.12297	0.12299	0.12309
α_i	0.01673	0.01707	0.01797
δ	2.8537	2.8014	2.6131
δ_1^*	1	0.9874	0.9453
δ_2	0.3859	0.3798	0.3591
$W_\infty \times 10^3$	2.9611	2.9238	2.7991
Zc	0.5625	0.5568	0.5378
Zn	2.44	2.41	2.31
$\lvert\phi_1'\rvert$max	0.7498	0.7552	0.7740
Z max	0.867	0.868	0.868
$\lvert h_1 \rvert$max	0.6998	0.7206	0.7943
Z max	1.434	1.450	1.483
$\lvert\phi_2'\rvert$max	2.274	2.221	2.101
Z max	0.509	0.507	0.503
$\lvert h_2 \rvert$max	4.044	3.996	3.899
Z max	0.888	0.888	0.888
$\lvert\phi_3'\rvert$max	9.187	8.656	7.445
Z max	0.353	0.351	0.344
$\lvert h_3 \rvert$max	20.48	19.63	17.74
Z max	0.654	0.648	0.634

same value as the wave velocity $C_r = Re(\beta/\alpha)$, and the magnitude of the factor $(\alpha U - \beta)$ has a minimum, which becomes zero when $\alpha_i = 0$. This leads to a singularity in the asymptotic methods of solution.

ϕ_1' always has a minimum of magnitude at which its phase reverses. The position of the phase reversal is tabulated as Z_n. It corresponds to the maximum of ϕ_1, normalised to unity. Since the imaginary part of ϕ_1' is much smaller than the real part,

$$\int_0^{Z_n} |\phi_1'| \, dz \simeq 1 .$$

When Z_n moves inwards, as is the case at this Reynolds number, the maximum value of $|\phi_1'|$ has to rise to maintain the integral constant. This maximum value and its position Z_{max} are tabulated.

The magnitude of the vorticity, h_1, has a large value on the plate, not shown in the figure. Away from the plate it first falls steeply to a minimum, at which it undergoes a phase change, then rises to a maximum. The value and position of this maximum has been tabulated.

The functions $|\phi_n'|$ and $|h_n|$ for the second and third harmonics have a more complex shape, with an additional maximum. Details of the largest maximum only are tabulated in each case. Its magnitude is slightly diminished by the perturbation.

The Results at R = 1000, F = 80×10^{-6}.

Table (6.7) is arranged as for Table (6.6). Numerical values derived from the functions in Figure (6.3) are compared with those obtained for other amplitudes.

At this position, the linear perturbation is amplified, but the effect of the non-linearity is to reduce the amount of amplification.

Each of the measures of boundary layer thickness indicates an increase caused by the perturbation. The Reynolds stress is almost entirely positive, meaning that over most of the boundary layer, energy is fed to the perturbation from the mean flow. As a consequence, the mean flow is reduced, and the boundary layer becomes thicker.

The energy fed into the perturbation pushes out the position of the phase change of ϕ_1', and therefore the maximum of $|\phi_1'|$ is slightly reduced.

The small reduction of $|\phi_1'|$ is insufficient to explain the much larger reduction in the harmonics, which are substantially reduced by the perturbation. The secondary peak of $|\phi_2'|$ and $|\phi_3'|$ observed in Figure (6.1) is lacking, although the inflexion seen in $|\phi_2'|$ may be a residual effect.

The Results at R = 1750, F = 80×10^{-6}

The properties at this position, found from Figure (6.6) and compared in Table (6.8) with those at different amplitudes, are more complex than those previously described.

TABLE 6.7

Computed values with R = 1000, F = 80 x 10^{-6}

C	0	.014	.028
α_r	0.23046	0.22883	0.22461
$\alpha_i x10^3$	-6.60	-6.08	-5.16
δ	2.8537	2.8599	2.8716
δ_1^*	1	1.0040	1.0140
δ_2	0.3859	0.3875	0.3912
$W_\infty x10^3$	1.4806	1.4865	1.5012
Z_c	0.6120	0.6189	0.6371
Zn	2.11	2.12	2.17
$\lvert\phi_1'\rvert$max	0.7929	0.7819	0.7543
Z max	0.624	0.639	0.677
$\lvert h_1\rvert$max	0.7150	0.7104	0.7007
Z max	1.298	1.346	1.446
$\lvert\phi_2'\rvert$max	8.052	7.511	6.196
Z max	0.263	0.263	0.264
$\lvert h_2\rvert$max	12.61	11.71	9.556
Z max	0.560	0.559	0.557
$\lvert\phi_3'\rvert$max	77.48	66.94	44.87
Z max	0.214	0.215	0.220
$\lvert h_3\rvert$max	157.4	137.0	95.04
Z max	0.575	0.586	0.618

The linear perturbation is in the second damping region, but the non-linear effects much reduce the damping, so much so that it appears possible that with sufficient amplitude, instability could be found. By extrapolation, the amplitude at which instability may begin was estimated to be $c = .023$, but since the value of $\frac{K_r}{C_g}$ decreases with increasing amplitude, it is possible that the amplitude required may be higher still. Since the iteration at $c = .014$ was difficult to converge, no attempt was made to solve for a higher amplitude.

The changes in the mean flow appear to be quite complicated An increasing amplitude of perturbation causes δ and δ_2 to decrease, but δ_1^* first falls then rises, and, since the fall in δ_2 when c increases from .007 to .014 is much smaller than that from $c = 0$ to $c = .007$, it seems that δ_2 may also have reached a minimum.

The key to this behaviour lies in the mean flow distortion and the Reynolds stress. These are shown for different amplitudes in Figure (6.7). The mean flow distortion has a positive and a negative peak. The negative peak grows with increasing perturbation size, whereas the positive peak is actually reduced. The Reynolds stress also has two peaks, a positive one close to the plate, and a very pronounced negative peak further out. The negative peak is reduced by the perturbation, but since this is a normalised function, to obtain the physical Reynolds stress, the factor c^2 must be included. When this is done, as shown in Figure (6.8),

TABLE 6.8

Computed values with R = 1750, F = 80×10^{-6}

c	0	.007	.014
α_r	0.38444	0.38355	0.37885
$\alpha_i \times 10^2$	2.631	1.718	0.774
δ	2.8537	2.8462	2.8426
δ_1^*	1	0.9983	1.0005
δ_2	0.3859	0.3846	0.3843
$W_\infty \times 10^3$	0.8460	0.8446	0.8465
Zc	0.6403	0.6450	0.6598
Zn	1.736	1.735	1.753
$\lvert\phi_1'\rvert$max	1.042	1.034	1.002
Z max	0.248	0.246	0.245
$\lvert h_1 \rvert$max	1.691	1.378	1.114
Z max	0.733	0.796	0.917
$\lvert\phi_2'\rvert$max	5.577 and 5.619	4.154and3.588	2.611 and 1.671
Z max	0.206 and 0.593	0.202and 0.538	0.215 and 0.833
$\lvert h_2 \rvert$max	42.61	26.25	13.61
Z max	0.726	0.723	0.711
$\lvert\phi_3'\rvert$max	69.8 and 105.6	54.02 and 59.47	37.66
Z max	0.190 and 0.780	0.199 and 0.810	0.207
$\lvert h_3 \rvert$max	1204	671.7	309.1
Z max	0.753	0.760	0.773

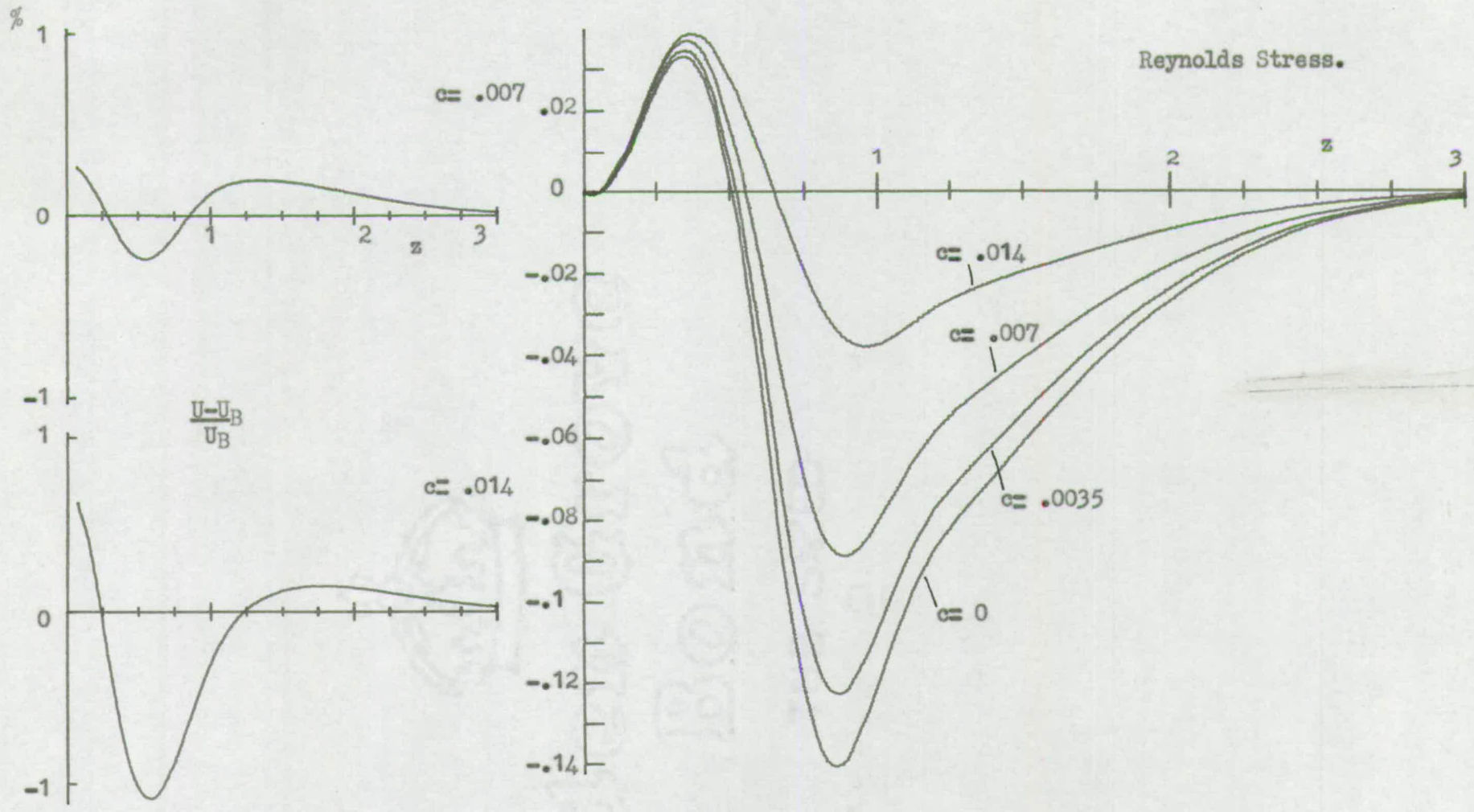

Figure 6.7 Mean flow distortion and Reynolds stress at different amplitudes, R= 1750.

Figure 6.8
Reynolds Stress,
Actual value,
R= 1750.

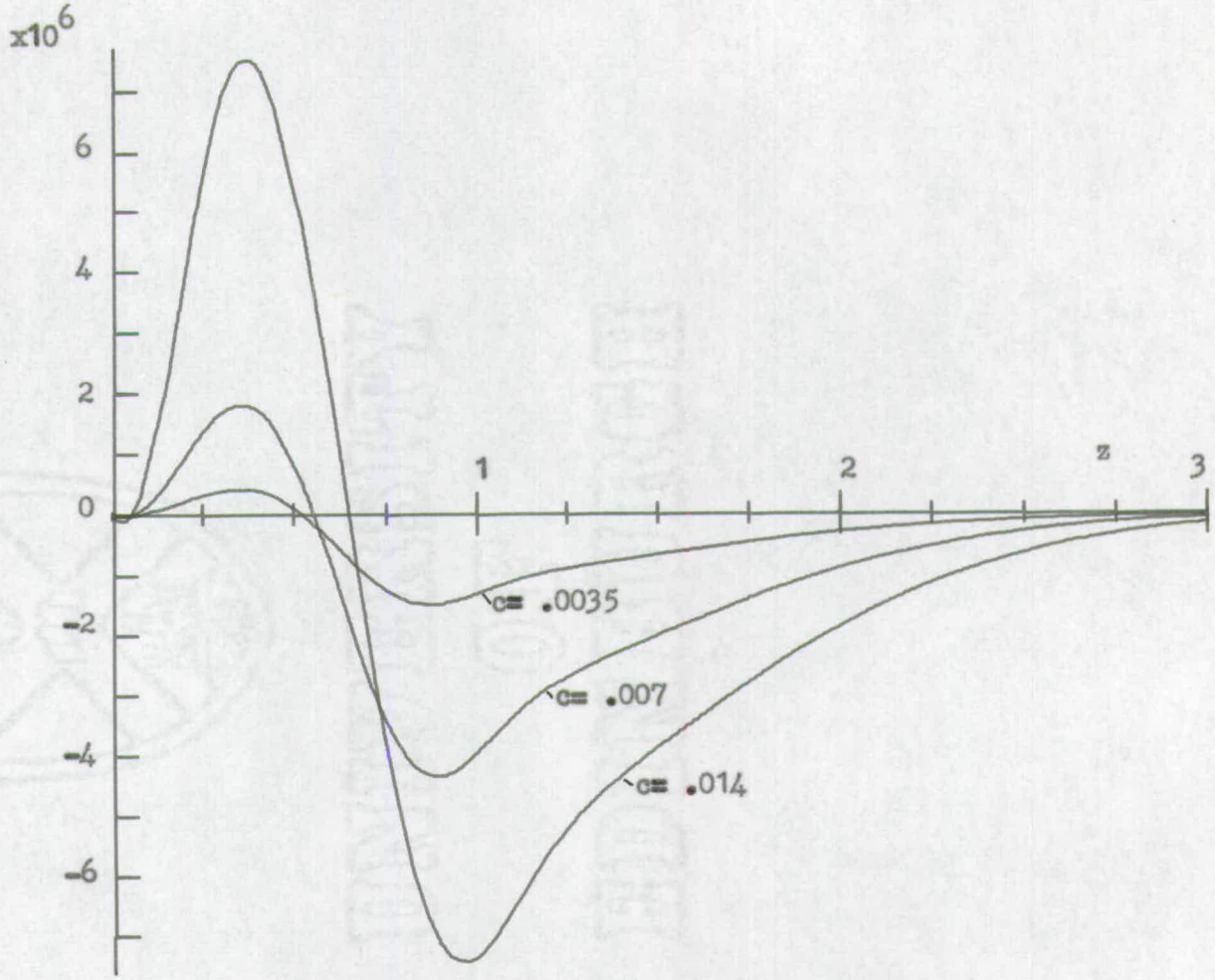

an increase in c from .007 to .014 doubles the negative peak, but the positive peak is increased by over fourfold.

It is this change of shape which causes the complicated behaviour. δ is found only from the boundary layer at its outer edge, whereas δ_1^* and δ_2 are found from an integration over the boundary layer. For δ_1^*, the boundary layer integration is evenly weighted, but for δ_2, more emphasis is given to the outer parts than to the region close to the plate.

An indication of what might happen to the Reynolds stress if it could be computed at still higher amplitudes is given in Figure (6.9), which is in fact the computed Reynolds stress at R = 1500. The linear perturbation and c = .007 are damped, but for c = .014 and .021, the perturbation is amplified. The damped solutions show traces of the large negative peak found with R = 1750, but the amplified solutions have the opposite sign at this position. The normalised positive peak is slightly larger than for R = 1750, being largest for c = .007, then moving outwards and decreasing at larger amplitudes.

The fundamental is also affected by these variations. At a low amplitude, the nett effect over the range $0 < Z < Z_n$ is a loss of energy to the mean flow. As the amplitude increases, the net effect changes towards a gain of energy. The gains and losses of energy which are present in this region cause a change in shape of the fundamental peak. The fundamental of the linear perturbation has a broader peak, and a sharper fall to the minimum value than

Figure 6.9

Reynolds Stress,
R= 1500.

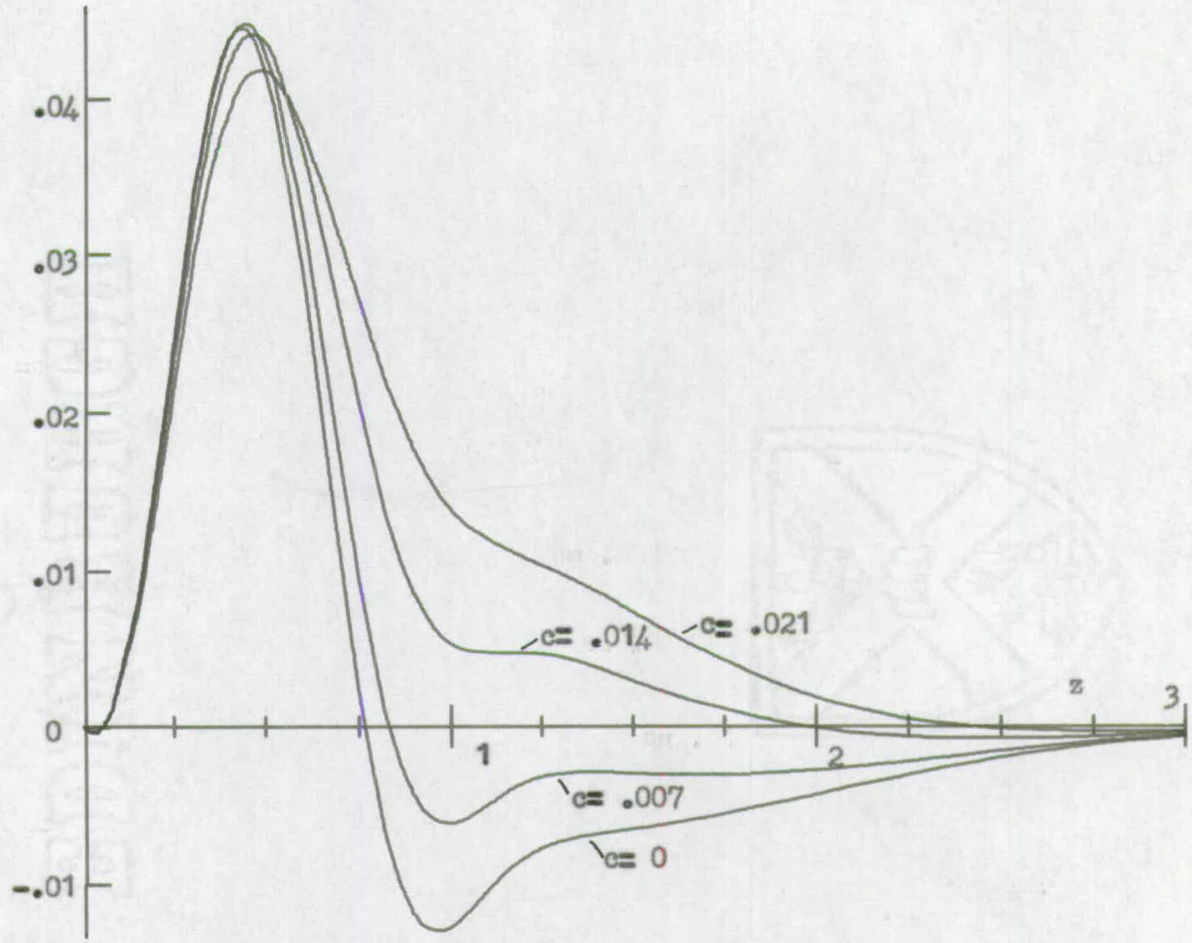

the distorted fundamental.

Both the second and third harmonics have two main peaks in the linear case, but the outer peak is strikingly reduced by the non-linear effects, almost to the extent of obliteration in the case of $c = .014$.

The vorticity peak occurs close to the position of the critical layer for each of the fundamental, second and third harmonics, and is very pronounced in the linear case.

The Relative Importance of the Non-linear Interactions

Two non-linear interactions cause changes to the eigenvalue α and the fundamental ϕ_1. One is the mean flow distortion, and the other the interaction between the first and second harmonics. Since a simultaneous solution has been found, these effects are not independent; for instance, the mean flow distortion will also modify the second harmonic.

An indication of the relative importance of these effects may be obtained by ignoring one of them. The non-linear calculations of Barry (1970) included only the mean flow distortion, obtaining a simultaneous solution of (2.20) and (2.24). To find the effect of the second harmonic interaction alone, a simultaneous solution of (2.21) and (2.22) was made. The results are given in Table (6.9). Δ_{MF} is the change in α_i caused by the mean flow distortion only, Δ_{2H} from the second harmonic interaction only, and Δ_T for both effects simultaneously.

The two effects differ in behaviour. The mean flow distortion appears to have a moderating effect. It changes α_i

TABLE 6.9

Comparison of Non-Linear Effects

R	$c \times 10^2$	$\alpha_i(0) \times 10^2$	$\Delta_{MF} \times 10^7$	$\Delta_{H2} \times 10^7$	$(\Delta_{MF}+\Delta_{H2}) \times 10^7$	$\Delta_T \times 10^7$
500	2.8	1.67342	- 800	4560	3760	3344
800	2.8	0.06923	-2173	19892	17719	13645
1000	1.4	-0.66047	1601	4461	6062	5214
1250	1.4	-0.80589	2874	-4886	-2012	-1124
1500	0.7	0.22218	-11623	-5018	-16641	-15594
1750	0.35	2.63145	-31686	1312	-30374	-31107
1750	1.4	2.63145	-182587	-9364	-191951	-185795

in such a way as to oppose the effect of the linear perturbation, by reducing the amplification or damping. One case, at $R = 1500$, is known at which the effect overshoots, and a stable perturbation becomes unstable.

The second harmonic interaction has a stabilising effect with $R < 1250$, and seems to be destabilising with $R \geqslant 1250$, although at $R = 1750$, the only Reynolds number at which two different amplitudes were used, there is a stabilising effect at small amplitudes. It may also vary in effect with amplitude at other Reynolds numbers, although this has not been tested, and this would explain the behaviour with amplitude at $R = 1250$.

Taking the two effects together, the larger is the second harmonic interaction with $R \leqslant 1250$, but for $R > 1250$, the mean flow distortion effect becomes very large, and obscures the effect of the second harmonic.

The difference between $\Delta_{MF} + \Delta_{2H}$ and Δ_T is quite small in each case, and its sign is consistent with a reduction of the second harmonic interaction.

Downstream Integration

It will be recalled that at each occurrence of the amplitude factor c in the non-linear equations (2.20) and (2.21), there also occurred a factor $e^{-\alpha_i x}$. This factor has been omitted, since each calculation hitherto has been made at a fixed x position. The factor indicates that c is not fixed, but varies with x position. x is a local variable used to remove the x-dependence of the

equations.

Since α_i varies with R and c, an integral is necessary:

$$\log \frac{c}{C_o} = \int_{R_o}^{R} -\alpha_i(R, c)dx$$

where C_o is the amplitude at $R = R_o$.

α_i has been calculated assuming constant R, and it must first be converted into its dimensional form. Then, by changing the integration parameter from dimensional x to R, the result

$$\log \frac{c}{C_o} = -\frac{2}{k^2} \int_{R_o}^{R} \alpha_i(R, c)dR$$

is obtained.

In order to minimise the length of the computation, an approximate form of integration was used:

$$\log (c(R+\Delta R)) = \log(c(R)) - \frac{2}{k^2} \alpha_i(R, c(R))\Delta R \ . \qquad (6.1)$$

Accurate results were not intended, but it was hoped that the general form of the downstream growth would be obtained.

Two integrations were made, both commencing from R = 1000, and using a steplength $\Delta R = 50$. The first had an initial value for c of 0.001, and the second 0.002. Table (6.10) shows the result of this integration, and for comparison, the corresponding values for the downstream growth for the linear case obtained using (6.1), Figure (6.10) is a graph of $\log \frac{c}{C_o}$.

TABLE 6.10

Amplitudes on integration

R	$Cx10^2$	$Cx10^2$	Linear case (relative values)
1000	0.1	0.2	1
1050	0.12498	0.24987	1.2499
1100	0.16190	0.32356	1.6194
1150	0.21478	0.42899	2.1487
1200	0.28799	0.57482	2.8818
1250	0,38494	0.76801	3.8525
1300	0.50563	1.01020	5.0575
1350	0.64362	1.29485	6.4178
1400	0.78405	1.60858	7.7410
1450	0.90524	1.93633	8.7190
1500	0.98334	2.26511	9.0003
1550	0.99732	2.58421	8.3497
1600	0.93236	2.88375	6.8223
1650	0.78460		4.8108
1700	0.57019		2.8719
1750	0.33649		1.4286
1800	0.15262		0.5874
1850	0.05383		0.2010
1900	0.01583		0.0588

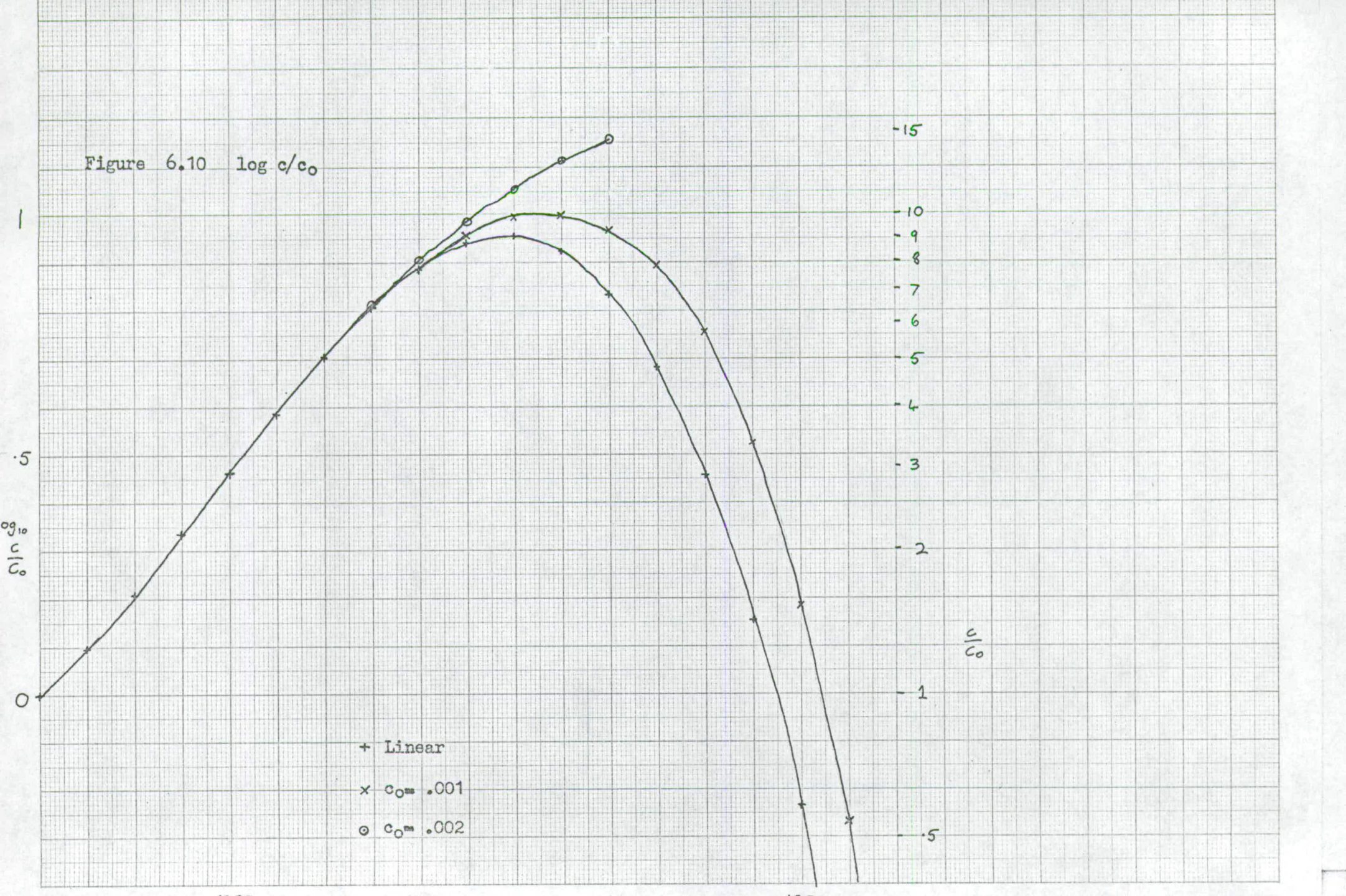
Figure 6.10 log c/c₀
1
.5
0
log c/c₀
15
10
9
8
7
6
5
4
3
2
1
.5
c/c₀
+ Linear
× c₀= .001
⊙ c₀= .002

The second integration was terminated when the iteration failed to converge. The iteration appeared to be diverging faster than the Δ^2 correction could contain.

From Figure (6.10) it can be seen that the effect of a small perturbation is to displace the maximum of amplitude downstream. The full effect of a larger perturbation can only be estimated, since the second integration was still growing when the solution method failed. It may continue to grow without limit if the amplitude is sufficient at each position to transform the stable linear perturbation into instability. The minimum amplitude required for this is about $1^{o}/o$ at $R = 1500$, and has been estimated to be about $2{,}3^{o}/o$ at $R = 1750$. It probably rises further at still larger values of R. Sustained growth may only occur if the amplitude is sufficiently above the minimum to supply enough amplification to maintain the amplitude sufficiently above the minimum at downstream positions. Whether this occurs or not cannot be found from the present investigation because of the failure of the iteration to converge.

An attempt was made to establish the error involved in the integration. In general, if $\frac{\partial \alpha_i}{\partial R} < 0$, the true solution will be greater than that found, and vice versa. It was estimated that a correction of $2.5^{o}/o$ should be added to each integration at $R = 1250$, and at $R = 1500$, the first integration was estimated to be $10^{o}/o$ too large, and the second $5^{o}/o$ too large.

CHAPTER 7

THE SPECTRUM OF EIGENVALUES

Determination of Eigenvalues

At an eigenvalue α of the matrix equation $M(\alpha)\underline{g} = 0$, the determinant of the matrix M is zero. To find the number of zeros of the determinant inside a closed contour C in the complex α plane, the principle of the argument method may be used.

Complex variable theory proves that for a function $f(z)$ analytic on and inside the contour C in the z-plane,

$$\frac{1}{2\pi i} \oint_C \frac{f'(z)}{f(z)}\, dz = \frac{1}{2\pi}\Big[\arg f(z)\Big]_C = N - P,$$

where N is the number of zeros and P the number of poles of f enclosed by C.

In any finite region of the α plane $\det M(\alpha)$ cannot become infinite, thus only zeros are possible. The number of zeros is found from the change in argument of $\det M(\alpha)$ after traversing the contour anticlockwise.

A rectangular contour was chosen, and arg det $M(\alpha)$ was evaluated along the contour at intervals small enough to ensure that the change in argument between successive points was less than π.

A development of this method was obtained from the late Dr. G.M. Thomas. A procedure was used which systematically subdivided the contour until it had located each zero to within a specified accuracy. This produced a good first approximation to α for use in the iterative procedure.

Modification of the Outer Boundary Condition

When dealing with the unstable mode, one term of the asymptotic outer boundary condition was ignored since it became so quickly negligible. In the area to be searched, however, the rate of decay of both terms could be of similar magnitude, and the boundary condition should take the form

$$\phi = Ae^{-\alpha z} + Be^{-\gamma z} \quad \text{x} \qquad (7.1)$$

In applying this boundary condition to the discretised matrix, it was assumed that the components $g_{(n-1)}$, $g_{(n)}$, $g_{(n+1)}$, $g_{(n+2)}$, $g_{(n+3)}$ fitted the boundary condition, i.e.

$$g_{(n+s)} = A\,e^{-sh\alpha} + B\,e^{-sh\gamma}, \quad s = -1,0,1,2,3 \ .$$

A and B can be found in terms of $g_{(n-1)}$ and $g_{(n)}$, and then substituted into the expressions for $g_{(n+1)}$, $g_{(n+2)}$, $g_{(n+3)}$ to give

$$\begin{aligned}
g_{(n+1)} &= (e^{-h\alpha} + e^{-h\gamma})g_{(n)} - e^{-h(\alpha+\gamma)}\,g_{(n-1)} \\
g_{(n+2)} &= (e^{-2h\alpha} + e^{-h(\alpha+\gamma)} + e^{-2h\gamma})g_{(n)} \\
&\quad - e^{-h(\alpha+\gamma)}(e^{-h\alpha} + e^{-h\gamma})g_{(n-1)} \qquad (7.2) \\
g_{(n+3)} &= (e^{-3h\alpha} + e^{-h(2\alpha+\gamma)} + e^{-h(\alpha+2\gamma)} + e^{-3h\gamma})g_{(n)} \\
&\quad - e^{-h(\alpha+\gamma)}(e^{-2h\alpha} + e^{-h(\alpha+\gamma)} + e^{-2h\gamma})g_{(n-1)}
\end{aligned}$$

---

x For the special case $\alpha = \gamma$, a different exponential form

$$\phi = Ae^{-\alpha z} + Bze^{-\alpha z}$$

is necessary, but (7.2) is also derived in this case.

In the case of the standard Orr-Sommerfeld equation

$$\gamma = (\alpha^2 + iR(\alpha - \beta))^{\frac{1}{2}} ,$$

and for the extended form

$$\gamma = \mu - \tfrac{1}{2}R\, W_\infty$$

where $$\mu = ((\tfrac{1}{2}R\, W_\infty)^2 + \alpha^2 + iR(\alpha-\beta))^{\frac{1}{2}} .$$

Since there is a square root in the definition of γ, for each value of α there are two possible values of γ. In order to preserve a one to one relationship between α and γ, complex variable theory considers the α plane to consist of two sheets. If α is on sheet I, it transforms to γ using the square root of positive real part, and if on sheet II, the other square root is used. At two values of α the square root is zero, and these are called branch points. A line, along which the real part of the square root is zero, connects these branch points and is called a branch line. If α crosses this branch line, it passes from one sheet to the other. Care must be taken when a contour integration is made, since a closed path must cross the branch line an even number of times, and, in particular, a single circuit of a branch point is not a closed path.

In the case of the standard Orr-Sommerfeld equation, the branch points occur at $\gamma = 0$, i.e. at approximately

$$\alpha = \beta - \frac{2\beta^3}{R^2} + \frac{i\beta^2}{R} \quad \text{and} \quad \alpha = -\beta - i(R + \frac{\beta^2}{R}) .$$

The branch line is the locus of $\gamma_i = 0$ with $\gamma_r < 0$, i.e.

$$\alpha_r = R\beta/(2\alpha_i + R)$$

with $\alpha_i > \frac{\beta^2}{R}$ or $\alpha_i < -(R + \frac{\beta^2}{R})$.

When $\alpha_i \ll R$ the locus is approximately $\alpha_r = \beta$.

In the extended case, the only difference is a small change in the position of the branch points, found at $\mu = 0$.

Only part of this double plane is physically meaningful. To have physical meaning, the real part of γ must be greater than zero. This occurs over the entire sheet I of the α plane in the standard Orr-Sommerfeld case, but for the extended case, since $W_\infty > 0$, there is a region of sheet I in which $\mu_r < \frac{1}{2}RW_\infty$, and hence any solution in this region is not physically meaningful.

Results

The positions of some of the eigenvalues found are plotted in Figures (7.1) and (7.2). Figure (7.1) compares different step-lengths, and also the standard and extended form of the equation. Figure (7.2) shows the results at a different Reynolds number for the standard form of the equation and one step-length only, but over a larger area of the α plane. The unstable mode is in this case slightly stable, and is shown on the figure at $\alpha = .341 + .002i$.

The dominant feature of both figures is the long line of eigenvalues with real part α_r slightly greater than β, and α_i positive. This line is moved by a change in step-length, tending to move with decreasing step-length across the branch

gure 7.1 Eigenvalues at R= 1000.

.075 ×
.05 ⊙
.0375 +

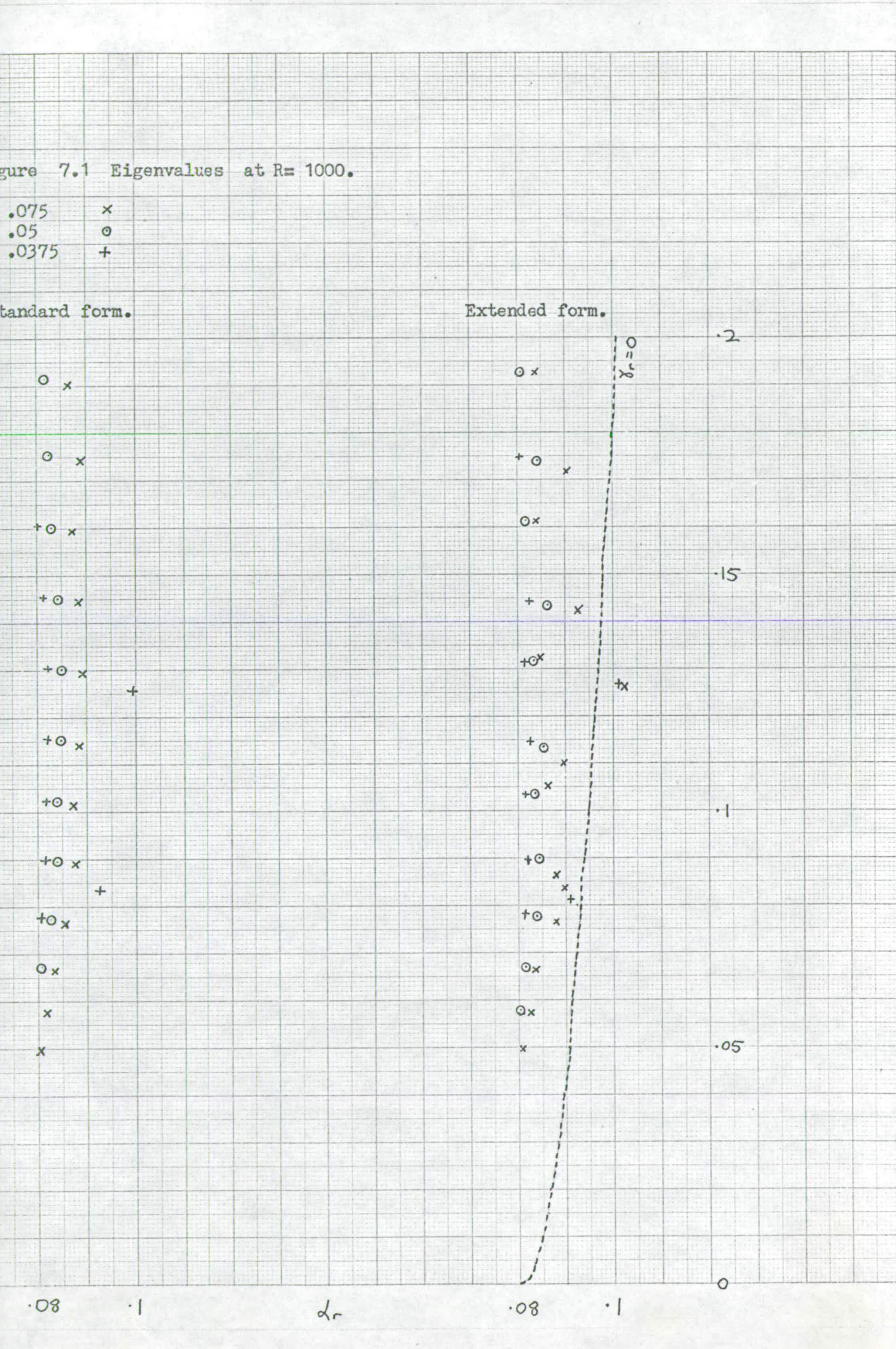

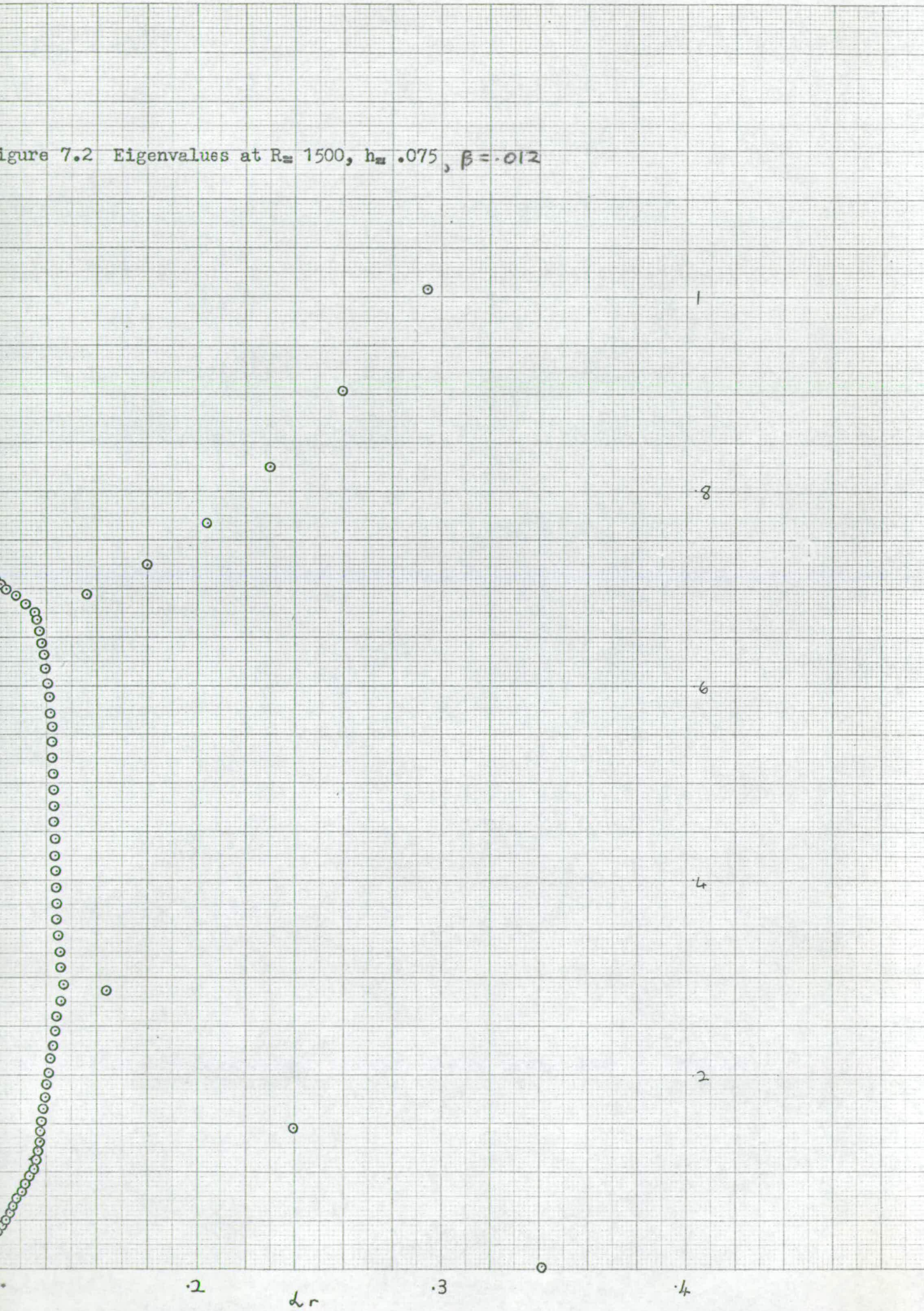

igure 7.2 Eigenvalues at R= 1500, h= .075, β = .012

line located approximately along the line $\alpha_r = \beta$.

Table (7.1) shows the effect of step-length on a single eigenvalue. α_i seems to be tending to some limit value, but it is not obvious whether α_r is tending to a limit or not. Similar behaviour was found for other eigenvalues. This seems to indicate that the line of eigenvalues is a property of the matrix representation, rather than the equation itself. If a limit value does exist, it will be physically unreal.

In each case two exceptions were found. These appear to be quite stable to step-length variation, and tend to a limit which is physically meaningful. It seems probable that these are solutions of the equation itself.

Figure (7.2) shows another feature. At large α_i the line of eigenvalues splits into two sections. It was found that this effect is highly sensitive to step-length variation, the effect of a smaller step-length being to raise the value of α_i at which the split occurs. At these large values of α_i the eigenvector is highly oscillatory, and it was thought that at this stage the discretisation is no longer a good representation of the differential equation. In order to make a rigorous investigation at these high α_i values, a step-length small enough to allow a satisfactory representation of the equation would have to be used.

The positions of the two modes stable to step-length variation were found along lines of constant F. By calculating

TABLE 7.1

Eigenvalues at different step-lengths, $R = 1000$, $\beta = .08$, extended form of equation.

Number of Points	Step-length	α_r	α_i
80	.075	.084774	.132370
120	.05	.083307	.131797
160	.0375	.081344	.131278
200	.03	.079551	.131021
240	.025	.077997	.130879
320	.01875	.075462	.130720
400	.015	.073462	.130619
480	.0125	.071823	.130536

$$\left[\frac{\partial \alpha}{\partial R}\right]_F = \left[\frac{\partial \alpha}{\partial R}\right]_\beta + F\left[\frac{\partial \alpha}{\partial \beta}\right]_R$$

at a value of R at which the solution is known, an approximation to the eigenvalue at $R + \Delta R$ with constant F can be obtained. Provided the interval ΔR is not too large, this approximation is a good starting value for an iteration.

Table (7.2) shows the calculated eigenvalues over the range of Reynolds number from 1000 to 1500 with $F = 80 \times 10^{-6}$, using the standard form of the equation. Figure (7.3) shows α_r and α_i for one mode plotted against R.

The shape of the eigenvector and its derivative is shown in figures (7.4) to (7.9) for several Reynolds numbers.

From Figure (7.3), it can be seen that both α_r and α_i increase with R, but that the rate of increase of α_i diminishes at larger R, whilst the rate of increase of α_r increases. Also, α_r increases at a faster rate than β. This suggests the question of what happens at lower R? It might be expected that α_r will become less than β, and so the mode would become physically unreal.

In fact, it was found that for R less than 1000, the position of the eigenvalue becomes step-length dependent, and only with a short step-length does the solution become physically unreal. Figure (7.10) shows this for R between 900 and 1000.

At this range of R, the eigenvalue of the mode is very close to the line of eigenvalues, and it seems possible that the position of the eigenvalue of the mode is modified by the step-length dependent factors which create the line of eigenvalues.

TABLE 7.2

Eigenvalues at $F = 80\times10^{-6}$, standard form of equation.

Reynolds Number	Mode 1		Mode 2	
	α_r	α_i	α_r	α_i
1000	.092690	.083280	.099548	.125715
1050	.104640	.090556	.104671	.138349
1100	.117338	.097334	.109709	.151357
1150	.130528	.103799	.115416	.165916
1200	.144196	.110071	.121137	.180790
1250	.158382	.116210	.127868	.196830
1300	.173146	.122243	.134399	.213854
1350	.188553	.128172	.141036	.231163
1400	.204672	.133989	.148271	.248927
1450	.221580	.139681	.155957	.267450
1500	.239369	.145235	.163965	.286661

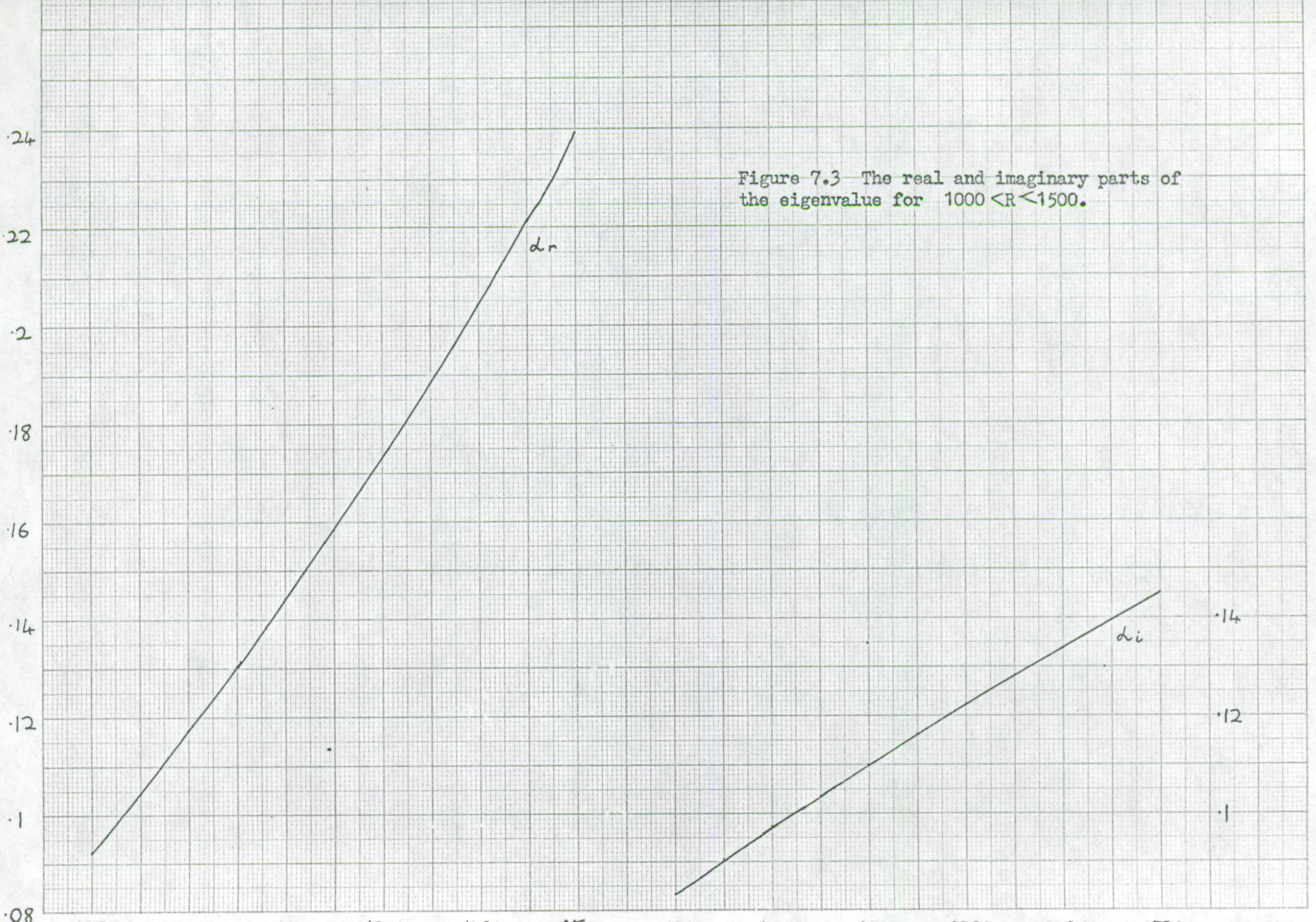

Figure 7.3 The real and imaginary parts of the eigenvalue for $1000 < R < 1500$.

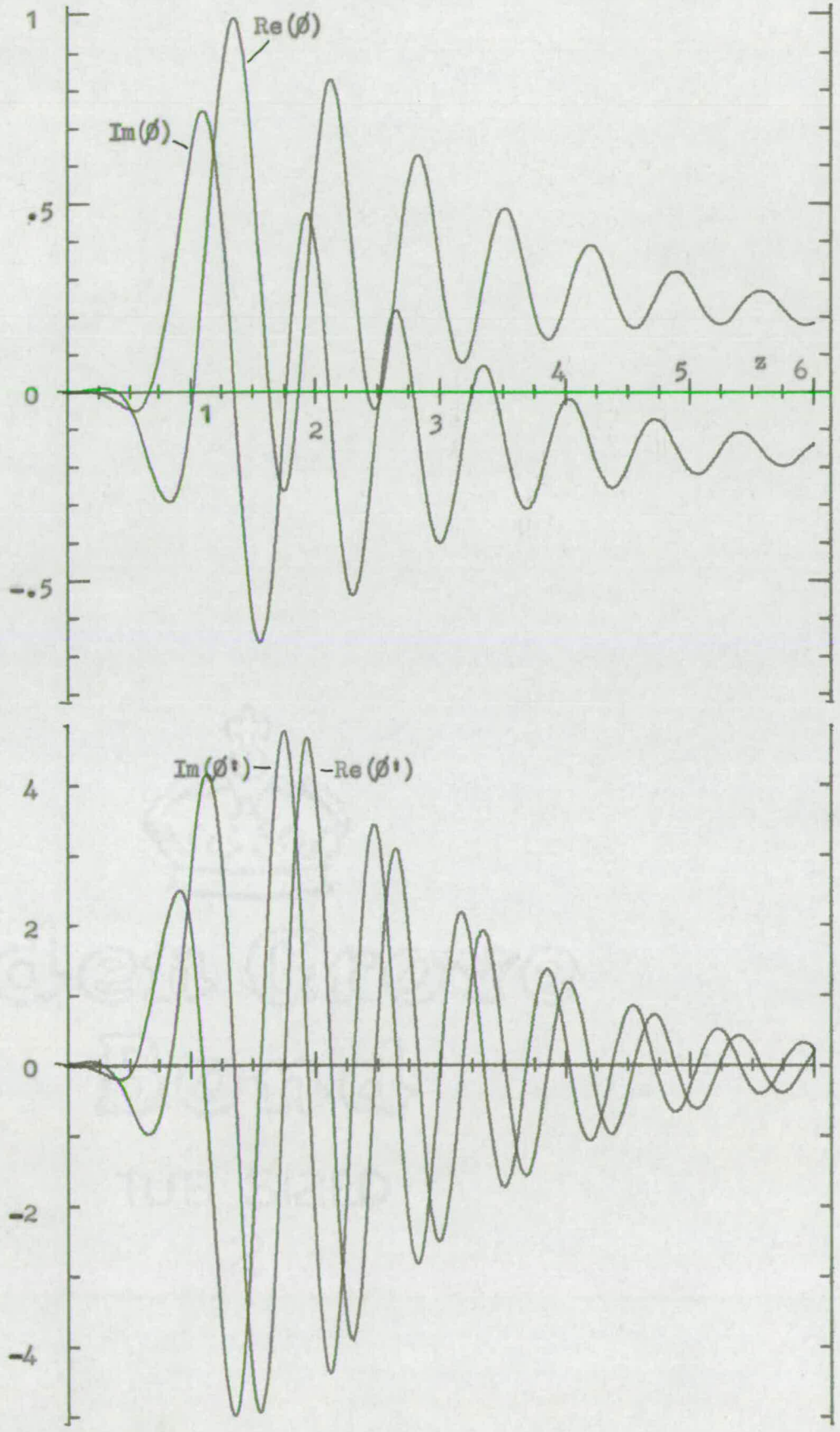

Figure 7.4 Eigenvector, standard form of equation, R= 1000, α = .092690 + .083280i.

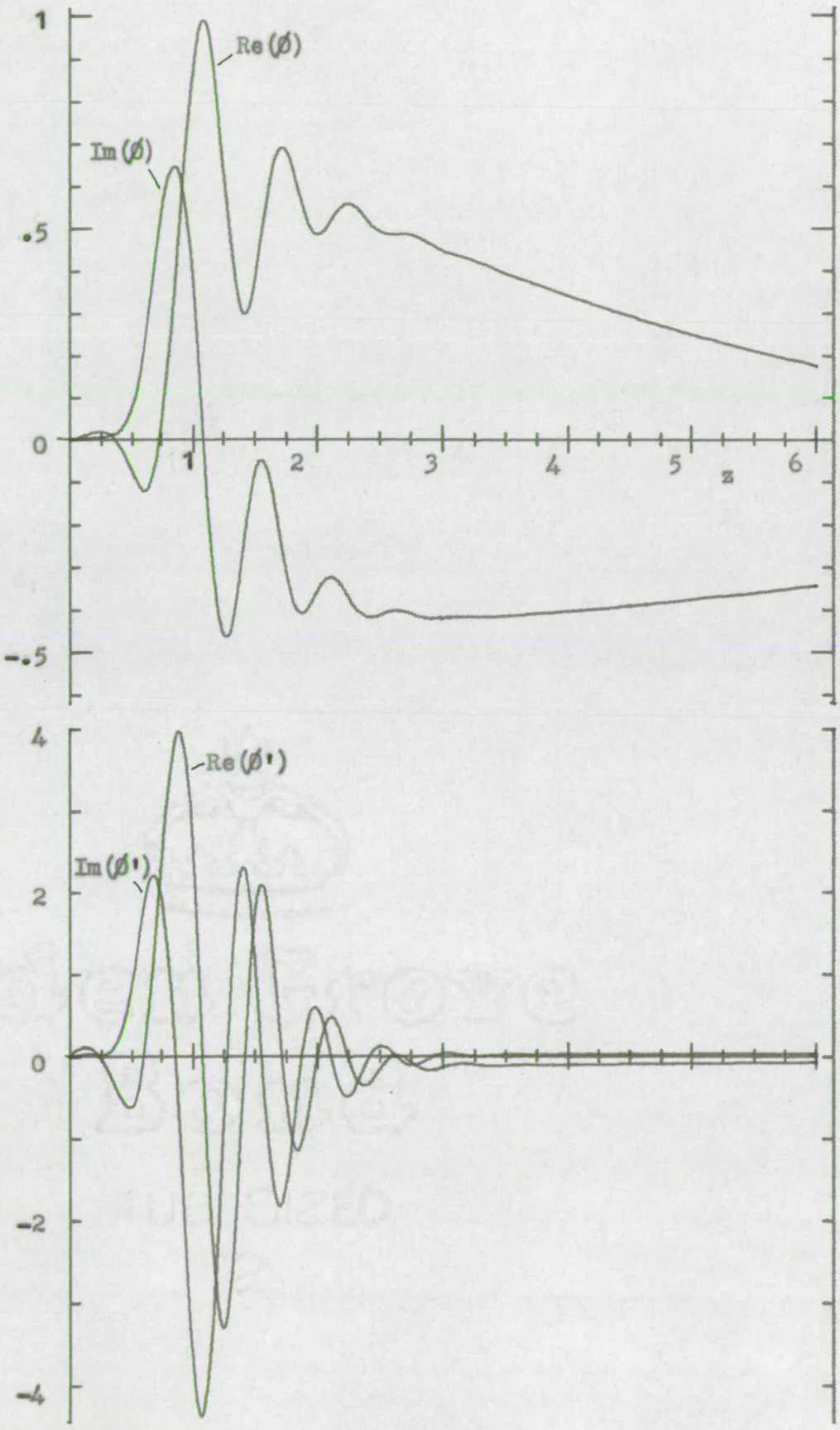

Figure 7.5 Eigenvector, standard form of equation, R= 1250, α = .158382 + .116210i.

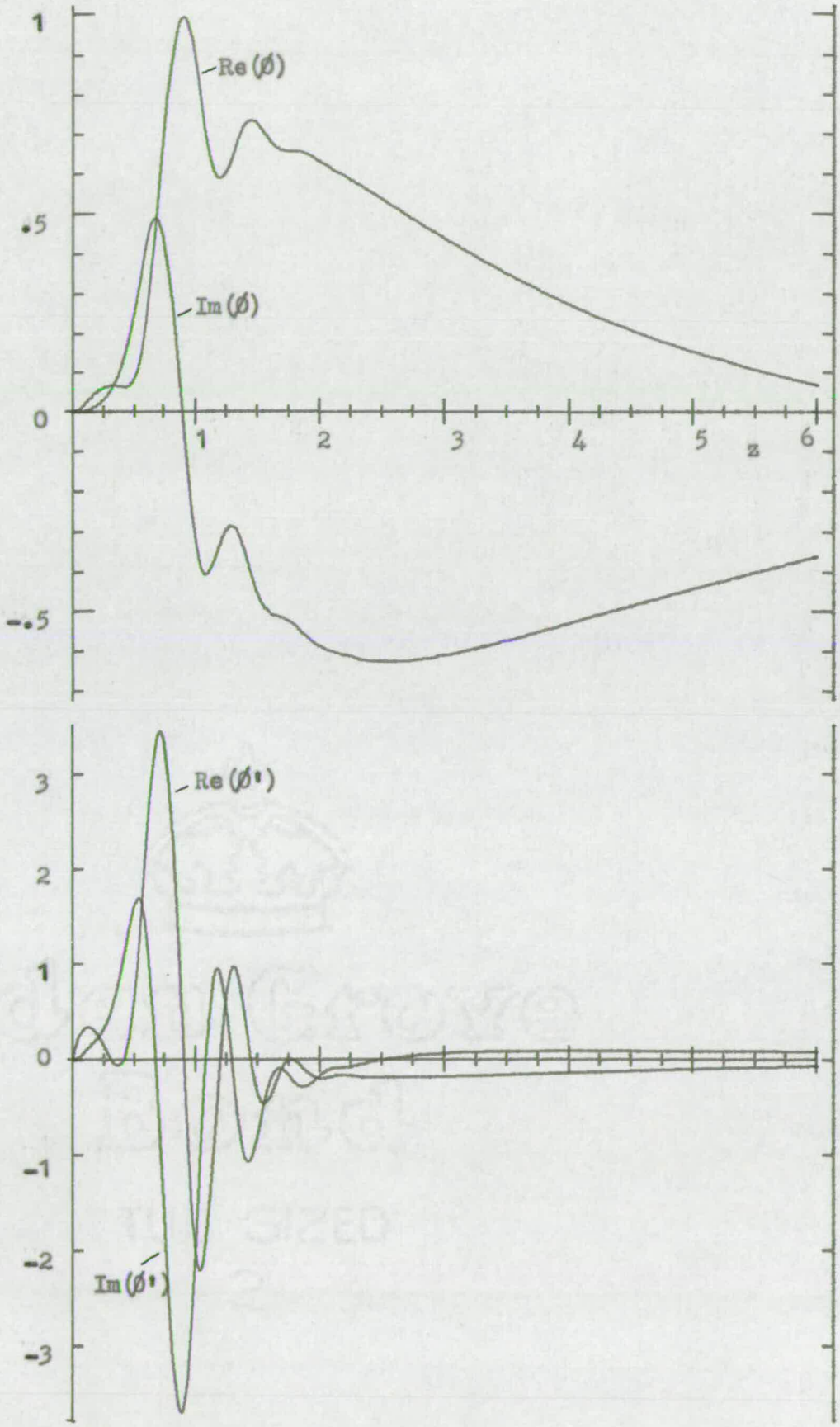

Figure 7.6 Eigenvector, standard form of equation, R= 1500, α = .239369 + .145235i.

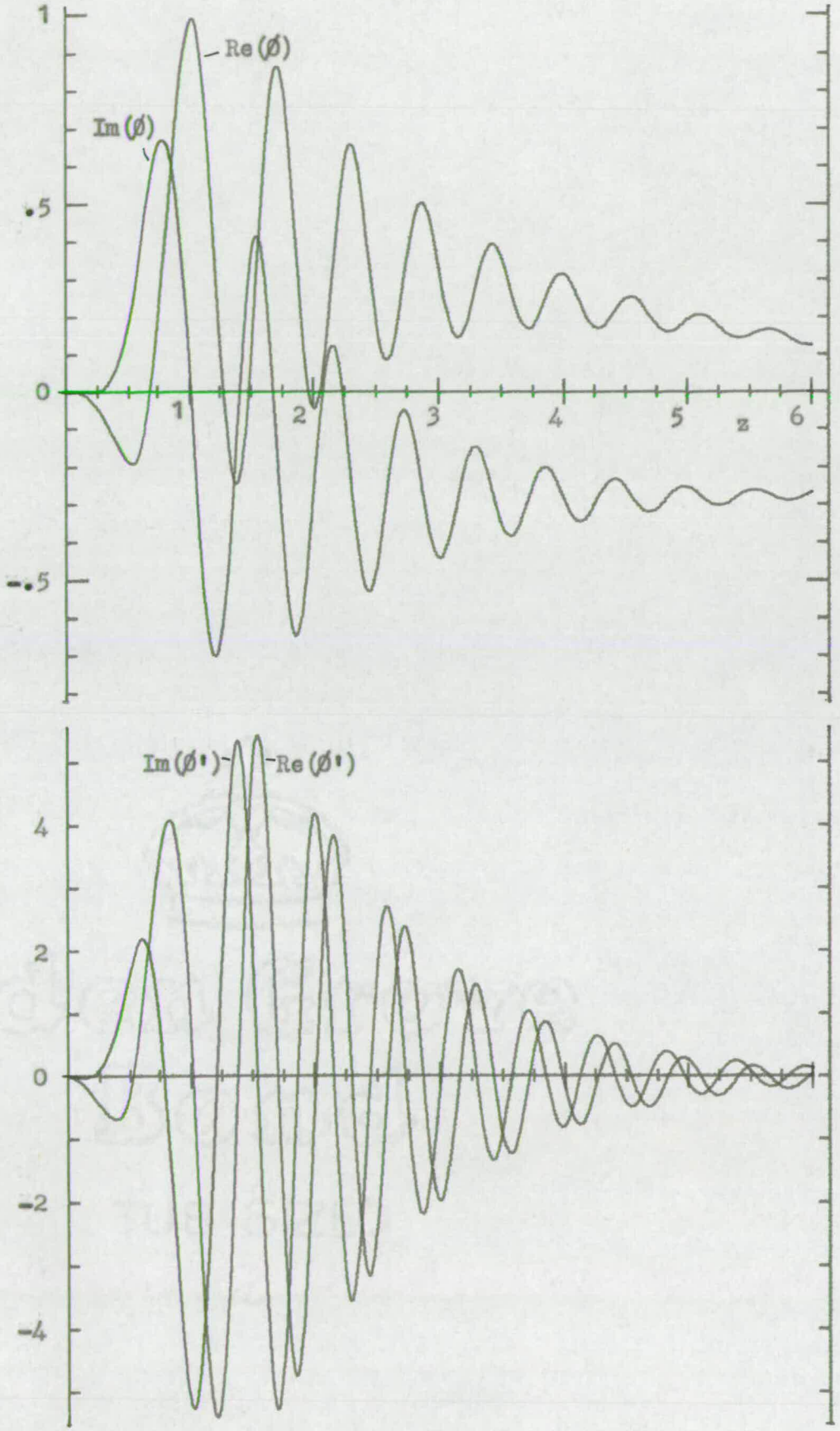

Figure 7.7 Eigenvector, standard form of equation, R= 1000, α = .099548 + .125715i.

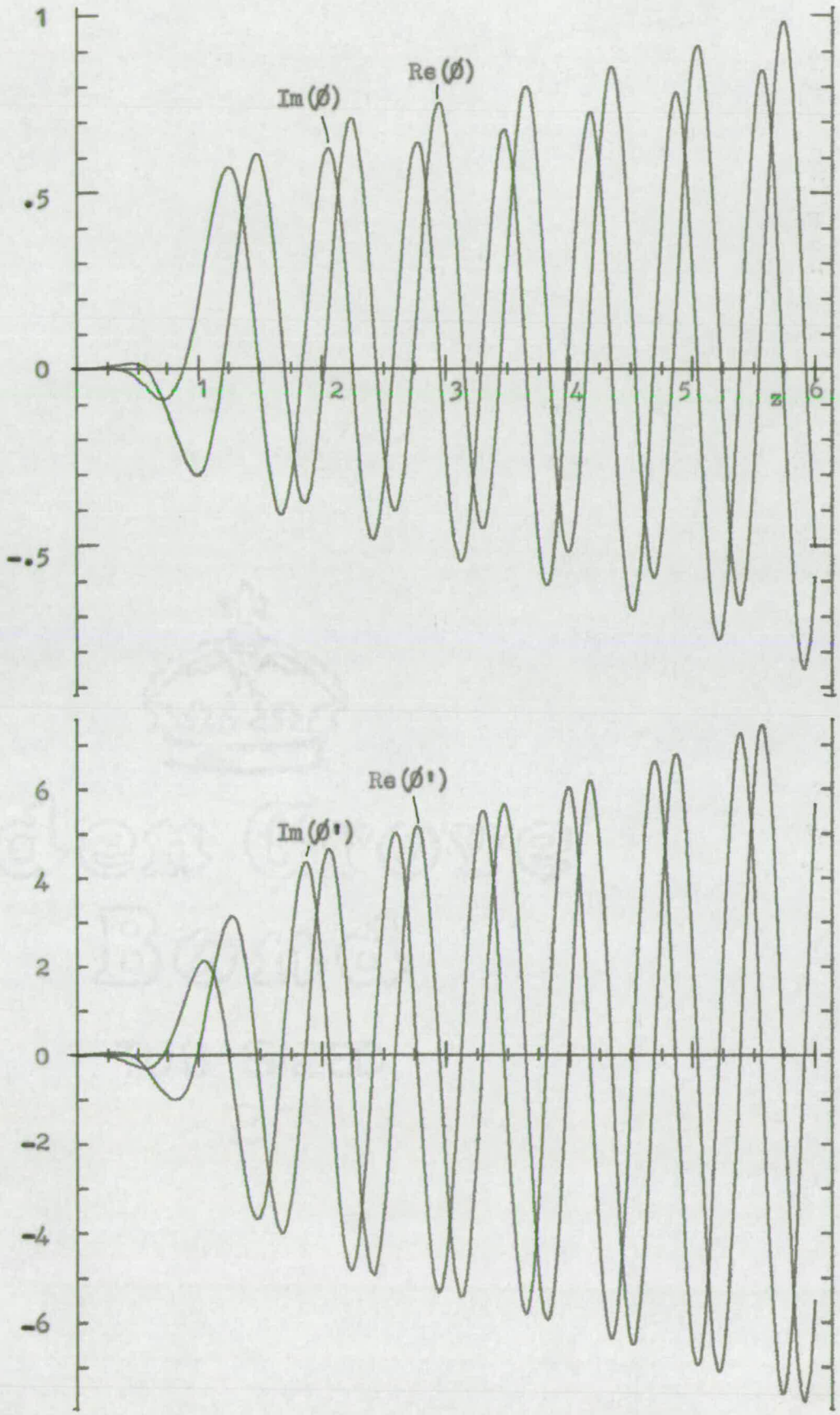

Figure 7.8 Eigenvector, extended form of equation, R= 1000, λ = .089760 + .083363i. (non-physical)

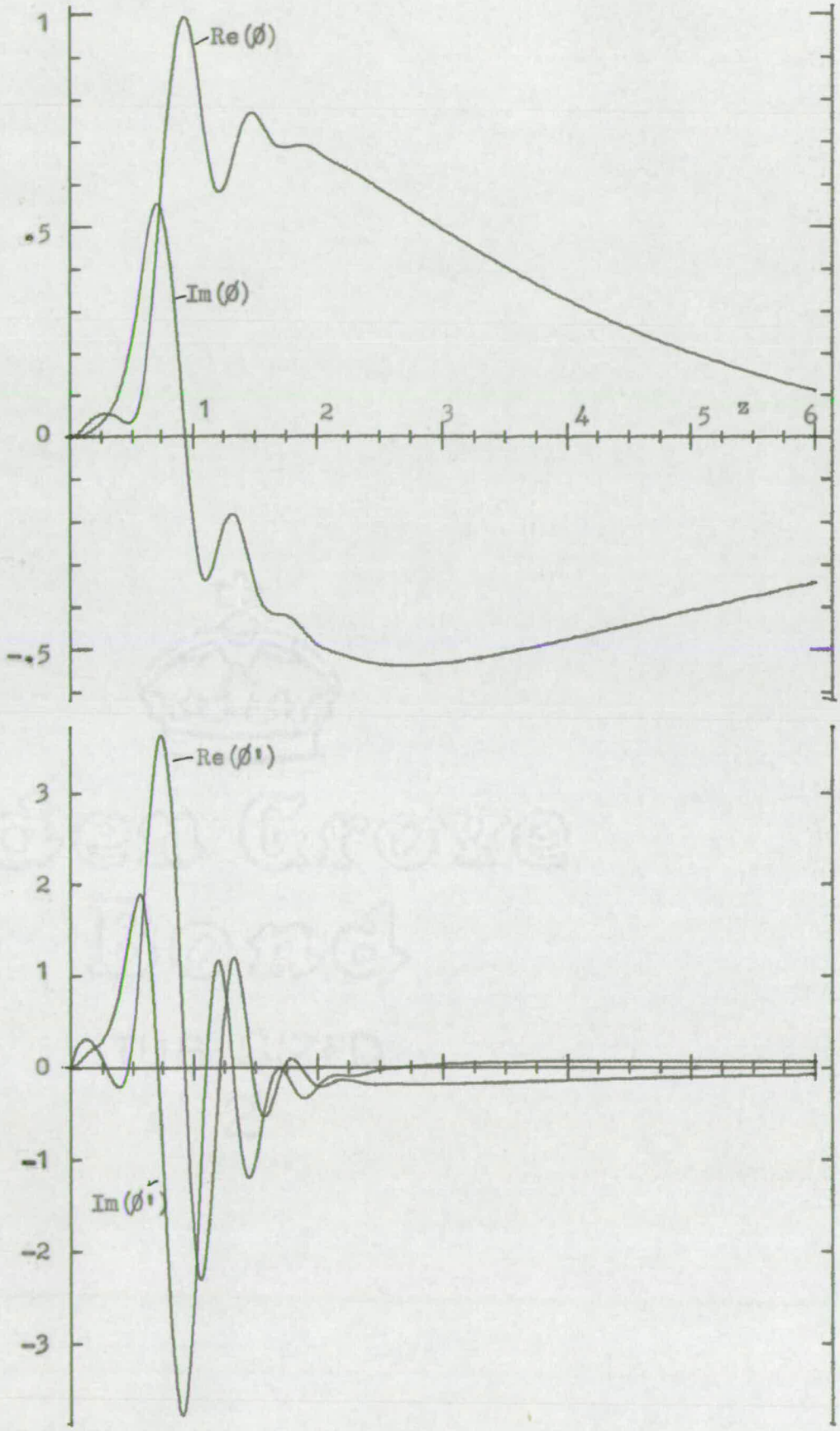

Figure 7.9 Eigenvector, extended form of equation, R= 1500, α = .237553 + .144677i.

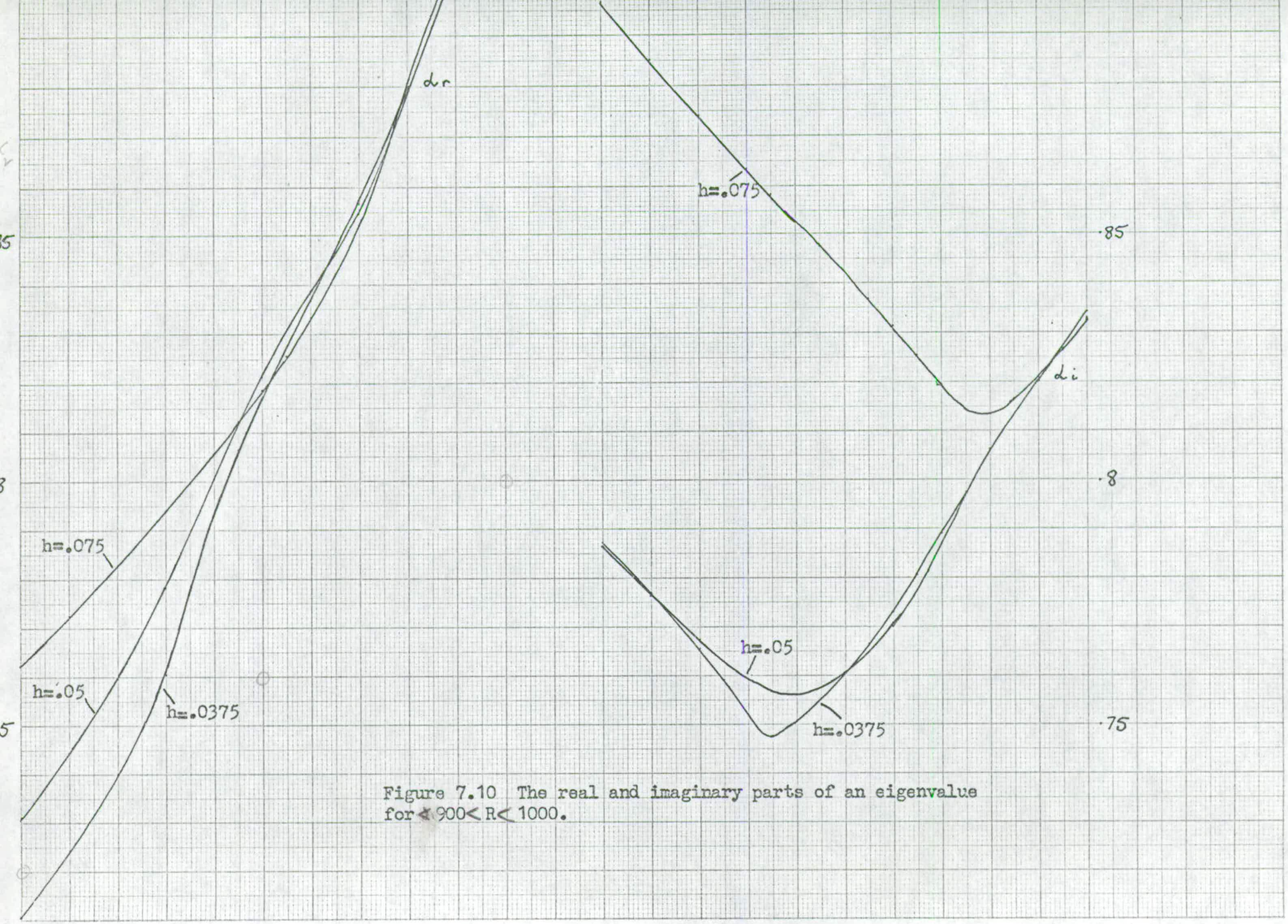

Figure 7.10 The real and imaginary parts of an eigenvalue for $900 < R < 1000$.

A second possibility is that the estimation of an eigenvalue was closer to an eigenvalue on the line than the eigenvalue sought, but, whilst this possibility cannot be overlooked, it is thought that the steplength ΔR was sufficiently small to avoid this.

If the former is the case, then the mode will seem to merge into the line. It is possible that a similar thing could happen at higher Reynolds numbers, and a mode up to then hidden in the line could emerge as a separate mode.

CHAPTER 8

SUGGESTIONS FOR FUTURE RESEARCH

Conclusions from Present Research

If the aim of the present research has been to predict breakdown to turbulence then this aim has not been attained. What has been found is that for a periodic perturbation of finite size, the boundary layer is first more stable, and then downstream less stable, than linear theory predicts. This, however, gives no sign of the rapid growth of the perturbation and its harmonics which heralds the onset of turbulence. Nor is there the slightest indication of the spot-like breakdown encountered by Klebanoff and Tidstrom. Clearly, these effects are caused by something omitted from the theory.

A few possible lines of inquiry which may lead to better agreement with experimental observations will now be discussed.

Inclusion of Higher Order Terms

Some of the terms of $O(\epsilon^4)$ and higher which have been ignored may require to be taken into account. The magnitude of these terms is higher than their order implies. The magnitude of ϕ_2 and ϕ_3 is greater than unity, and in one test case, it has been found that higher harmonics are even greater. At $R = 1000$, the magnitude of ϕ_{10} was found to be 10^9. It seems reasonable, from the increase of ϕ_3 at larger Reynolds numbers, to expect ϕ_{10} also to increase in magnitude.

There are two effects which may moderate the influence of the harmonics. It has been found that the non-linearities reduce the magnitudes of ϕ_2 and ϕ_3, and it is a reasonable postulation that the same thing happens to the higher harmonics. Also, at the larger Reynolds numbers, despite the larger amplitude of the harmonics, the predominant influence is the mean flow distortion.

It has to be decided how many harmonics ought to be included. In calculations in plane Poiseuille flow Pekeris and Shkoller (1971b) included 55 harmonics, but the present technique cannot be extended to that degree because of computer storage limitations.

The solution method for the next stage, when terms in (2.12), (2.13), (2.14) up to $O(C^5)$ are included, will be outlined. It is necessary to solve five simultaneous equations, given here schematically:

$$
\begin{aligned}
MF(\psi_o) + C^2NL(\psi_1, \psi_1) + C^4NL(\psi_2, \psi_2) &= 0 \\
G_1(\psi_1) + C^2NL(\psi_2, \psi_1) + C^4NL(\psi_3, \psi_2) &= 0 \\
G_2(\psi_2) + NL(\psi_1, \psi_1) + C^2NL(\psi_3, \psi_1) &= 0 \\
G_3(\psi_3) + NL(\psi_2, \psi_1) + C^2NL(\psi_4, \psi_1) &= 0 \\
G_4(\psi_4) + NL(\psi_3, \psi_1) + NL(\psi_2, \psi_2) &= 0 \ .
\end{aligned}
$$

MF denotes the mean flow terms, and NL the non-linear terms.

In order to obtain an eigenvalue type of matrix equation, it is necessary to solve simultaneously for ψ_1 and ψ_3.

$$\begin{bmatrix} L_1 & c^2 NL(\psi_2) & c^4 NL(\psi_2) \\ NL(\psi_2) & c^2 NL(\psi_4) & L_3 \end{bmatrix} \begin{bmatrix} \psi_1 \\ \psi_1 \\ \psi_3 \end{bmatrix} = \begin{bmatrix} 0 \\ 0 \end{bmatrix}$$

This can be turned into a real matrix equation and solved using (4.18), (4.19). There is no difficulty with the solution for ψ_o, ψ_2, ψ_4.

The method may be extended further in a similar manner. The solution for the odd harmonics has to be simultaneous, and the remainder can be found individually. The disadvantage is that the size of the matrix required for the simultaneous solution will limit the number of terms which can be included.

An alternative is to attempt a solution of the partial differential equation over a region of the boundary layer. A periodic disturbance may be imposed at an upstream position and its evolu tion followed downstream. If the time dependence is retained, then as many harmonics as are necessary will be included.

Inclusion of Other Modes of Solution

A different line of inquiry involves the other modes of solution of the Orr-Sommerfeld equation investigated in Chapter 7. A possible mechanism by which these may be generated and amplified is non-linear resonance. The conditions for the non-linear resonance of three modes of oscillation are:

$$\beta_1 + \beta_2 = \beta_3$$
$$\alpha_{r_1} + \alpha_{r_2} = \alpha_{r_3} \ .$$

If the latter is not satisfied there is still an interaction, but its phase varies with distance, and it tends to cancel itself out. In the boundary layer, the wave numbers are not constant, but vary with distance. This may make the phase-matching condition unnecessary.

It appears possible that highly damped modes can still be generated. In the equation coupling $\phi^{(1)}$ and $\phi^{(2)}$ non-linearly to $\phi^{(3)}$, the non-linear terms have a coefficient $\frac{C_1 C_2}{C_3} e^{(\alpha_{i_3} - \alpha_{i_1} - \alpha_{i_2})x}$ where C_n is the amplitude of the mode $\phi^{(n)}$. If $\phi^{(3)}$ is heavily damped, the non-linear terms will become very large and the result may be the generation of $\phi^{(3)}$ despite its damping.

One possible resonance is known. It occurs at about $R = 1300$, $F = 80 \times 10^{-6}$. The difference between α_r for the fundamental mode and its second harmonic is the same as α_r for mode 1 in Table (7.1).

There is no reason why the frequencies should be harmonically related. The only conditions for the non-linear coupling are that initially two oscillations of arbitrary frequency are present, and that the oscillation at the sum or difference of these frequencies satisfies, or perhaps it is only necessary that it nearly satisfies, the phase-matching condition. The second oscillation could possibly be part of the residual turbulence present in an experiment.

Once a resonance condition is reached, there are a number of effects which may then occur to initiate turbulence. The

resonant oscillations may grow in amplitude, they may generate further oscillations, they may interact with the mean flow. Which effects do in fact occur, and how they occur is a subject for investigation.

Three-dimensional Effects

No two-dimensional experiment can be perfect. There must always be a trace of three-dimensionality in the experiment. To what extent these imperfections affect transition is an interesting problem, and it would be a useful comparison if some three-dimensional effects were added.

The linear problem is relatively simple. The equation derived by Squire (1933) is a small extension of the Orr-Sommerfeld equation, and it would not be difficult to make the necessary modifications.

The non-linear problem is less straightforward. The mean flow becomes three-dimensional, and unless some simplifying assumptions can be made, it may be necessary to solve a partial differential equation directly. This is more difficult, but there are a number of recently developed techniques available.

This problem has only been looked at superficially, and it will require a closer examination before a solution can be attempted, but it is possible that a detailed three-dimensional solution will reveal more about the structure of transition.

APPENDIX I

Programming Methods

The programs used to conduct the calculations were written in IMP, a local variant of Atlas Autocode. Two computers were available, an ICL 4/70 and an IBM 370/155.

The language structure and operating system permitted the use of precompiled routines, and most of the basic procedures were precompiled. These were stored on disc, and the inclusion of the appropriate routines was automatic.

IMP does not include complex arithmetic, and to represent a complex variable two real variables were used. The naming convention was adopted that the suffices -r and -i denoted real and imaginary parts respectively. Double precision arithmetic, accurate to 16 significant figures, was used throughout.

The matrix M in (4.2) has a band structure, with most of its elements zero, and the only non-zero elements in a band centred on the diagonal. It is therefore unnecessary to store the entire matrix of n^2 elements (with n normally 80, but occasionally higher) and instead only the band of non-zero elements need be stored. The parameter dim denotes the number of non-zero elements on each side of the diagonal, and the band width is then 2dim + 1. In the standard Orr-Sommerfeld form, dim takes the value 2, and in the extended form 3.

The iteration requires the solution of sets of linear equations $M\underline{x} = \underline{y}$. The solution was achieved by means of

two routines, csolve1 and csolve2, written to take account of the band structure of M. The former performs a L.U. factorisation with partial pivoting on M, and the latter finds $\underline{x}$ using forward and back substitution. Some additional elements of storage are required by the partial pivoting, increasing the total storage required for M to (3dim + 1)xn elements.

The factorised matrix may be used to calculate detM. The lower triangular factor has a unit diagonal, and therefore the determinant is the product of the diagonal elements of the upper triangular factor, changed in sign by each application of pivoting. The problem of underflow requires the product to be scaled to keep it within the range of the machine. The modulus of the determinant is about 10^{-200}, but the computer treats values under 10^{-75} as zero. The scaling has no effect on the argument.

M in (5.3) is real, but larger, with dim = 7. To solve a set of real equations, procedures solve1 and solve2, real counterparts of csolve1 and csolve2 were used.

Solution of (2.24)

A routine iterate2 was written to perform one step of the iteration (4.7), (4.8). The longer iteration step required initially was performed by a routine iterate. A routine eigen2 performed a complete solution.

These routines called others to perform sections of the iteration, and it was arranged that by the modification of only two small routines, the solution could be made for a different type of flow profile. For a flow profile with the

same boundary conditions on the Orr-Sommerfeld equation, no change is required; it is only when the boundary conditions are different that it is necessary to alter the routines bound and extend.

The routines matrix and dm calculate the matrices M and $\frac{\partial M}{\partial \alpha}$ independently of the boundary conditions. A separate routine, bound, then applies the boundary conditions.

A point to notice is that the eigenvalue occurs explicitly in the boundary conditions. After application of the boundary conditions to M, a few elements have the form

$$t_o + t_1 e^{-h\alpha} + t_2 e^{-2h\alpha} \quad .$$

The corresponding element in $\frac{\partial M}{\partial \alpha}$ must be

$$\frac{\partial t_o}{\partial \alpha} + (\frac{\partial t_1}{\partial \alpha} - ht_1)e^{-h\alpha} + (\frac{\partial t_2}{\partial \alpha} - 2ht_2)e^{-2h\alpha} \quad .$$

Care must be taken to include these elements of the unbounded matrix M in $\frac{\partial M}{\partial \alpha}$. Their omission, although minor, is sufficient to upset the convergence rate of the iteration. It was arranged so that bound applied the boundary conditions to M alone, or to both, using elements of M for $\frac{\partial M}{\partial \alpha}$.

The routine extend is called after the completion of the iteration. It calculates elements of $\underline{g}$ outside the limits of the matrix, utilising the boundary conditions.

The routines matrix and dm can produce either the standard or the extended form of the Orr-Sommerfeld equation. Depending on the setting of the parameter dim, the additional terms required for the extended form are included or excluded.

On entry to the routine eigen2, ar, ai, gr, and gi contain the first approximations to the eigenvalue and the eigenvector. To indicate a good eigenvector approximation, s contains a value corresponding to a component of the approximation, usually the component of largest magnitude; if the value of s is outside the range of the eigenvector approximation, it is assumed that only a poor approximation has been given, and the first step of the iteration is made using the longer method. After each iteration s contains the coefficient of the component of largest magnitude.

The parameter z is the outer limit of the solution, and usually takes the value 6. The convergence limit of the iteration is e ; if the change in eigenvalue after a step of the iteration is less than e, convergence is assumed. The value of e was usually 10^{-8}. The solution is then as accurate as the computer precision will allow.

On the ICL 4/70, one step of the iteration, with n = 80, required less than a second c.p.u. time, and with a moderately good initial eigenvalue approximation, three or four seconds was required for the complete solution.

Listing of Procedure iterate2

```
Program
routine iterate2 (realname ar, ai, dar, dai,
realarrayname  u, d2u, w, d2w, integername s,
integer n, dim)
realarray  mr, mi(-dim:2dim,0:n),dmr,dmi(-2:2,0:n)
realarray  xr, xi, str, sti(0:n)
integerarray  c(0:n-1)
eq(str,sti,gr,gi,0,n)                    copy initial approx. g
dm(dmr,dmi,u,dzu,w)                      calculate ∂M/∂α
matrix(mr,mi,u,dzu,w,dzw)                calculate M
bound(mr,mi,dmr,dmi,1)                   fit boundary conditions to
                                         M and ∂M/∂α
csolvel(mr,mi,c,0,n,dim)                 perform L.U. factorisation
dmmult(xr,xi,gr,gi,dmr,dmi)              set X = ∂M/∂α g
csolve2(gr,gi,xr,xi,mr,mi,c,0,n,dim)     set g = M^-1 x
s = maxcom(gr,gi,r)                      find maximum component of g
pr = gr(s); pi = gi(s)
cdiv(dar,dai,1,0,pr,pi)                  da = 1/g_s
cycle  i = 0,1,n
cdiv(gr(i),gi(i),gr(i),gi(i),pr,pi)      normalise g
repeat
ar = ar - dar
ai = ai - dai
newline; print(ar);print(ai)
print(dar); print(dai)
print(evnorm(str,sti,gr,gi,n))           print change in g
setupl(ar,ai)                            recompute e^-hα etc
end
```

Listing of Procedure eigen2

```
Program                                                    Intention
routine  eigen2 (realname ar, ai,
realarrayname gr, gi,u,dzu,w,dzw, integername s
real b,r,z,e, integer n,dim)
setup(ar,ai,b,r,z,n,dim)                          calculate values such as
                                                        e^-hα etc.
unless  0≤s≤n  then iterate (ar,di,dar,dai,       perform one step
 gr,gi,u,dzu,w,dzw,s,n,dim)                       of the longer iteration
newa:iterate2(ar,ai,dar,dai,gr,gi,u,
 dzu,w,dzw,s,n,dim)                               normal iteration
if  dar*dar + dai*dai > e*e  then -> newa         check for convergence
extend (gr,gi)
end
```

In order to fit the boundary conditions (7.2), an alternative set of routines was produced. The necessary changes were made to the routines bound and extend, and in addition the routine setupl was changed. In addition to calculating $e^{-h\alpha}$, the routine calculated γ, $\frac{\partial\gamma}{\partial\alpha}$, and $e^{-h\gamma}$. The routine setf was provided to specify which sign of square root should be taken in the calculation of γ, but if α later crossed the branch line, the square root of opposite sign was taken. In this way, contour integration was simplified. After first specifying on which sheet of the α plane the integration began, the contour was allowed to cross and recross the branchline without any special precautions

Calculation of the Second Harmonic

Since the left hand side operator of (2.22) is the same as that of (2.24), with the replacement of α, β, by 2α, 2β, the same matrix routines can be used. The program excerpt below shows the steps in the calculation of g_2 following the calculation of the non-linear terms on the right hand side of (2.22), which have been stored in the arrays g2r, g2i.

Program	Intention
setup(2ar,2ai,2b,r,z,n,dim)	Note that 2α,2β are used.
matrix(mr,mi,u,dzu,w,dzw)	calculate M
bound(mr,mi,mr,mi,0)	0 means bound M only
csolvel(mr,mi,c,0,n,dim)	
csolve2(g2r,g2i,g2r,g2i,mr,mi,c,0,n,dim)	g2r,g2i now contain the solution g_2
extend(g2r,g2i)	

The third harmonic is calculated in the same way, using 3α, 3β

Solution of (2.21)

The iteration (4.18), (4.19) is applied to solve (2.21), and one step of the iteration is performed by the routine, iteratem. The matrix M and the vector $\underline{g}$ are the discretization of both the real and imaginary parts of a non-analytic complex equation. The even numbered rows of M, and the even numbered elements of $\underline{g}$ correspond to the real

part, and the following odd numbered row or element to the imaginary part of each of the set of simultaneous complex equations and the complex vector.

Two derivative matrices are required, $\frac{\partial M}{\partial \alpha_r}$ and $\frac{\partial M}{\partial \alpha_i}$. A separate routine could have been written for each, but instead a method was devised to calculate each by the same routine matrixm. The routine was written so as to calculate M, but, since each element in M is the sum of multiples of the real and imaginary parts of powers of α, it was possible to replace the power of α by its derivative and calculate a derivative of M.

No separate routine was written to fit the boundary conditions; instead this was done in two parts. The inner boundary condition is the same for M and its derivatives, and was fitted by matrixm. The outer boundary condition is a function of α and therefore different for each derivation of M. It was fitted inside iteratem.

In the abbreviated listing of iteratem given below, p1,p2,p3 and p4 are functions of ϕ_2 which occur on the righthand side of (2.21), and contain the powers of 2α which are considered to be constant for the solution of the equation. The position of the maximum component of $\underline{g}$ is given by pi, and is fixed throughout the iteration.

Program	Intention
setupm	
matrix(m,u,d2u,w,d2w,p1,p2,p3,p4)	form M
setupdl	
matrixm(mm,u,d2u,w,d2w,p1,p2,p3,p4)	form $\frac{\partial M}{\partial \alpha_r}$
.	
.	fit outer boundary
.	condition to $\frac{\partial M}{\partial \alpha_r}$
spmult(dm1,g,mm)	set dm1 = $\frac{\partial M}{2\alpha_r}$ g
matrixm(mm,u,d2u,w,d2w,p1,p2,p3,p4)	form $\frac{\partial M}{\partial \alpha_i}$
.	
.	fit outer boundary
.	condition to $\frac{\partial M}{\partial \alpha_i}$ and M
spmult(dm2,g,mm)	set dm2 = $\frac{\partial M}{\partial \alpha_i}$ g
solve1 (m,c,7)	
solve2(dm1,dm1,m,c,7)	set dm1 = M^{-1}dm1
solve2(dm2,dm2,m,c,7)	set dm2 = M^{-1}dm2
p=dm1(pi)*dm2(pi+1)-dm1(pi+1)*dm2(pi)	
dar=-dm2(pi+1)/p ; dai=dm1(pi+1)/p	calculate
ar=ar+dar ; ai=ai+dai	new eigenvalue
cycle i = 0,1, 2n+1	
g(i) = -(dar*dm1(i)+dai*dm2(i))	calculate
	new eigenvector
repeat	

One iteration, again with n=80, required two or three seconds on the ICL 4/70.

The longest complete simultaneous solution required about 100 seconds.

APPENDIX II

Comparison of Theory with Experiment

One of the objects of these calculations was to produce results using finite amplitude perturbations for comparison with the experiments of Robertson (1971). Those comparisons which were made are inconclusive, but for completeness they are given here.

1) Perturbation distributions.

Figures (A.1) and (A.2) show two comparisons of the measured and the calculated distributions of the fundamental and second harmonic of the perturbation. The experimental points are of the R.M.S. value of u'/U_o, and the calculated values have been converted to R.M.S. values by multiplying by $\sqrt{2}$.

In Figure (A.1), the calculated distribution had been calculated at the amplitude shown, but no previously calculated distribution was available for Figure (A.2), and in this figure a distribution for a higher amplitude was scaled down by a factor of .4 for the fundamental and $(.4)^2$ for the second harmonic.

Figure (A.1) shows the better fit, but in both cases the second harmonic peak is larger than predicted.

At the amplitudes at which these comparisons were made, the difference between the linear and non-linear calculations

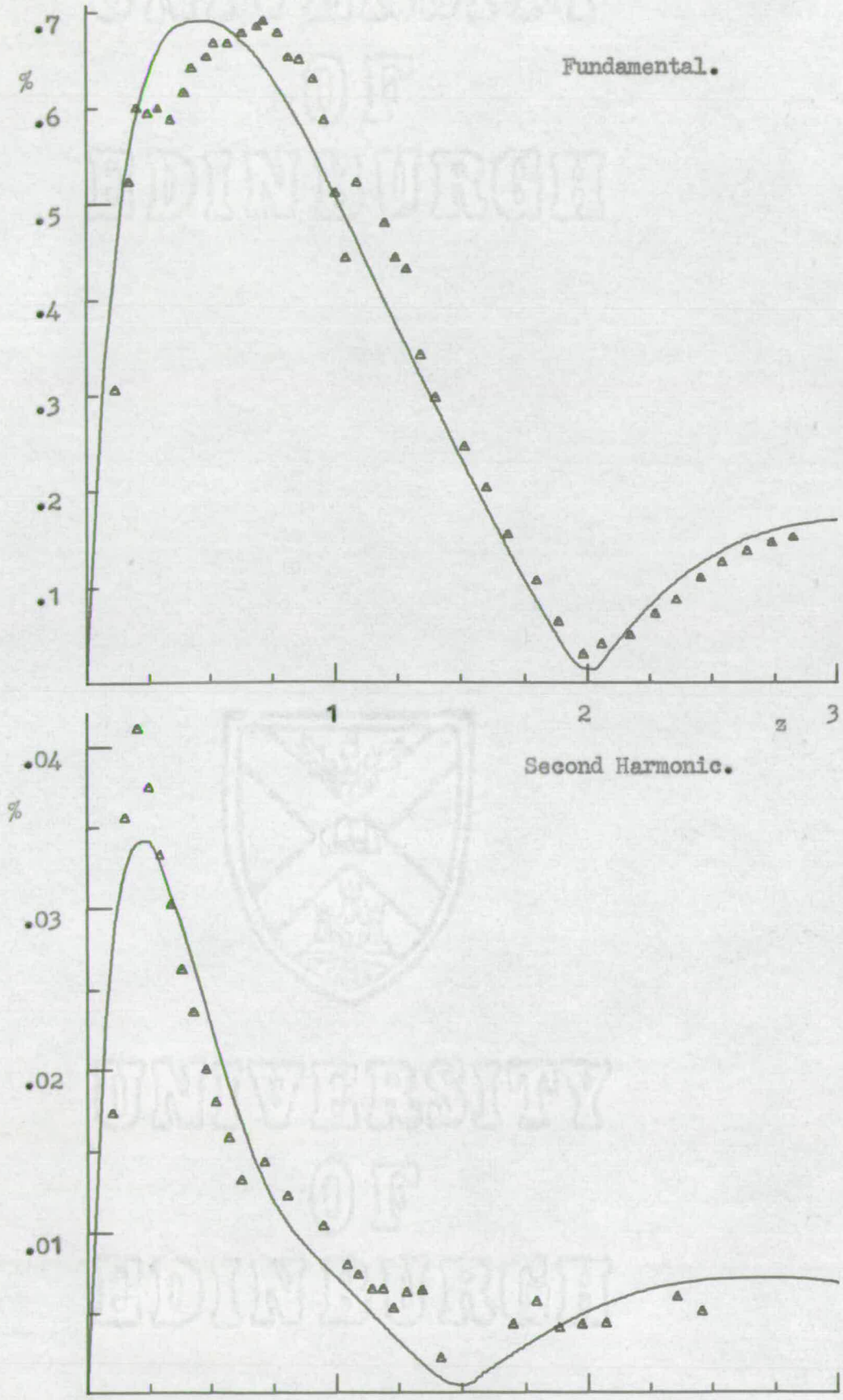

Figure A.1 Comparison of experimental (points) and calculated (line) distributions of the fundamental and second harmonic, R= 1200

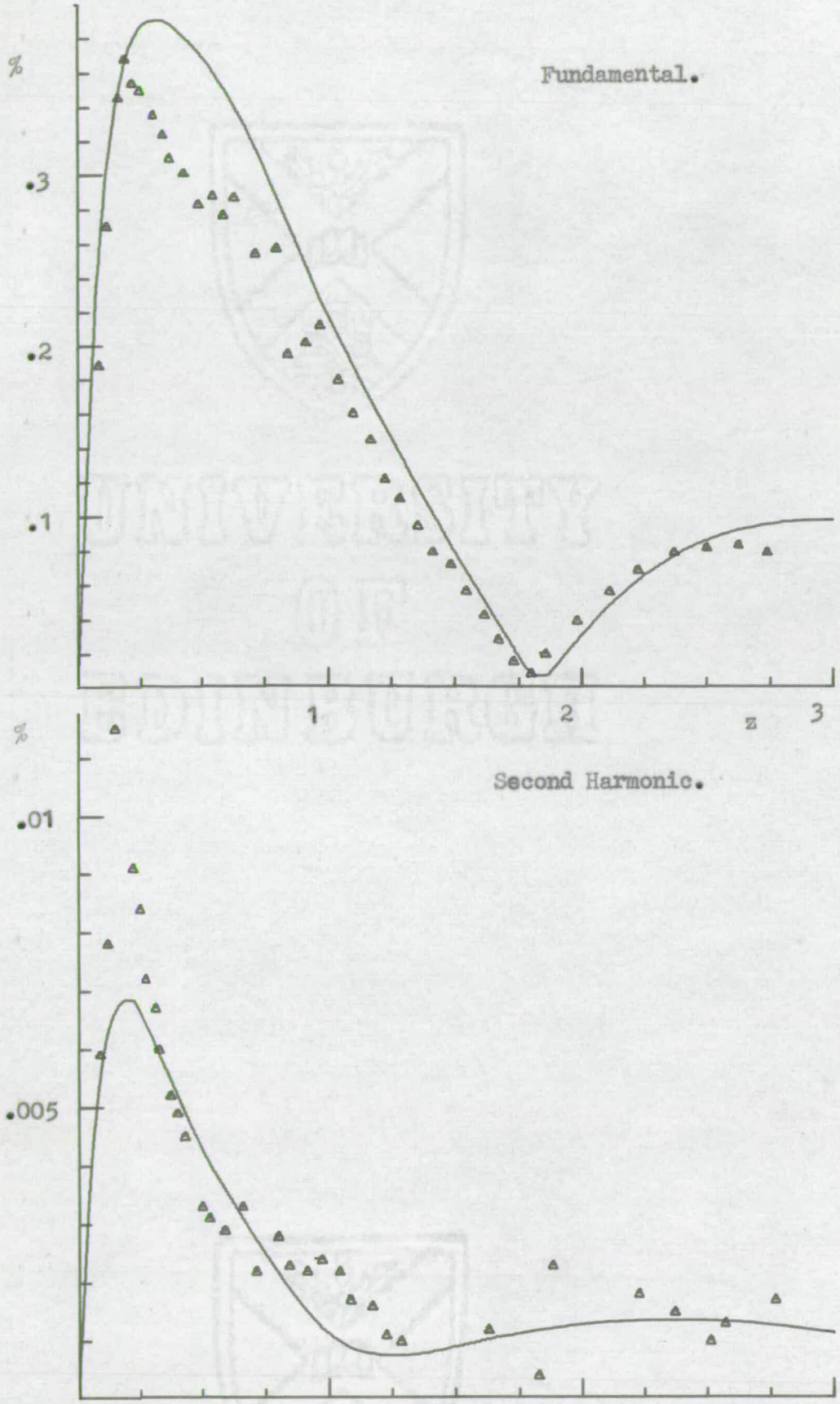

Figure A.2 Comparison of experimental and calculated distributions of the fundamental and second harmonic, R= 1500.

is small, and the departures of the experimental points from theoretical curve are larger, therefore no conclusion can be drawn from non-linear theory which could not be drawn using linear theory.

2) Downstream Integration.

Figures (A.3) and (A.4) compare the results of two downstream integrations with observed values taken during a downstream traverse of the boundary layer at a constant non-dimensional distance from the plate. The calculated values at this non-dimensional distance were found by multiplying the amplitude, corrected approximately for the inaccuracy of the integration method, by the magnitude of the perturbation distribution at the position of measurement.

The figures show the relative amplitudes $\frac{A}{A_o}$ on a logarithmic scale. The values of A_o for the calculated and experimental results are not the same, but the relative amplitudes may be compared. In Figure (A.3), A_o for the calculated values is about $0.1^o/o$, and for the observations about $0.05^o/o$. The corresponding values for Figure (A.4) are $0.21^o/o$ and $0.25^o/o$. In order to present a good comparison, the amplitude A_o for the observations has been slightly adjusted so that $\frac{A}{A_o}$ for both theory and experiment coincide at $R = 1100$.

Figure (A.3) shows that there is less observed gain than predicted. This deficit in amplification was also observed in the linear case by Ross et al. (1970). A possible reason

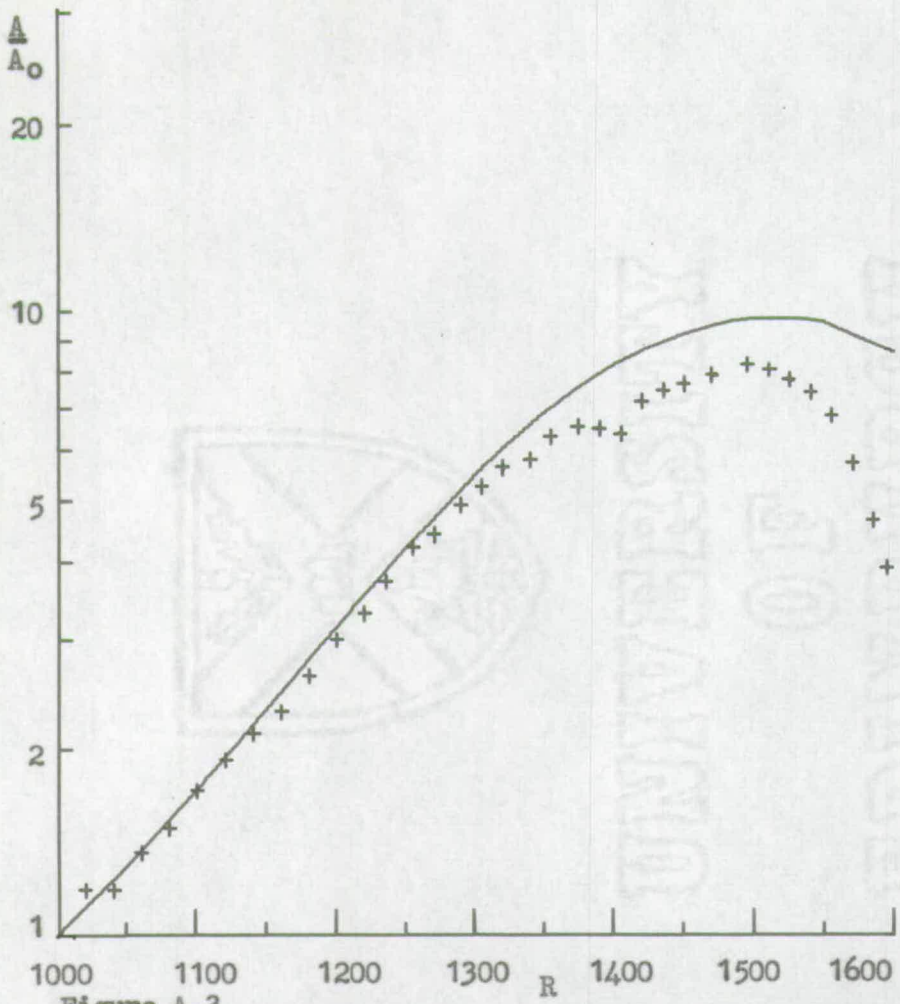

Figure A.3

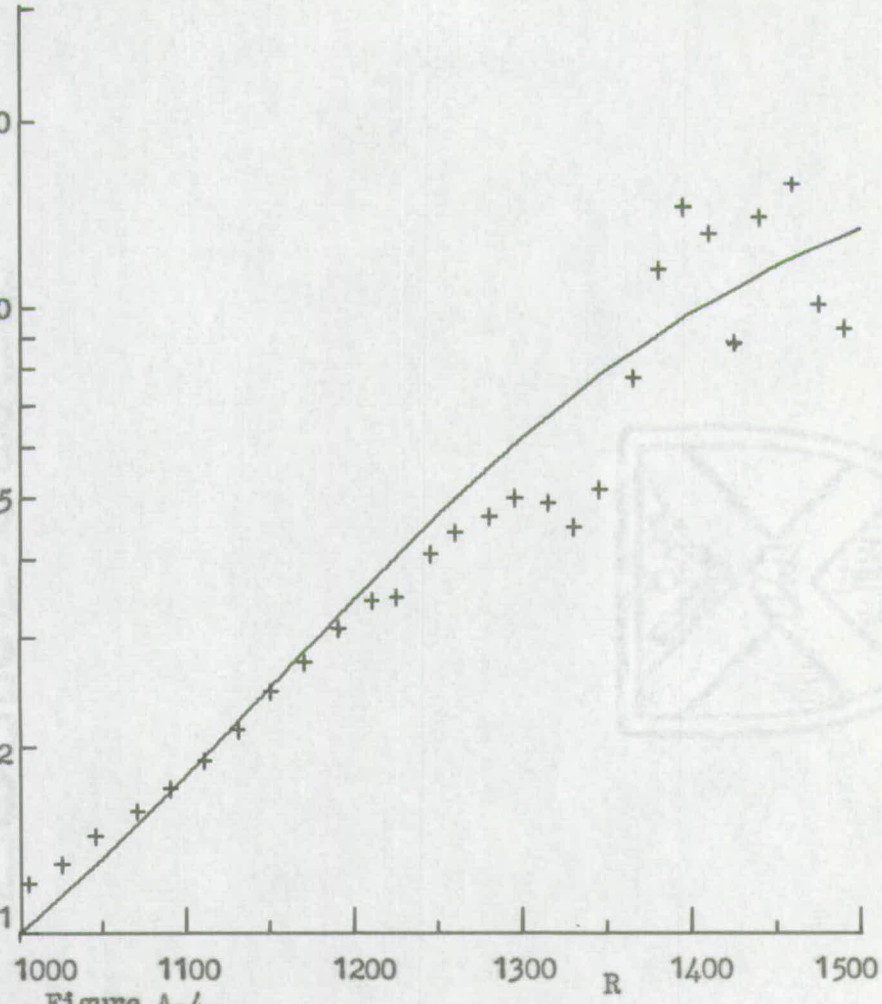

Figure A.4

Downstream integrations (line) and experimental values (points).

was suggested. The assumption made in deriving the Orr-Sommerfeld equation, that $\psi(x,z)$ is separable into $\phi(z)e^{i\alpha x}$, is incorrect. A more accurate equation given by Gregory et al. (1955) includes terms in $\frac{\partial\phi}{\partial x}$. The Orr-Sommerfeld equation appears to be a good approximation, and its error can only be found if a solution of the more accurate partial differential equation can be obtained.

There is also the possibility of three-dimensionality. The perturbation is limited in extent to the width of the ribbon which generates it, and, although measurements are normally taken at the centre, where the distribution is almost two-dimensional locally, the traces of the three-dimensional nature of the perturbation may have an effect even on infinitesimal perturbations. When non-linearity is also present, the mean flow may become three-dimensional also.

Again the deviation from the predicted values is larger than the changes caused by the non-linear effects, and no conclusion can be drawn.

At the larger amplitude of Figure (A.4), the experiment becomes turbulent at about $R = 1350$. The amplitude of the fundamental first dips, then rises abruptly. This is not predicted by the present theory, and indicates that the theory is incomplete.

Acknowledgements

I should like to thank Dr. M.A.S. Ross, not only for suggesting the research project, but also for her helpful advice and guidance throughout. Advice and helpful comments on the previous work were given by Dr. R. Jordinson and Dr. M.J. Barry. The development of the numerical work was assisted by discussions with Mr. D. Kershaw.

Part of the computational cost was met by a grant from the Procurement Executive of the Ministry of Defence. A studentship was provided by the Science Research Council.

REFERENCES

Barnes, F.H., 1966, Ph.D. Thesis, University of Edinburgh.

Barry, M.J., 1970, Ph.D. Thesis, University of Edinburgh.

Barry, M.J. and Ross, M.A.S, 1970, J. Fluid Mech. 43, 813.

Benney, D.J., 1961, J. Fluid Mech. 10, 209.

Blasius, H., 1908, Z. Math. u. Physik 56, 1.

Emmons, H.W., 1951, J. Aero Sci. 18, 490.

Fox, L., 1960, In Boundary Problems in Differential Equations (Ed. R.E. Langer), Univ. Wisconsin Press.

Gregory, N., Stuart, J.T. and Walker, W.S., 1955, Phil. Trans. A248, 155.

Heisenberg, W., 1924, Ann. Phys. Lpz. (4), 74, 577.

Jones, C.W. and Watson, E.J., 1963, in Laminar Boundary Layers, Oxford University Press.

Jordinson, R., 1968, Ph.D. Thesis, University of Edinburgh.

Jordinson, R., 1970, J. Fluid Mech., 43, 801.

Jordinson, R., 1971, Phys. Fluids 14, 2535.

Klebanoff, P.S. and Tidstrom, K.D., 1959, Tech. Notes nat. Aero. Space Admin., Wash. D-195.

Klebanoff, P.S., Tidstrom, K.D. and Sargent, L.M., 1962, J. Fluid Mech. 12, 1.

Lin, C.C., 1958, in Boundary Layer Research, p. 146, I.U.T.A.M. Symposium, Freiburg, 1957 (ed. H. Görtler), Berlin: Springer.

Meksyn, D. and Stuart, J.T., 1951, Proc. Roy. Soc. A208, 517.

Noumerov, B.V., 1924, Mon. Not. Roy. Astr. Soc. 84, 592.

Orr, W.M.F., 1907, Proc. Roy. Irish Acad. A27, 9.

Osborne, M.R., 1964, Comput. J. 7, 66.

Osborne, M.R., 1967, SIAM J. Appl. Math. 15, 539.

Prandtl, L., 1904, Verh. III int. Math. Kongr., Heidelberg, 484.

REFERENCES (Contd.)

Pekeris, C.L. and Shkoller, B., 1969, J. Fluid Mech. 39, 611.

Pekeris, C.L. and Shkoller, B., 1971a, Proc. Nat. Acad. Sci. U.S.A., 68, 197.

Pekeris, C.L. and Shkoller, B., 1971b, Proc. Nat. Acad. Sci. U.S.A., 68, 1434.

Pretsch, J., 1941, Jb. dtsch. Luftfahrtf. 1, 158.

Reynolds, O., 1883, Phil. Trans. 174, 935.

Robertson, T., 1971, Ph.D. Thesis, University of Edinburgh.

Ross, J.A., 1970, Ph.D. Thesis, University of Edinburgh.

Ross, J.A., Barnes, F.H., Burns, J.G. and Ross, M.A.S., 1970, J. Fluid Mech. 43, 819.

Schlichting, H., 1935, Nachr. Ges. Wiss. Göttingen Math.-phys. Kl. Fachgruppe, 1, 47.

Schubauer, G.B. and Skramstad, H.K., 1947, Rep. nat. adv. Comm. Aero., Wash. No. 909.

Squire, H.B., 1933, Proc. Roy. Soc. A142, 621.

Stewartson, K. and Stuart, J.T., 1971, J. Fluid Mech. 48, 529.

Thomas, L.H., 1953, Phys. Rev. (2) 91, 780.

Tollmein, W., 1929, Nachr. Ges. Wiss. Göttingen, 21.

Watson, J., 1962, J. Fluid Mech. 14, 221.

PUBLICATION

A paper describing the numerical methods developed and used to solve the non-linear equations has been published in the Proceedings of the Royal Society of Edinburgh. A copy of this paper is attached.

In addition, a paper discussing the results of the solution of the non-linear equations has been submitted for publication by the Aeronautical Research Council.

PROC. R.S.E. (A), 70, 24, 1971/72

24.—Eigenvalue and Eigenvector Solutions of a Wave System in a Non-Linear Dissipative Medium.* By M. A. S. Ross and D. F. Corner, Fluid Mechanics Unit, Department of Physics, University of Edinburgh. (With 1 text-figure)

Synopsis

This paper gives an account of some numerical methods which have been applied to solve the equations of second order stability theory in the flat plate boundary layer.

Over the last twenty-five years, in a number of branches of physics, interest has tended to shift from the study of linear fields to the study of non-linear fields. The solving of the non-linear partial differential equations which are then encountered raises formidable difficulties both for the pure mathematician and for the physicist. The mathematician examines questions of the existence and uniqueness of solutions, but the physicist approaches these difficulties from a different standpoint. If the equations from which the physicist starts are a correct and complete statement of the problem he can confidently assume that a solution exists, although, in some cases, it may not be a unique solution. The observable physical phenomena are themselves an 'analogue' solution of the equations. The question at issue for the physicist is whether the equations are correct and complete, and an affirmative answer can be given only when there is sufficiently close agreement between theory and experiment. What the physicist requires in order to carry out his test is a sufficiently accurate solution given not only in numerical form but also in a form which fits the experimental conditions. The development of fast, high capacity computers and of powerful numerical methods has contributed greatly to meet these requirements. The present paper gives an example of some methods which have recently been found practicable for the solution of the second order stability theory of the flat plate boundary layer.

The corresponding problem for Poiseuille flow has been dealt with analytically by Meksyn and Stuart (1951), Stuart (1958, 1960) and Watson (1960). The mean flow in this case can be expressed analytically, but this is not possible for boundary layer flow.

We assume that a semi-infinite flat plate lies in the plane $z = 0$ with its leading edge coincident with the y-axis, the fluid surrounding the plate moving parallel to the x-axis. It is usual to express the equations of fluid dynamics in non-dimensional form, and to do so we use units of velocity, length and time which are characteristic of the flow geometry. In boundary layer theory the unit of velocity is the main stream velocity which we shall call U_0, the unit of length is δ_1, the *local* displacement thickness of the boundary layer, and the unit of time is δ_1/U_0. The stream function is then expressed in units of $U_0\delta_1$ and the non-dimensional ratio of density to viscosity is the *local* Reynolds number $R = U_0\delta_1\rho/\mu$. If the flow in the boundary layer is assumed to take place over a flat plate under zero pressure gradient, the boundary layer geometry

* This paper was assisted in publication by a grant from the Carnegie Trust for the Universities of Scotland.

is considerably simplified: δ_1 and R increase as the square root of the *dimensional* distance from the leading edge, and the *non-dimensional* distance $x = 0{\cdot}341\ R$. These relations apply to all the equations which follow, subject to the restriction that R and x are not very small.

When a two-dimensional periodic perturbation is introduced into the two-dimensional laminar boundary layer on a flat plate, the equations governing the total flow in the layer are the linear continuity equation and the non-linear equation for the rate of change of the vorticity. The continuity equation is satisfied by expressing the components of total velocity in terms of a (scalar) stream function:

$$\psi = \psi_0 + \psi_p$$

where ψ_0 refers to the mean flow and ψ_p to the perturbation. The non-dimensional vorticity equation is then:

$$\frac{\partial \nabla^2\psi}{\partial t} + \frac{\partial \psi}{\partial z}\frac{\partial \nabla^2\psi}{\partial x} - \frac{\partial \psi}{\partial x}\frac{\partial \nabla^2\psi}{\partial z} = \frac{1}{R}\nabla^4\psi \tag{1}$$

The fact that the boundary layer is extensive in the x direction and very thin in the z direction led Prandtl to a simplification of the boundary layer equations which we introduce in the form:

$$\nabla^2\psi_0 = \frac{\partial^2\psi_0}{\partial z^2}.$$

The functions contained in ψ must satisfy boundary conditions at the surface of the plate and at the outer edge of the boundary layer, and within this bounded region the layer behaves like a two-dimensional wave guide for waves travelling downstream within it. The mean flow velocity components are now represented by $U = \partial\psi_0/\partial z$, $W = -\partial\psi_0/\partial x$.

Equation (1) is accepted as a correct and complete mathematical model. Since it is clearly separable in time, the stream function ψ_p may be expressed by terms of the general form

$$\tfrac{1}{2}[\Phi(x, z)e^{i\beta t} + \tilde{\Phi}(x, z)e^{-i\beta t}] \tag{2}$$

where β is a real angular velocity and $\sim$ represents a complex conjugate. The substitution of terms such as (2) in the non-linear terms of (1) will produce terms containing $\exp[2i\beta t]$ and $\exp[-2i\beta t]$, representing the generation of a second harmonic, and also terms containing the exponent of zero, representing a contribution to the steady flow and usually called 'mean flow distortion'. The total stream function is therefore assumed to have the form:

$$\psi(x, z;\ t) = \psi_0(x, z) + \tfrac{1}{2}\sum_{n=1}^{\infty} C^n\phi_n(z)e^{in(\alpha x - \beta t)} + \tfrac{1}{2}\sum_{n=1}^{\infty} C^n\tilde{\phi}_n(z)e^{-in(\tilde{\alpha}x - \beta t)} \tag{3}$$

where α is a complex wave number and C is a real amplitude factor of the order of 0·01. The form of the fluctuation terms in (3) involves the assumption that the variables x and z are separable in the travelling wave, and reduces the equation for $\phi_n(z)$ to an ordinary differential equation in which x does not appear explicitly. It is known that this assumption is not strictly accurate but does not lead to serious error when integration is performed at constant x.

Substitution of (3) in (1) and separation of terms in powers of $\exp[i\beta t]$ leads to an infinite series of equations, each with an infinite number of terms. Taken in order,

these equations are the relations governing the mean flow, the fundamental perturbation, and the second and higher harmonics. The factor $\exp[i(\alpha-\tilde{\alpha})x]$ which does not cancel out in the equations represents the downstream local rate of amplification or damping, and may be absorbed into the local amplitude constant C^2. The number of terms which are retained in the equations depends on the number of non-linear interactions which should be taken into account. Since the second harmonic is generated by the fundamental, the consequent distortion of the fundamental should be included. To this order of approximation the third harmonic is generated but is too weak to appear in non-linear terms.

The equations which are derived in this manner are arranged so that the terms appearing on the right-hand side are of second order, i.e., non-linear in the perturbation:

$$\frac{\partial}{\partial z}\left\{\frac{\partial\psi_0}{\partial z}\frac{\partial^2\psi_0}{\partial x\partial z}-\frac{\partial\psi_0}{\partial x}\frac{\partial^2\psi_0}{\partial z^2}-\frac{1}{R}\frac{\partial^3\psi_0}{\partial z^3}\right\}=\frac{C^2}{4}\{i\alpha[\phi_1\tilde{\phi}_1'''-\phi_1''\tilde{\phi}_1'+(\alpha^2-\tilde{\alpha}^2)\phi_1\tilde{\phi}_1']$$
$$-i\tilde{\alpha}(\tilde{\phi}_1\phi_1'''-\tilde{\phi}_1''\phi_1'+(\tilde{\alpha}^2-\alpha^2)\tilde{\phi}_1\phi_1']\} \qquad (4a)$$

$$G[\phi_1]=\frac{C^2}{2}\{2i\alpha[\phi_2\tilde{\phi}_1'''-\phi_2''\tilde{\phi}_1'+(4\alpha^2-\tilde{\alpha}^2)\phi_2\tilde{\phi}_1']-i\tilde{\alpha}[\phi_2'''\tilde{\phi}_1-\phi_2'\tilde{\phi}_1''-(4\alpha^2-\tilde{\alpha}^2)\phi_2'\tilde{\phi}_1]\} \qquad (4b)$$

$$G[\phi_2]=\tfrac{1}{2}i\alpha[\phi_1\phi_1'''-\phi_1'\phi_1''] \qquad (4c)$$

$$G[\phi_3]=\tfrac{1}{2}\{2i\alpha[\phi_2\phi_1'''-\phi_2''\phi_1'+3\alpha^2\phi_2\phi_1']+i\alpha[\phi_1\phi_2'''-\phi_1''\phi_2'-3\alpha^2\phi_1\phi_2']\} \qquad (4d)$$

The terms which are linear in the perturbation are contained in the operator $G[\phi]$, where

$$G[\phi_n]\equiv\left\{\left[in\alpha U-in\beta+W\frac{d}{dz}\right]\left[\frac{d^2}{dz^2}-n^2\alpha^2\right]-\frac{1}{R}\left[\frac{d^2}{dz^2}-n^2\alpha^2\right]^2-\left[W''\frac{d}{dz}+in\alpha U''\right]\right\}\phi_n,$$

and U'' and W'' are second differentials with respect to z of the mean flow velocity components.

The numerical integration of these equations provides a number of interesting problems. If we assume that $C\approx 0$ then (3) shows that the second and third harmonics together with (4*c*) and (4*d*) disappear and the terms on the right-hand sides of (4*a*) and (4*b*) will vanish. This reduces the equations to those of the first order perturbation problem:

$$\frac{\partial\psi_0}{\partial z}\frac{\partial^2\psi_0}{\partial x\partial z}-\frac{\partial\psi_0}{\partial x}\frac{\partial^2\psi_0}{\partial z^2}-\frac{1}{R}\frac{\partial^3\psi_0}{\partial z^3}=0$$

with boundary conditions (5*a*)

$$\frac{\partial\psi_0}{\partial x}=\frac{\partial\psi_0}{\partial z}=0 \text{ at } z=0, \quad \frac{\partial\psi_0}{\partial z}=1 \text{ at } z=\infty.$$

and $G[\phi_1]=0$ with boundary conditions

$$\phi_1(0)=\phi_1'(0)=0, \quad \phi_1\sim e^{-\alpha z} \text{ as } z\to\infty. \qquad (5b)$$

(5*a*) is now a third order partial differential equation, and (5*b*) has become analytic

and remains linear and homogeneous in ϕ_1. The solutions of these first order equations must be obtained before the second order equations can be dealt with.

The Mean Flow Equations in First and Second Order

The solution of (5*a*) is well known and was first obtained by Blasius in 1908. The equation is of similarity type, i.e., it can be reduced to an ordinary differential equation for ψ_0 as a function of a new variable η which is itself a function of x and z. Following Jones and Watson (1963) we use the substitutions

$$\psi_0 = [2x/R]^{\frac{1}{2}} f(\eta), \quad \eta = [R/2x]^{\frac{1}{2}} z,^* \tag{6}$$

reducing (5*a*) to $f'''(\eta)+f(\eta)f''(\eta) = 0$, with $f(0) = f'(0) = 0$ and $f'(\infty) = 1$. This equation can be solved by the Runge-Kutta method if the value of $f''(0)$ is known. At this preliminary stage it is sufficiently accurate to use the value given to five significant figures by Jones and Watson.

After (5*b*) has been solved to give first order values for α and ϕ_1, these values may be substituted in the right-hand side of (4*a*) to give an equation for the next approximation to the mean flow. It is obvious, however, that the addition of the z-dependent term on the right-hand side may invalidate the similarity principle which has been invoked to reduce the partial to an ordinary differential equation. If the added term is sufficiently small the similarity principle, although not holding exactly, will be a good approximation. Since the distortion function is proportional to C^2, various values of C may be used to find out what limitation applies to the use of the similarity principle. The application of the similarity relations to (4*a*) gives:

$$f''''(\eta)+f(\eta)f'''(\eta)+f'(\eta)f''(\eta) = -R^{-\frac{1}{2}}(2x)^{3/2}C^2F(z) = \mathscr{F}(z), \tag{7}$$

where $C^2F(z)$ represents the complete expression on the right-hand side of (4*a*).

We now have to integrate a fourth order equation and therefore require a fourth boundary condition: $\partial^2\psi_0/\partial z^2 = 0$ at $z = \infty$. The integration is performed by the Runge-Kutta method, and four initial values are required. These are the two boundary conditions $f(0) = f'(0) = 0$ together with good approximations for $f''(0)$ and $f'''(0)$. After performing the integration with these starting values it will, in general, be found that the values of $f'(l)$ and $f''(l)$ at the outer limit of integration $\eta = l$ are not consistent with the outer boundary conditions, indicating the need to find improved values of $f''(0)$ and $f'''(0)$. For this purpose we have used an iteration process similar to one employed by Fox (1960) for the determination of eigenvalues when the eigenvector was found by a shooting method. The method uses Newton's equation for finding the zero of a function, and therefore has second order convergence.

Let us first take $f''(0) = p$ and $f'''(0) = q$. When a shooting method is used to solve (7) starting from $\eta = 0$ then $f(\eta)$ and its differentials with respect to η are functions of p and q as well as of η, while $\mathscr{F}(z)$ is independent of p and q. Differentiating (7) with respect to p, writing $\partial f/\partial p = r$, and retaining dashes to represent partial differentiation with respect to η, we obtain:

$$r''''+rf'''+fr'''+r'f''+f'r'' = 0. \tag{7a}$$

* The variable x must be retained in (6) until the differential operations have been performed. Thereafter the substitution $x = 0{\cdot}341R$ is introduced, making $\eta = kz$, where k is a constant whose value to four significant figures is 1·217. The same substitution for x is used in (7). R is a local constant, and z is the only surviving independent variable.

Also differentiating (7) with respect to q and writing $\partial f/\partial q = s$,

$$s'''' + sf''' + fs''' + s'f'' + f's'' = 0. \tag{7b}$$

At $\eta = 0$ we have $f(0) = f'(0) = r(0) = r'(0) = r'''(0) = s(0) = s'(0) = s''(0) = 0$, $r''(0) = s'''(0) = 1$, and as $\eta \to \infty, f'(\eta) \to 1$ and $f''(\eta) \to 0$. The lower boundary conditions permit integration of (7*a*) and (7*b*) to be carried out from $\eta = 0$ to find $r'(l)$, $r''(l)$, $s'(l)$ and $s''(l)$ at the outer limit of integration. The equations of Newton's method may now be used in the following form to find Δp and Δq:

$$r'(l)\Delta p + s'(l)\Delta q + [f'(l) - 1] = 0$$

$$r''(l)\Delta p + s''(l)\Delta q + f''(l) \qquad = 0$$

The numerical solution of these equations was normally found for the range $0 \leqq z \leqq 6$, equivalent to about twice the total thickness of the boundary layer. Adequate accuracy was obtained when this range was divided by the net points into 80 equal intervals. After completing the integration the results were examined to estimate the extent of the departure from the similarity principle. The function $f''''(\eta) - \mathscr{F}(z)$ for the distorted flow was compared with the function $f''''(\eta)$ for the undistorted flow. Text-figs. 1*a* and 1*b* show that quite large variations in $\mathscr{F}(z)$ may occur without giving rise to a large difference between the two functions mentioned above. The figures illustrate the case: $\beta = 0{\cdot}08$, $R = 1000$ and (*a*) $C = 1{\cdot}4$ per cent., (*b*) $C = 5{\cdot}6$ per cent.

The Equations for the Fundamental Perturbation in First Order

In early work carried out to obtain a solution for the fundamental, (5*b*) was used in a simplified form: W, the normal component of the mean flow velocity was assumed to be zero everywhere. The constant β which occurs only to the first power was taken as the complex eigenvalue, and α which occurs in powers up to the fourth was taken as a known real constant. In experiments, however, β is known and real and α is the eigenvalue. Calculations in which α was treated as the eigenvalue and with $W = 0$ were first carried out by Wazzan *et al.* (1968) and independently by Jordinson (1968). The solution of the complete equation with α as eigenvalue was given by Barry (1970). The numerical methods used by Jordinson and Barry, and in the present paper, were developed by Osborne (1967). In the following account of this method, the suffix 1 which has been used to indicate the first harmonic will be omitted.

The differential equation is first replaced by a set of finite difference equations expressed in terms of the values $\phi_{(j)}$ of ϕ at the successive net points (j). Using D to represent d/dz, and h to represent the distance between successive net points, the following central difference relations for differentials of ϕ are used:

$$hD\phi_{(j)} = [\mu\delta - \tfrac{1}{6}\mu\delta^3 + \tfrac{1}{30}\mu\delta^5 - \ldots]\phi_{(j)} \tag{8a}$$

$$h^2D^2\phi_{(j)} = [\delta^2 - \tfrac{1}{12}\delta^4 + \tfrac{1}{90}\delta^6 - \ldots]\phi_{(j)} \tag{8b}$$

$$h^3D^3\phi_{(j)} = [\mu\delta^3 - \tfrac{1}{4}\mu\delta^5 + \tfrac{7}{120}\mu\delta^7 - \ldots]\phi_{(j)} \tag{8c}$$

$$h^4D^4\phi_{(j)} = [\delta^4 - \tfrac{1}{6}\delta^6 + \tfrac{7}{240}\delta^8 - \ldots]\phi_{(j)} \tag{8d}$$

The highest order differentials in (5*b*) are of fourth order, and it is desirable to limit the order of finite differences to δ^4, so that the boundary conditions for the differential

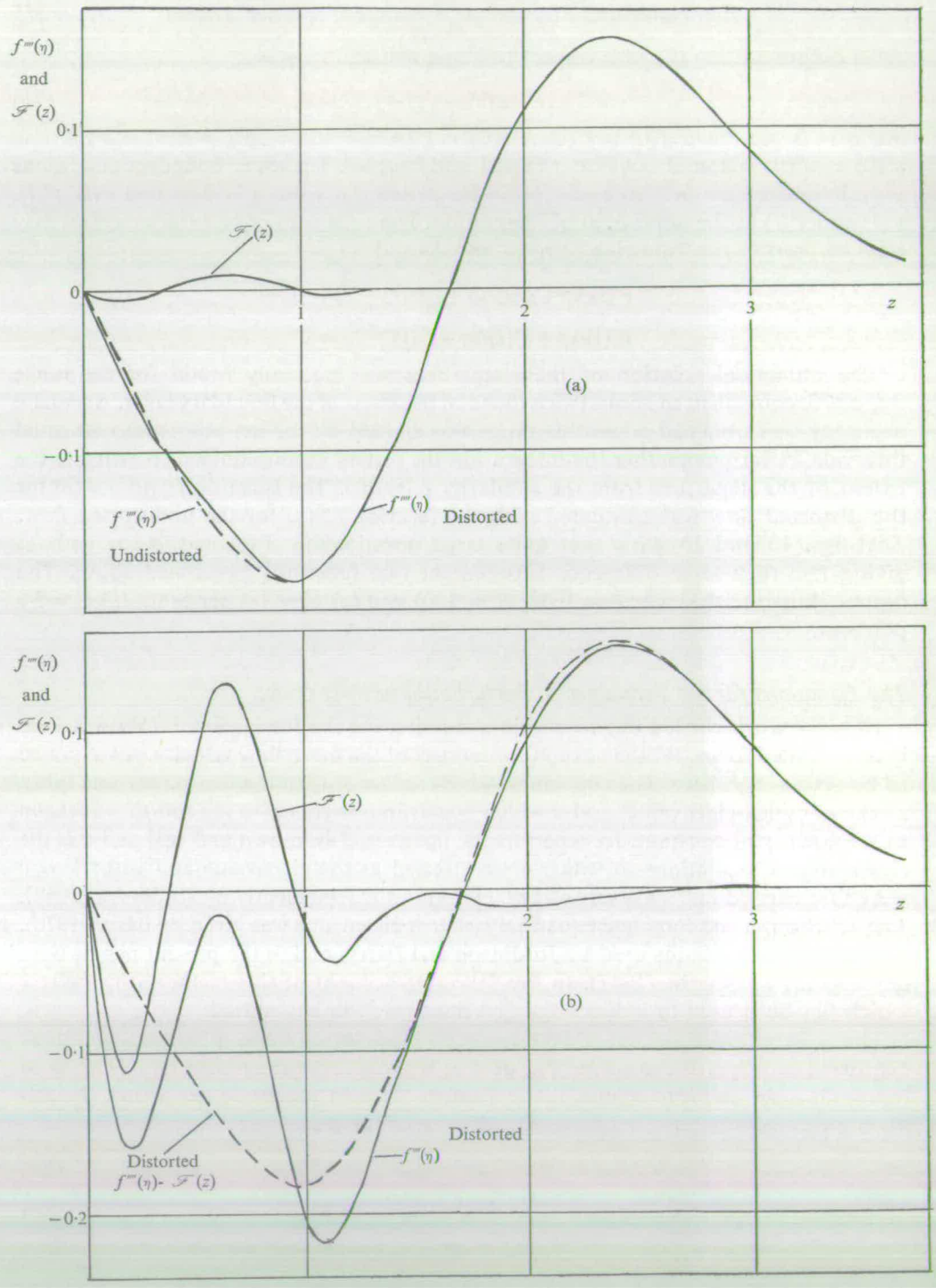

TEXT-FIG. 1.—Graphs of $f^{iv}(\eta)$ and $\mathscr{F}(z)$versus z; $\eta = 1{\cdot}217z$. $R = 1000$, $\beta = 0{\cdot}08$; (*a*) $C = 1{\cdot}4$ per cent., (*b*) $C = 5{\cdot}6$ per cent. Continuous lines show the distortion function $\mathscr{F}(z)$ and the distorted function $f^{iv}(\eta)$; dashed lines: (*a*) undistorted $f^{iv}(\eta)$, (*b*) distorted function $f^{iv}(\eta) - \mathscr{F}(z)$ for $C = 5{\cdot}6$ per cent.

equation will be easily transformed for the difference equations. To achieve this, we substitute in the right-hand side of (8*d*) the Numerov-type transformation:

$$\phi_{(j)} = [1+k_1\delta^2+k_2\delta^4]g_{(j)},$$

and choose k_1 and k_2 so that the coefficients of δ^6 and δ^8 in the resulting equation are zero. The required values are $k_1 = \frac{1}{6}$, $k_2 = -\frac{1}{720}$. This transforms (8*d*) to

$$h^4D^4\phi_{(j)} = \delta^4 g_{(j)}+0(\delta^{10}) \tag{9d}$$

and also gives:

$$hD\phi_{(j)} = \mu\delta g_{(j)}+0(\delta^5) \tag{9a}$$

$$h^2D^2\phi_{(j)} = [\delta^2+\tfrac{1}{12}\delta^4]g_{(j)}+0(\delta^6) \tag{9b}$$

$$h^3D^3\phi_{(j)} = [\mu\delta^3-\tfrac{1}{12}\mu\delta^5]g_{(j)}+0(\delta^7) \tag{9c}$$

The differential equation for ϕ is multiplied throughout by h^4 and the transformation equations (9) are substituted. A truncation error of $0(h^4)$ is adopted, and terms of appreciably lower magnitude, e.g. h^4R^{-1}, are omitted. The various orders of central differences are then expressed in terms of net-point values of g. The j'th equation involves all net points from $g_{(j-3)}$ to $g_{(j+3)}$, each equation of the set having seven terms. In the calculations 80 such equations were normally used, covering the range $0 \leqq z \leqq 6$ and values of j from -2 to $+83$. Finally the boundary conditions must be introduced. In the neighbourhood of the outer boundary the condition to be satisfied is

$$g_{(j+s)} = e^{-s\alpha h}g_{(j)}, \quad s = 1, 2, \ldots, \text{etc.}$$

At the lower boundary, $z = 0$, values are required for $g_{(-1)}$ and $g_{(-2)}$, and these are derived from the boundary conditions:

$$[1+\tfrac{1}{6}\delta^2-\tfrac{1}{720}\delta^4]g_{(0)} = 0, \quad \mu\delta_{g(0)} = 0,$$

giving $g_{(-1)} = g_{(1)}$ and $g_{(-2)} = 474g_{(0)}+248g_{(1)}-g_{(2)}$.

The simultaneous solution of the 80 equations is the solution of

$$M(\alpha)g = 0 \tag{10}$$

where $M(\alpha)$ is a heptadiagonal matrix operator involving the complex eigenvalue α, and g is a vector with 80 complex components. The real constants R and β which occur in M are given arbitrary values. The vector g must be normalised and (10) is therefore solved in conjunction with the vector equation

$$S^T.g = 1 \tag{11}$$

where S^T is a transposed vector having one component unity and all other components zero. By applying this normalisation at one of the net points, the arbitrary amplitude and the arbitrary phase angle of the function g are made definite. The operation of this process can be most simply explained in terms of ϕ. If we write $\alpha = \alpha_r+i\alpha_i$ and $\phi(z) = \phi_r(z)+i\phi_i(z) = |\phi(z)| \exp[i\gamma(z)]$ then the two terms in (3) representing the fundamental perturbation may be replaced by $C \exp[-\alpha_i x] |\phi(z)| \cos(\alpha_r x-\beta t+\gamma(z))$ which represents at fixed x a vector rotating in time in the complex ϕ plane. The normalisation is applied at the net point having the maximum value of $|\phi(z)|$ and makes $\phi_r(z) = 1$ and $\phi_i(z) = 0$ or $\gamma(z) = 0$ at this point. The previously arbitrary

origin of γ is thus defined. At the normalisation point the function g is so nearly equal to ϕ that it is sufficient to normalise g.

The simultaneous solution of (10) and (11) is carried out by an iteration process, assuming a good approximation for α (known from previous work) and a coarse approximation for g. In practice g is taken to be a vector with every element unity. If after the i'th iteration approximate values $\alpha^{(i)}$ and $g^{(i)}$ are known, it is then required to find corrections $\Delta\alpha^{(i)}$ and $\Delta g^{(i)}$ such that

$$M(\alpha^{(i)}+\Delta\alpha^{(i)})(g^{(i)}+\Delta g^{(i)}) = M(\alpha^{(i+1)})g^{(i+1)} = 0$$

with

$$S^T g^{(i)} = S^T g^{(i+1)} = 1.$$

Expanding $M(\alpha^{(i+1)})$ and $g^{(i+1)}$ by Taylor's Theorem we obtain

$$M(\alpha^{(i+1)}) = M(\alpha^{(i)}) + \frac{\partial M(\alpha^{(i)})}{\partial\alpha}\Delta\alpha^{(i)} + \tfrac{1}{2}\frac{\partial^2 M(\alpha^{(i)})}{\partial\alpha^2}(\Delta\alpha^{(i)})^2 + 0(\Delta\alpha^{(i)})^3$$

$$g^{(i+1)} = g^{(i)} + \frac{\partial g^{(i)}}{\partial\alpha}\Delta a^{(i)} + \tfrac{1}{2}\frac{\partial^2 g^{(i)}}{\partial\alpha^2}(\Delta\alpha^{(i)})^2 + 0(\Delta\alpha^{(i)})^3$$

and

$$M(\alpha^{(i+1)})g^{(i+1)} = M(\alpha^{(i)})g^{(i)} + \Delta\alpha^{(i)}\left[M(\alpha^{(i)})\frac{\partial g^{(i)}}{\partial\alpha} + \frac{\partial M(\alpha^{(i)})}{\partial\alpha}g^{(i)}\right]$$

$$+\tfrac{1}{2}(\Delta\alpha^{(i)})^2\left[M(\alpha^{(i)})\frac{\partial^2 g^{(i)}}{\partial\alpha^2} + 2\frac{\partial M(\alpha^{(i)})}{\partial\alpha}\frac{\partial g^{(i)}}{\partial\alpha} + \frac{\partial^2 M(\alpha^{(i)})}{\partial\alpha^2}g^{(i)}\right] + 0(\Delta\alpha^{(i)})^3 \qquad (12)$$

Premultiplying (12) by $M(\alpha^{(i)})^{-1}$ and retaining only first and second order terms,

$$0 = g^{(i)} + \Delta\alpha^{(i)}\frac{\partial g^{(i)}}{\partial\alpha} + M^{-1}\frac{\partial M}{\partial\alpha}g^{(i)}(\Delta\alpha^{(i)}) \qquad (13)$$

Premultiplying (13) by S^T and noting that $S^T\Delta g^{(i)} = 0$,

$$S^T g^{(i)} = -S^T M^{-1}\frac{\partial M}{\partial\alpha}g^{(i)}(\Delta\alpha^{(i)}) \qquad (14)$$

The iteration equations are then

from (14)
$$\Delta\alpha^{(i)} = -\frac{S^T g^{(i)}}{S^T M^{-1}\dfrac{\partial M}{\partial\alpha}g^{(i)}} \qquad (15)$$

from (13)
$$g^{(i+1)} = -(\Delta\alpha^{(i)})M^{-1}\frac{\partial M}{\partial\alpha}g^{(i)} \qquad (16)$$

When the third order terms in (12) are retained we have:

$$g^{(i)} + \frac{\partial g^{(i)}}{\partial\alpha}\Delta\alpha + \tfrac{1}{2}\frac{\partial^2 g^{(i)}}{\partial\alpha^2}(\Delta\alpha)^2 = -(\Delta\alpha)\left[M^{-1}\frac{\partial M}{\partial\alpha}(g^{(i)}+\Delta g^{(i)}) + \tfrac{1}{2}(\Delta\alpha)M^{-1}\frac{\partial^2 M}{\partial\alpha^2}g^{(i)}\right]$$

Substituting for $g^{(i)}+\Delta g^{(i)}$ from (13), for one factor $\Delta\alpha$ from (15), and multiplying by S^T we obtain:

$$\Delta\alpha^{(i)} = -\frac{S^T M^{-1}\frac{\partial M}{\partial \alpha} g^{(i)}}{S^T\left[M^{-1}\frac{\partial M}{\partial \alpha} M^{-1}\frac{\partial M}{\partial \alpha} g^{(i)} - \frac{1}{2}M^{-1}\frac{\partial^2 M}{\partial \alpha^2} g^{(i)}\right]} \tag{17}$$

$$g^{(i+1)} = (\Delta\alpha)^2\left[M^{-1}\frac{\partial M}{\partial \alpha} M^{-1}\frac{\partial M}{\partial \alpha} g^{(i)} - \frac{1}{2}M^{-1}\frac{\partial^2 M}{\partial \alpha^2} g^{(i)}\right] \tag{18}$$

Equations (17) and (18) in their complete form give an iteration with third order convergence (Osborne 1967). If the term containing $\partial^2 M/\partial\alpha^2$ is omitted, (17) and (18) give second order convergence, but the iteration is more stable with respect to a coarse eigenvector approximation than that obtained with (15) and (16). We have therefore used this reduced form of (17) and (18) for the first iteration when the coarse initial approximation to g is used. Subsequent iterations have been performed with (15) and (16).

From the solution for g the function ϕ_1 is obtained by direct application of the Numerov transformation equation. When the calculations were carried out by this method on an ICL 4/70 Computer using double precision numbers, a solution of (5*b*) could be obtained in about 3 seconds.

The Equations for the Second and Third Harmonics

Equations (4*c*) and (4*d*) are obviously not eigenvalue equations, and the constant α is given by the solution of (5*b*) or (4*b*). The first step in solving (4*c*) is to evaluate at all net points (j) the complex vector Z_2, representing the function on the right-hand side. The left-hand side is then replaced by the application of (9) with the finite differences of the function g_2, and the finite differences are expressed in terms of the net-point values of this function. The equation to be solved is now $M_2 g_2 = Z_2$, where M_2 is a matrix operator with complex elements and g_2 is an 80-component vector with complex components. The solution is directly given by

$$g_2 = (M_2)^{-1} Z_2$$

From the solution for g_2 the function ϕ_2 is obtained by the Numerov transformation equation. It will be noted that ϕ_2 is automatically normalised, since the normalised function ϕ_1 has been used in the equation.

Having obtained solutions for ϕ_1 and ϕ_2, the solution for (4*d*) may be undertaken by a process similar to that used for (4*c*). The intermediate function g_3 is given by an equation of the form

$$g_3 = (M_3)^{-1} Z_3.$$

The solution of (4*d*) is, however, not found until final values are available for ψ_0, ϕ_1 and ϕ_2 after simultaneous solution of (4*a*), (4*b*) and (4*c*) has been completed.

The Second Order Equation for the Fundamental

When ψ_0 and ϕ_2 are known, a solution of (4*b*) may be found. The equation is not analytic since ϕ_1, $\tilde{\phi}_1$, α and $\tilde{\alpha}$ are all present, but it is nevertheless linear and homogeneous in ϕ_1, and its solution gives the eigenvalue and the eigenvector. It should be noted, however, that α enters the equation in association both with ϕ_1 and with ϕ_2.

We are solving for ϕ_1 and assuming ϕ_2 to be known, and have therefore treated the α which is associated with ϕ_2 as a known constant and taken the α associated with ϕ_1 as the constant to be determined.

The equation is first expressed in terms of its real and imaginary parts, writing it in the form:

$$(A_r+iA_i)(\phi_r+i\phi_i)+(B_r+iB_i)(\phi_r-i\phi_i)=0,$$

leading to two real equations expressible as a matrix equation:

$$\begin{pmatrix}(A_r+B_r) & (B_i-A_i)\\ (A_i+B_i) & (A_r-B_r)\end{pmatrix}\begin{pmatrix}\phi_r\\ \phi_i\end{pmatrix}=0$$

where A_r, A_i, B_r and B_i are operators which act on both ϕ_r and ϕ_i, and each operator contains two real parameters, α_r and α_i, whose values must be found to obtain the eigenvalue.

The application of the usual Numerov transformation gives two new functions g_r and g_i, and discretisation leads to a matrix equation:

$$M(\alpha_r, \alpha_i)g=0 \tag{19}$$

where M is a square matrix with real components, and g is a vector with 160 real components. In order to keep M as nearly as possible in diagonal form, the order of components in g is $(\ldots, g_{r(j)}, g_{i(j)}, g_{r(j+1)}, g_{i(j+1)}, \ldots)$ and successive columns of M operate alternately on g_r and g_i. A normalisation process is required, as in the solution of (5*b*), for both g_r and g_i. For this purpose the matrix relation

$$Sg=K \tag{20}$$

is used, where K is a two-component vector and S a 2×160 matrix.* The normalisation is applied, as before, at the net point (j) where $|\phi|$ reaches its maximum value, and makes $\phi_{r(j)}=1$ and $\phi_{i(j)}=0$. S therefore consists of zero elements except at $(1,2j-1)$ and $(2,2j)$ where the value is unity. K is the vector (1,0). The general principle which underlies the inclusion of normalisation equations is simply that the number of equations used in a solution must equal the number of quantities to be determined.

The iteration equations are most simply derived from Newton's equation for finding the zero of a function. We assume that the starting values of g, α_r and α_i satisfy (19) and (20) nearly but not exactly. Differentiating (19) and (20) we obtain corrections $\Delta\alpha_r$, $\Delta\alpha_i$ and a vector correction Δg.

$$M\Delta g+\frac{\partial M}{\partial\alpha_r}g\Delta\alpha_r+\frac{\partial M}{\partial\alpha_i}g\Delta\alpha_i=-Mg \tag{21}$$

$$S\Delta g=K-Sg \tag{22}$$

The values of g, α_r and α_i in (21) and (22) are assumed to have been obtained from the i'th iteration. Premultiplying (δ21) by M^{-1} we find

$$g^{(i+1)}=-M^{-1}\frac{\partial M}{\partial\alpha_r}g^{(i)}\Delta\alpha_r^{(i)}-M^{-1}\frac{\partial M}{\partial\alpha_i}g^{(i)}\Delta\alpha_i^{(i)} \tag{23}$$

* Equation (20) represents a simple case of a more general normalising relation $S(\lambda)\,g=\chi(\lambda)$ in which S and χ are functions of the eigenvalue parameters. In the general case the iteration equations involve differentiations of S and χ with respect to these parameters.

Premultiplying (23) by S and subtracting (22)

$$-K = SM^{-1}\frac{\partial M}{\partial \alpha_r} g^{(i)}\Delta\alpha_r^{(i)} + SM^{-1}\frac{\partial M}{\partial \alpha_i} g^{(i)}\Delta\alpha_i^{(i)}$$

$$= T\Delta\lambda^{(i)}$$

Where T is a 2×2 matrix and $\Delta\lambda$ is the vector $(\Delta\alpha_r, \Delta\alpha_i)$
Then

$$\Delta\lambda^{(i)} = -T^{-1}K \tag{24}$$

The iteration equations are then (24) followed by (23). Since in this calculation a good first approximation for g is known, no difficulties arise in the first iteration for g.

The Complete Solution

When the computer programs for the solution of all the equations (4) have been prepared and tested, the separate programs must be built into a single complete program which first obtains a convergent simultaneous solution for (4*a*), (4*b*) and (4*c*) and thereafter finds the solution of (4*d*). The order in which the separate programs are used is (5*a*), (5*b*), (4*a*), (4*c*), (4*b*), (4*a*), (4*c*), (4*b*), . . . recycling the last three programs until a criterion of convergence is met. The criterion used in our program is: $(\Delta\alpha_r)^2+(\Delta\alpha_i)^2<10^{-16}$ in the last iteration. When this condition is met it is found in practice that the norm of variations in ψ_0, ϕ_1 and ϕ_2 in the last iteration does not appreciably exceed 10^{-8}.

The program requires central storage of about 60 K bytes, and its operation requires central storage of 200 K bytes. The total time required on an ICL 4/70 Computer is about 10 seconds per cycle of (4*a*), (4*c*) and (4*b*).

Acknowledgments

The computational methods which have been described in this paper for the solution of the eigenvalue problem were originally developed by Osborne (1967) for our work. The development of other parts of the program was greatly assisted by discussions with Mr Donald Kershaw. The derivation of the Numerov transformation equations follows Jordinson (1968). The computational costs were met in part by a grant from the Ministry of Trade and Industry, and one of the authors (D. F. C.) has been supported by an S.R.C. Studentship.

References to Literature

Barry, M. D. J., 1970. Ph.D. thesis, Edinb. Univ. (Unpublished).
Fox, L., 1960. In *Boundary Problems in Differential Equations* (Ed. R. E. Langer). Univ. Wisconsin Press.
Jones, C. W. and Watson, E. J., 1963. In *Laminar Boundary Layers*. Oxford University Press.
Jordinson, R., 1968. Ph.D. thesis, Edinb. Univ. (Unpublished).
Meksyn, D. and Stuart, J. T., 1951. *Proc. Roy. Soc.*, **A208**.
Numerov, B. V., 1924. *Mon. Not. Roy. Astr. Soc.*, **84**, 592.
Osborne, M. R., 1967. *SIAM J. Appl. Math.*, **15**, 539.
Stuart, J. T., 1958. *J. Fluid Mech.*, **4**, 1.
——, 1960. *J. Fluid Mech.*, **9**, 353.
Watson, J., 1960. *J. Fluid Mech.*, **9**, 371.
Wazzan, A. R., Okamura, T. T. and Smith, A. M. O., 1968. Douglas Aircraft Co. Rep. DAC-67086.

ABSTRACT OF THESIS

Name of Candidate DAVID FRANCIS CORNER

Address PHYSICS DEPARTMENT, JAMES CLERK MAXWELL BLDG., MAYFIELD ROAD.

Degree DOCTOR OF PHILOSOPHY *Date* SEPTEMBER, 1973.

Title of Thesis NUMERICAL STUDIES IN NON-LINEAR BOUNDARY LAYER STABILITY THEORY.

The main part of this thesis is devoted to the study of a finite periodic perturbation imposed on a Blasius boundary layer.

Some non-linear terms are included, causing distortion of the mean flow by the perturbation, generation of second and third harmonics, and modification of the fundamental of the perturbation by the second harmonic. The problem requires the solution of a set of three non-linear coupled equations.

The linearised problem of an infinitesimal perturbation is also stated, and the equation for the perturbation, the Orr-Sommerfeld equation is given.

The numerical methods used to solve the individual equations are derived. The undistorted mean flow is found by a step-by-step method, but in the application of this step-by-step method to the distorted mean flow, an initial value has first to be found.

An iterative method is used for the solution of the Orr-Sommerfeld equation. It has been used previously, but a more concise derivation is given. A development of the iteration is derived in order to solve for the fundamental of the non-linear problem. The method of solution for the higher harmonics is also given.

The solution of the set of coupled equations is accomplished by iteration of the individual equations until convergence is attained.

The results of some solutions of the coupled equations at different amplitudes, Reynolds numbers, and frequencies are presented, and a few cases considered in more detail.

In addition, the results of some investigations into the existence of/

Use other side if necessary.

of other modes of solution of the Orr-Sommerfeld equation are presented. The possibility of non-linear interaction between these modes is suggested.